THEORETICAL STUDY OF SPIN-WAVE EFFECTS IN QUANTUM FERROMAGNETS

by

SRIPOORNA PANIYADI KRISHNA BHARADWAJ

A DISSERTATION

Presented to the Department of Physics
and the Graduate School of the University of Oregon
in partial fulfillment of the requirements
for the degree of
Doctor of Philosophy

June 2017

DISSERTATION APPROVAL PAGE

Student: Sripoorna Paniyadi Krishna Bharadwaj

Title: Theoretical Study of Spin-wave Effects in Quantum Ferromagnets

This dissertation has been accepted and approved in partial fulfillment of the requirements for the Doctor of Philosophy degree in the Department of Physics by:

Dr. John Toner	Chairperson
Dr. Dietrich Belitz	Advisor
Dr. Hailin Wang	Core Member
Dr. James Isenberg	Institutional Representative

and

Scott L. Pratt	Dean of the Graduate School

Original approval signatures are on file with the University of Oregon Graduate School.

Degree awarded June 2017.

DISSERTATION ABSTRACT

Sripoorna Paniyadi Krishna Bharadwaj

Doctor of Philosophy

Department of Physics

June 2017

Title: Theoretical Study of Spin-wave Effects in Quantum Ferromagnets

In this dissertation, we examine quantum ferromagnets and determine various effects of the magnetic Goldstone modes or "magnons" in these systems.

Firstly, we calculate the magnon contribution to the transport relaxation rate of conduction electrons in metallic ferromagnets and find that at asymptotically low temperatures, the contribution behaves as $T^2 e^{-T_0/T}$ and not as T^2 predicted previously. To perform these calculations, we derive and use a very general effective theory for metallic ferromagnets. This activation barrier-like behavior is due to the fact that spin waves only couple electrons from different Stoner subbands that arise from the splitting of the conduction band in presence of a nonzero magnetization. The T^2 behavior is found to be valid only in a pre-asymptotic temperature window. The temperature scale T_0 is the energy of the least energetic ferromagnon that couples electrons of different spins.

Second, we discuss magnon-induced long-range correlation functions in quantum magnets. In the ordered phases of both classical ferromagnets and antiferromagnets, the long-range correlations induced by the magnons lead to a singular wavenumber

dependence of the longitudinal order-parameter susceptibility in spatial dimensions $2 < d < 4$. We investigate the quantum analog of this singularity using a nonlinear sigma model. In a quantum antiferromagnet at $T = 0$, a weaker nonanalytic behavior is obtained, which is consistent with power counting. The analogous result for a quantum ferromagnet is absent if the magnon damping is neglected. This is due to the lack of magnon number fluctuations in the quantum ferromagnetic ground state. Magnon damping due to quenched disorder restores the expected nonanalyticity.

Finally, we use an effective field theory for clean, strongly interacting electron systems to calculate the magnon contribution to the density of states, the longitudinal magnetic susceptibility and the conductivity in an itinerant ferromagnet. Utilizing a loop expansion that does not assume the electron-electron interaction to be a small parameter, we obtain the leading nonanalytic corrections to the Stoner saddle-point results for these observables, as functions of the frequency and wavenumber in the hydrodynamic limit.

The dissertation includes previously published and unpublished co-authored material.

CURRICULUM VITAE

NAME OF AUTHOR: Sripoorna Paniyadi Krishna Bharadwaj

GRADUATE AND UNDERGRADUATE SCHOOLS ATTENDED:

University of Oregon, Eugene, Oregon
Indian Institute of Technology Madras, Chennai, India

DEGREES AWARDED:

Doctor of Philosophy, Physics, 2017, University of Oregon
Master of Science, Physics, 2014, University of Oregon
Bachelor of Technology, Engineering Physics, 2011, Indian Institute of Technology Madras

AREAS OF SPECIAL INTEREST:

Strongly-correlated Electrons
Magnetism
Machine Learning

PROFESSIONAL EXPERIENCE:

Graduate Research Assistant, University of Oregon, 06/2015 - 06/2017

Graduate Teaching Fellow, University of Oregon, 09/2011 - 06/2015

GRANTS, AWARDS AND HONORS:

Doctoral Research Fellowship, 2016-17, University of Oregon

Weiser Senior Teaching Assistant Award, 2016, Department of Physics, University of Oregon

Physics Qualifier Exam Prize, Fall 2011, Department of Physics, University of Oregon

PUBLICATIONS:

S. Bharadwaj, D. Belitz and T. R. Kirkpatrick, Phys. Rev. B, 94:144404, 2016

S. Bharadwaj, D. Belitz and T. R. Kirkpatrick, Phys. Rev. B, 89:134401, 2014

ACKNOWLEDGEMENTS

I am immensely grateful to my advisor Prof. Dietrich Belitz for his guidance and insightful discussions throughout the duration of my PhD research. It was great fun learning about magnets, soft-modes, etc. and working with him. His meticulousness and organized approach to research is something that I hope to incorporate in whatever I do in the future.

My sincere thanks also go to Prof. John Toner, the chair of my committee. I will always remember his entertaining lectures, challenging homeworks and many illuminating conversations.

I will be forever thankful to Rajesh Narayanan, for stoking my interest in Condensed Matter Physics and for pointing the way to Eugene and Dietrich.

I am deeply indebted to Nirmal Raj; for convincing me to come to Eugene, for being a great housemate for four years, for our long conversations about physics and beyond, and for being an all-round awesome dude.

My sincerest gratitude goes to George de Coster, for being incredibly supportive, a great friend and helping me open up and enjoy life.

I would also like to acknowledge Chris Jackson for his exemplary ways. It was a sheer joy and a privilege to listen to his unique insights into physics and stuff in general.

My thanks go to Prof. Davison Soper, Prof. Graham Kribs, Prof. Hailin Wang, Prof. Jim Isenberg and Prof. Spencer Chang for their entertaining and informative courses.

My fellow Oregon physics students: Wes Erickson, Chris Newby, Gabriel Barello, Dileep Reddy, Herbert Grotewohl, Richard Wagner, Bill Watterson; Thank you for being great friends and enriching my life.

I would like to acknowledge the musician Steven Wilson and his band 'Porcupine Tree' for being the soundtrack to my life for the past five years.

Finally, my thanks go to the University of Oregon for supporting me in my final year through the Doctoral Research Fellowship.

To my parents.

TABLE OF CONTENTS

Chapter Page

I. INTRODUCTION 1
Heisenberg Model 1
Order Parameter and Spontaneous Symmetry Breaking 4
Magnons 6
Ferromagnon Dispersion Relation 6
Antiferromagnon Dispersion Relation 8
Outline 10

II. SPIN-WAVE CONTRIBUTION TO THE ELECTRONIC RELAXATION RATES IN METALLIC FERROMAGNETS 12
Motivation 12
Model: Magnon-mediated Electron-electron Interaction 15
Effective Action 15
Stoner Model for Itinerant Ferromagnetism 22
Single-particle Relaxation Rate 28
Transport Relaxation Rate 32
Validity of the Effective Action 40
Discussion and Conclusions 44

III. MAGNON-INDUCED LONG-RANGE CORRELATION FUNCTIONS IN QUANTUM MAGNETS 49
Motivation 49
NLσM for Quantum Ferromagnets 52
NLσM for Quantum Antiferromagnets 63
Effects of Damped Ferromagnetic Magnons 70
Nonconserved Order Parameter 72
Conserved Order Parameter 74
Renormalization-group Interpretation of the Results 75
Conclusions 78

IV. AN EFFECTIVE FIELD THEORY APPROACH TO ITINERANT FERROMAGNETS 82
Motivation 82
Q-matrix Formalism 84
Action in terms of Composite Variables 84
Stoner Saddle Point 87

Chapter Page
Gaussian Approximation . . . 89
Spin Waves and Longitudinal Susceptibility . . . 93
One-loop Contribution . . . 93
Effects of Damping . . . 101
Some Finite Temperature Results . . . 104
Electrical Conductivity . . . 104
Density of States . . . 111
Conclusions . . . 116

V. SUMMARY . . . 118

APPENDIX: CAUSAL FUNCTIONS AND LONG-TIME TAILS . . . 121
Non-integer Powers . . . 121
Even Powers . . . 122
Odd Powers . . . 123

REFERENCES CITED . . . 125

LIST OF FIGURES

Figure Page

1. (a) A ferromagnetic and (b) an antiferromagnetic arrangement of lattice spins 2
2. A helical magnet with the spins modulated along the z-axis 3
3. A spin wave on a line of spins, showing one wavelength. In the top row, the spins are viewed in perspective. In the bottom row, the spins are viewed from above 6
4. Splitting of the conduction band Fermi surface. Here, $k_0 = k_{\rm F}^+ - k_{\rm F}^-$. The blue and red Fermi surfaces represent the up-spin and down-spin electrons, respectively. 19
5. Effective electron-electron interaction mediated via magnon exchange. The dashed line represents the effective potential $\mathcal{V}_{\sigma\sigma'}(k)$ 21
6. Self-energy contributions $\Sigma_\sigma(p)$ for the σ-spin Green function 29
7. Diagrammatic representation of the current-current correlation function, which describes the linear response of the system to an applied external electric field 33
8. Ladder approximation for the vertex function $\mathbf{\Gamma}$ 34
9. Diagrammatic representation of the coupling between the longitudinal and the transverse spin fluctuations in the classical case: A longitudinal (L) mode couples to two transverse (T) modes. The resulting contribution to the longitudinal susceptibility $\chi_{\rm L}$ has the form given in Eq. (3.1) 50
10. Diagrammatic representation of the coupling between longitudinal and transverse spin fluctuations in the quantum case 57
11. The one-loop contribution to the longitudinal part of the dynamical structure factor for a ferromagnet, Eq. (3.24), normalized by $\sqrt{\omega_{\boldsymbol{k}}}/4\pi D^{3/2}$, for $H = 0$ as a function of the frequency ω for various values of the temperature T. ω and T are measured in units of $\omega_{\boldsymbol{k}}$. On the scale shown, the result for $T/\omega_{\boldsymbol{k}} = 10$ is almost distinguishable from the classical result, Eq. (3.25) 61
12. The one-loop contribution to the longitudinal part of the dynamical structure factor for a ferromagnet, Eq. (3.24), normalized as in Fig. 11, for $T/\omega_{\boldsymbol{k}}$ as a function of the frequency ω for various values of the magnetic field H. ω and H are measured in units of $\omega_{\boldsymbol{k}}$ and $\omega_{\boldsymbol{k}}/\mu$, respectively. Even a very weak magnetic field broadens the resonance feature. 62

13. The one-loop contribution to the longitudinal part of the dynamical structure factor for an antiferromagnet (left panel) and a ferromagnet (right panel), normalized by $N_0^2 c/4\pi\rho_s^2$ and as Figs. 11 and 12, respectively, for $T/\omega_{\boldsymbol{k}} = 0.05$ as functions of the frequency ω measured in units of $\omega_{\boldsymbol{k}}$. The inset in the left panel separately shows the $T = 0$ contribution to the antiferromagnetic structure factor (blue curve) and the contribution that vanishes as $T \to 0$ (red curve). The structure factor shown in the main panel is the sum of these two contributions, as expressed in Eq. (3.38) 68
14. The solid lines represent $\delta\tilde{\Lambda}$ and the wavy lines represent JL 95
15. One-loop (a) and two-loop (b) contribution to the one-point vertex function $\langle \delta Q \rangle$ 112

CHAPTER I

INTRODUCTION

Magnets are among the most widely-researched condensed matter systems. They have a wide variety of technological applications ranging from electric motors to magnetic data storage devices and medicine. At the atomic level, the origin of magnetism can be attributed to an intrinsic property of the electron, namely, the angular momentum known as "spin". Due to its spin, each electron basically behaves like a tiny magnet. At low enough temperatures, the various interactions between these electronic spins lead to a plethora of magnetic systems with interesting arrangements of spins. At high temperatures, the thermal fluctuations in the system cause disorder and the spins point in random directions.

Heisenberg Model

A model widely used to describe various magnetic systems is the Heisenberg model. Consider a collection of atoms at lattice sites i, each with an associated classical spin $\boldsymbol{S}_i$, a three dimensional vector. According to the Heisenberg model, the energy of this system, in the absence of an external magnetic field, is given by the Hamiltonian [1, 2]

$$H = -J \sum_{\langle ij \rangle} \boldsymbol{S}_i \,.\, \boldsymbol{S}_j, \tag{1.1}$$

where J is the exchange integral. It is related to the overlap of the charge distributions of atoms at sites i, j and represents the characteristic magnetic energy scale. The symbol $\langle ij \rangle$ indicates that the interaction is only between nearest-neighbor pair of spins [3].

When the quantity $J > 0$, the ground state of the system is the one where all the spins are aligned parallel to each other, leading to a nonzero net magnetization, as shown in Fig. 1(a). This state with a nonzero magnetization, exists below a certain temperature known as the "Curie temperature". This particular ground state corresponds to a ferromagnet. Eq. (1.1) adequately describes simple ferromagnetic insulators like $CrBr_3$, EuO and EuS. In these materials, all the spins are ionic in origin and in their ground states, the ionic spins are aligned parallel to each other as in Fig. 1(a).

However, the Heisenberg model does not describe metallic ferromagnets like Fe, Co and Ni. These metals obey a band or itinerant electron model of ferromagnetism [4], which will be discussed in Chapter II. In short, the ferromagnetism in these materials is due to the different populations of up-spin and down-spin electrons in the system.

FIGURE 1. (a) A ferromagnetic and (b) an antiferromagnetic arrangement of lattice spins

The case $J < 0$ corresponds to an antiferromagnet, where the classical ground state has neighboring spins anti-parallel to each other as shown in Fig. 1(b), with a net zero magnetization. This state is known as the "Néel state", which exists below a temperature known as the "Néel temperature" [5]. Some examples of antiferromagnets are Cr, MnO and FeO. The spins in an antiferromagnet can be interpreted as belonging to two sublattices A and B. The spins in a particular sublattice are parallel to each other. But, the spins belonging to two different sublattices have the same

magnitude but are antiparallel to each other, i.e. $\boldsymbol{S}_A = -\boldsymbol{S}_B$. Above the ordering temperature, in both ferromagnets and antiferromagnets, the spins point in random directions and there is no long-range order in the system. This is the paramagnetic state.

Some other ordered arrangements of electron spins are ferrimagnets, canted antiferromagnets and helical magnets. A ferrimagnet is a more general version of an antiferromagnet, where the antiparallel spins of the two sublattices have different magnitude, i.e. $|\boldsymbol{S}_A| > |\boldsymbol{S}_B|$. Examples of ferrimagnets are magnetite (Fe_3O_4), ferrites of the form MO.Fe_2O_3 where M is often Zn, Cd, Fe, Ni, Cu, Co or Mg [3].

Helical magnets are another interesting class of materials. The inversion symmetry in the system is broken and the Hamiltonian has a Dzhyaloshinksi-Moriya term [6, 7]. This leads to a helical or spiral order in the ground state, where the magnetization is ferromagnetic in planes perpendicular to some pitch vector $\boldsymbol{q}$, with a helical modulation along the $\boldsymbol{q}$- axis as shown in Fig. 2. A well-known helimagnet is MnSi [8, 9].

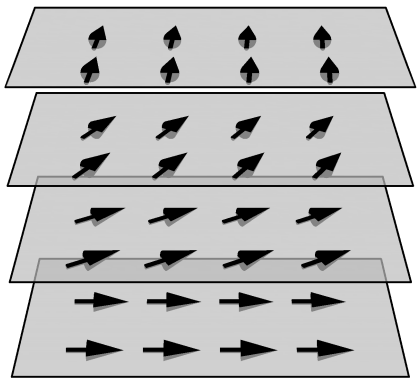

FIGURE 2. A helical magnet with the spins modulated along the z-axis

There also exist more complicated forms of magnetism like spin glasses, spin liquids, spin-density waves etc [10, 11, 12, 13]. This dissertation only considers isotropic ferromagnets and antiferromagnets.

Order Parameter and Spontaneous Symmetry Breaking

The preceding section discussed some ordered arrangements of classical spins that exist below an ordering temperature. In order to describe these systems, it is useful to introduce a quantity that signifies the degree of ordering in the system. This quantity is known as the "order parameter" of the system. Usually, the order parameter is nonzero in the ordered phase and is zero in the disordered phase. For ferromagnets, the net magnetization $\boldsymbol{M}$ is the order parameter. For antiferromagnets, the net magnetization is zero even in the ordered phase. Therefore, one needs to use the "staggered magnetization" as the order parameter. It is defined as $\boldsymbol{M}' = 1/V \sum_i (-1)^i \boldsymbol{S}_i$, where alternate sites are labeled even or odd.

In both cases, the lattice model of spins can be coarse-grained into a continuum model where the order parameter is a spatially-varying classical vector field $\boldsymbol{\phi}(\boldsymbol{x})$ [14]. Then, a continuum description of the ferromagnetic or the antiferromagnetic state can be obtained in terms of a free-energy which is a function of the order parameter $\boldsymbol{\phi}$. In short, the partition function for the Heisenberg model, which is in terms of the spins at individual sites, can be rewritten purely in terms of the continuous field by integrating out the site-specific spin variables $\boldsymbol{S}_i$. What is left behind is the Landau-Ginzburg free-energy functional [15],

$$F[\boldsymbol{\phi}(\boldsymbol{x})] = \int d^d\boldsymbol{x}\, [\frac{c}{2}|\nabla\boldsymbol{\phi}(\boldsymbol{x})|^2 + \frac{r}{2}|\boldsymbol{\phi}(\boldsymbol{x})|^2 + \frac{u}{4}(|\boldsymbol{\phi}(\boldsymbol{x})|^2)^2 + \ldots]. \tag{1.2}$$

The coefficients $c, u, r, \ldots$ are functions of the exchange energy J and temperature T. Eq. (1.2) is more general than Eq. (1.1) and describes both metallic and insulating magnets.

Considering a spatially uniform $\boldsymbol{\phi}$, one now analyzes the free-energy density $f(M) = (r/2)\varphi^2 + (u/4)\varphi^4$. Here, φ is the magnitude of the order parameter. For stability, it is assumed that $u > 0$. If $r > 0$, the free-energy is minimized when $\varphi = 0$. This represents the disordered paramagnetic state. When $r < 0$, the free-energy is minimized at nonzero φ, which represents the ordered state. Generically, $r \propto T - T_c$ for $T \simeq T_c$. Therefore, T_c represents the ordering temperature which is the Curie temperature in ferromagnets and Néel temperature in antiferromagnets.

In the disordered phase, the symmetry of the system, namely the spin-rotation symmetry, is unbroken. That is, the free energy remains invariant under arbitrary rotations of the field $\boldsymbol{\phi}(\boldsymbol{x})$. However, in the ordered phase, the system chooses to order along some arbitrary direction, e.g., $\boldsymbol{\phi}(\boldsymbol{x}) = (0, 0, \varphi)$ and it is no longer invariant under arbitrary rotations of $\boldsymbol{\phi}$. Therefore, the spin-rotation symmetry has been broken in the ordered phase. This phenomenon is known as "spontaneous symmetry breaking" and it occurs in many physical systems like superconductors, liquid crystals, particle physics etc [16, 17, 18]. The word "spontaneous" signifies that these systems develop a nonzero order parameter on their own at sufficiently low temperatures, without being subjected to an external magnetic field.

An important consequence of a generic continuous symmetry which is spontaneously broken is the necessary presence of massless or soft excitations, predicted by Goldstone's theorem. These massless excitations are known as "Goldstone modes". In solids, spontaneously broken translational and rotational symmetry results in phonons, which are the Goldstone modes. In both ferromagnets

and antiferromagnets, the breaking of the continuous spin-rotation symmetry results in Goldstone modes known as "magnons".

Magnons

As mentioned in the previous section, a spontaneously broken continuous symmetry is accompanied by massless Goldstone modes. In ordered spin systems, the Goldstone modes are magnons. These massless excitations have a wavelike form, as shown in Fig. 3, and are analogous to lattice vibrations or phonons. Magnons are oscillations in the relative orientations of spins on a lattice. In this dissertation, the terms "magnons" and "spin waves" are used interchangeably. In the following, the derivations of the ferromagnetic and the antiferromagnetic magnon dispersion relation in [3] are briefly recapitulated.

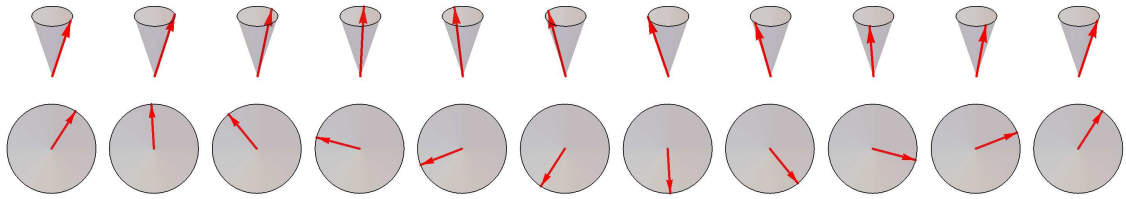

FIGURE 3. A spin wave on a line of spins, showing one wavelength. In the top row, the spins are viewed in perspective. In the bottom row, the spins are viewed from above

Ferromagnon Dispersion Relation

To derive the magnon dispersion relation, one assumes, for simplicity, a chain of spins that prefer to align parallel to each other, i.e. $J > 0$ in the Heisenberg model. From Eq. (1.1), the effective magnetic field felt by the lth spin is

$$\boldsymbol{B}_l = (-2J/g\mu_B)\,(\boldsymbol{S}_{l-1} + \boldsymbol{S}_{l+1}), \tag{1.3a}$$

where g is the electronic g-factor and μ_B is Bohr magneton. From mechanics, the effective magnetic field causes a torque on the lth spin. Then, the rate of change of the angular momentum $\hbar \boldsymbol{S}_l$ is

$$\hbar \frac{d\boldsymbol{S}_l}{dt} = (-g\mu_B)\boldsymbol{S}_l \times \boldsymbol{B}_l = (2J/\hbar)\left[\boldsymbol{S}_l \times \boldsymbol{S}_{l-1} + \boldsymbol{S}_l \times \boldsymbol{S}_{l+1}\right]. \tag{1.3b}$$

In general, these equations are nonlinear. Assume that the spins predominantly point along the z-direction, i.e. $S_l^z \approx S$. Then, the transverse components $S_l^x, S_l^y \ll S$, which means that the amplitude of the excitations are small. With these assumptions, the following linearized equations are obtained:

$$\frac{dS_l^x}{dt} = (2JS/\hbar)\left[2S_l^y - S_{l-1}^y - S_{l+1}^y\right] \tag{1.4a}$$

$$\frac{dS_l^y}{dt} = -(2JS/\hbar)\left[2S_l^x - S_{l-1}^x - S_{l+1}^x\right] \tag{1.4b}$$

$$\frac{dS_l^z}{dt} = 0. \tag{1.4c}$$

To solve these linearized equations, plane wave solutions for S^x and S^y can be assumed. Taking $S_l^x = u\exp[i(lka - \omega t)]$ and $S_l^y = v\exp[i(lka - \omega t)]$, with u, v constants, k the wavenumber and a the lattice constant, Eqns. (1.4a) yield

$$-i\omega u = (4JS/\hbar)(1 - \cos(ka))v, \tag{1.5a}$$

$$-i\omega v = -(4JS/\hbar)(1 - \cos(ka))u. \tag{1.5b}$$

For nonzero u and v, the determinant of the coefficients must be zero. This yields the ferromagnetic dispersion relation

$$\hbar\omega = 4JS(1 - \cos(ka)). \tag{1.6a}$$

The above expression is the magnon dispersion relation for a ferromagnetic spin chain. For a ferromagnetic cubic lattice with nearest-neighbor interactions,

$$\hbar\omega = 4JS(\mathcal{N} - \sum_{\delta} \cos(\boldsymbol{k}.\boldsymbol{\delta})). \tag{1.6b}$$

The summation is over $\mathcal{N}$ vectors that join the central atom to its nearest neighbors. For small wavenumbers, or equivalently long wavelengths, $ka \ll 1$. Thus, we obtain a quadratic dispersion relation

$$\hbar\omega = (2JS\mathcal{N}a^2)|\boldsymbol{k}|^2. \tag{1.6c}$$

For comparison, phonons have a linear dispersion relation. The coefficient of $|\boldsymbol{k}|^2$ is the spin-wave stiffness, which can be measured by neutron-scattering experiments.

Antiferromagnon Dispersion Relation

For antiferromagnets, the steps for the ferromagnetic case follow through in a similar fashion. First, it is assumed that spins with even indices $2l$ belong to the sublattice A with $(S^z = S)$ and the spins with odd indices $2l + 1$ belong to the sublattice B with $(S^z = -S)$. Considering only nearest-neighbor interactions with $J < 0$ in Eq. (1.1), the set of linearized equations now read; for the up spins

$$\frac{dS^x_{2l}}{dt} = (2JS/\hbar)\left[-2S^y_{2l} - S^y_{2l-1} - S^y_{2l+1}\right] \tag{1.7a}$$

$$\frac{dS^y_{2l}}{dt} = -(2JS/\hbar)\left[-2S^x_{2l} - S^x_{2l-1} - S^x_{2l+1}\right], \tag{1.7b}$$

$$\frac{dS^x_{2l+1}}{dt} = (2JS/\hbar)\,[2S^y_{2l+1} + S^y_{2l} + S^y_{2l+2}] \tag{1.8a}$$
$$\frac{dS^y_{2l+1}}{dt} = -(2JS/\hbar)\,[2S^x_{2l+1} + S^x_{2l} + S^x_{2l+2}] \tag{1.8b}$$

for the down spins. Defining a new variable $S^+ = S^x + iS^y$, the equations can be combined to yield

$$\frac{dS^+_{2l}}{dt} = (2iJS/\hbar)\,[2S^+_{2l} + S^+_{2l-1} + S^+_{2l+1}] \tag{1.9a}$$
$$\frac{dS^+_{2l+1}}{dt} = -(2iJS/\hbar)\,[2S^+_{2l+1} + S^+_{2l} + S^+_{2l+2}]. \tag{1.9b}$$

Looking for solutions of the form

$$S^+_{2l} = u\exp[i(2lka - \omega t)]; \quad S^+_{2l+1} = v\exp[i((2l+1)ka - \omega t)], \tag{1.10a}$$

one obtains

$$\omega u = \frac{4|J|S}{\hbar}(u + v\cos(ka)), \tag{1.10b}$$
$$\omega v = -\frac{4|J|S}{\hbar}(v + u\cos(ka)). \tag{1.10c}$$

As before, the above system of equations has nonzero solutions for u and v if

$$\omega^2 = (\frac{4|J|S}{\hbar})^2\,(1 - \cos^2(ka)) \implies \omega = \frac{4|J|S}{\hbar}|\sin(ka)|. \tag{1.10d}$$

For long wavelengths, $\omega \approx (4|J|S/\hbar)|ka|$, which is a linear dispersion relation.

The preceding discussion was in the context of classical spins. At very low temperatures, quantum effects become relevant and the spins in the system must

be treated quantum mechanically. Therefore, the spins $\boldsymbol{S}_i$ in Eq. (1.1) are now quantum mechanical operators. In a spin 1/2 system, that is $S = 1/2$, the individual components of $\boldsymbol{S}_i$ are the Pauli matrices. Then, the spin waves in the ordered state are quantized, analogous to photons and phonons.

Outline

In this dissertation, we are interested in studying the various effects of magnons on certain thermodynamic and transport observables. In metallic quantum ferromagnets, the conduction electrons can be scattered by magnons in a similar fashion to their scattering by phonons and photons. In Chapter II, the magnon contributions to the electronic single-particle and transport relaxation rates are calculated. These relaxation rates are in turn related to the thermal and electrical conductivity, respectively. At asymptotically low temperatures, both the relaxation rates display an activation-barrier like behavior, which is in contrast to a previous result [19].

In Chapter III, the zero-temperature magnon contributions to the longitudinal order-parameter susceptibility of both quantum ferromagnets and quantum antiferromagnets are calculated and compared, using some very general models that are insensitive to the origin of the magnetic ordering. Since the magnons are massless, one expects that they give rise to nonanalyticities in the long-wavelength/low-frequency dependence of transport coefficients and thermodynamic quantities. These nonanalyticities correspond to a power-law behavior of correlation functions in real-time/real-space. However, the ferromagnetic magnon contribution vanishes at $T = 0$, whereas the antiferromagnetic magnon contribution does not. Chapter III explains the reason and examines the robustness of this null result.

Chapter IV considers a particular class of ferromagnets known as itinerant ferromagnets and briefly introduces an effective field theory for these systems. This field-theoretical approach allows for a systematic identification and analysis of the soft modes in the system. Within the framework of this effective field theory, the spin-wave contributions to the longitudinal susceptibility, the dynamical electrical conductivity and the electronic density of states are calculated. The magnon contribution to the longitudinal susceptibility matches the result from Chapter III. The corresponding contribution to the conductivity is also found to vanish at $T = 0$ and differs from a previous result [20]. The reason for this discrepancy is a sign error in the original paper that led to an incorrect result. Chapter IV points out where exactly this error occured and gives the correct result for the conductivity.

Chapters II and III contain previously published material co-authored with D. Belitz and T. R. Kirkpatrick. Chapter IV contains unpublished material co-authored with D. Belitz and T. R. Kirkpatrick.

CHAPTER II

SPIN-WAVE CONTRIBUTION TO THE ELECTRONIC RELAXATION RATES IN METALLIC FERROMAGNETS

This work was published in volume 89 of the journal *Physical Review B* in April 2014. Dietrich Belitz and Theodore R. Kirkpatrick were the principal investigators for this work; Sripoorna Bharadwaj performed the calculations and produced the figures in this chapter.

Motivation

In a metallic system, the electronic relaxation rates contain important information about the various excitations. The single-particle relaxation rate $1/\tau$ corresponds to the lifetime of the electrons and also determines the thermal conductivity $\kappa = v_{\mathrm{F}}^2 c_V \tau/3$. The transport relaxation rate $1/\tau_{\mathrm{tr}}$ determines the Drude electrical conductivity, $\sigma = n_e e^2 \tau_{\mathrm{tr}}/m_{\mathrm{e}}$. In this dissertation, we alternate between referring to the electrical conductivity and its reciprocal, the electrical resistivity (which is directly proportional to the transport relaxation rate). Here, and in what follows, m_{e} and n_e are the conduction electron effective mass and number density, respectively, v_{F} is the Fermi velocity and c_V is the specific heat. The different excitations present in the system contribute to these relaxation rates. The excitations can be propagating or particle-like − for example, longitudinal phonons. Coupling of these phonons with the conduction electrons leads to the famous T^5 Bloch behavior of the electrical resistivity and T^3 behavior of the thermal conductivity [21]. If the system has some form of magnetic order, the coupling of the conduction

electrons to the magnetic Goldstone modes contributes to the relaxation rates. In isotropic Heisenberg ferromagnets, the Goldstone modes are the "ferromagnons" or "spin waves". Ueda and Moriya found that the ferromagnons contribute a T^2 term to the transport relaxation rate [19, 22, 23, 24]. In helimagnets [7, 25], which have a helically modulated magnetic ordering, the corresponding Goldstone mode − the "helimagnon", leads to a $T^{5/2}$ contribution to the electrical resistivity at low temperatures [26, 27, 28]. In antiferromagnets, the corresponding contribution is proportional to T^3 [29]. It should be noted that the aforementioned results are dimensionality-dependent and in particular, hold only for three dimensional systems − the only physical dimension in which magnetic order exists for $T > 0$ [30]. In a generic dimension $d > 2$, the ferromagnons, which have the frequency-momentum relation $\omega \sim k^2$, are expected to contribute a $T^{(d+1)/2}$ term to the resistivity.

There are also the dissipative excitations: excitations with a continuous spectrum. An example of such excitations contributing to transport coefficients is the well known Fermi liquid T^2 behavior of both the single-particle and transport relaxation rates due to the Coulomb interaction between the electrons in a metal. In metallic ferromagnets, in addition to the propagating spin waves, there are longitudinal magnetization fluctuations and "Stoner excitations" in the transverse channel, which are opposite spin electron-hole excitations [24]. These excitations are dissipative and non-hydrodynamic in nature, and are also found to contribute a T^2 behavior to the resistivity, with a prefactor inversely proportional to the magnetization [19].

The primary topic of discussion in this chapter is the ferromagnon contribution to the electronic relaxation rates in ferromagnets. As mentioned previously, Ueda and Moriya found that at low temperatures, the ferromagnons contribute a T^2 term to the

electrical resistivity. A problem with this established result was first noted in context of helimagnets [31]. It turns out that if the T^2 behavior is valid at asymptotically low temperatures, then the helimagnetic and ferromagnetic cases are not mutually consistent. To elaborate, when the ferromagnetic limit of the helimagnetic result was taken by letting the wavelength of the helically modulated spin-ordering go to infinity, the leading contribution to the resistivity, which yields a power law, vanishes. What remains in the ferromagnetic limit is an exponential behavior of the form

$$1/\tau_{\rm tr} \propto (T^2/\lambda) \exp(-T_0/T), \tag{2.1}$$

where the temperature scale T_0 is related to the conduction band splitting or "Stoner gap" λ, which in turn is directly proportional to the magnetization, and the Fermi energy $\epsilon_{\rm F}$. This result is particularly noteworthy, given that the leading magnetic Goldstone mode contribution to the relaxation rates in both helimagnets and antiferromagnets are power laws. Understanding the difference between the scattering of electrons with ferromagnons and other magnetic Goldstone modes is important. Additionally, the electrical resistivity is a basic physical property that can be easily measured and is very useful, for example, in tracking and identifying magnetic phase transitions. Therefore, correctly establishing its true low temperature behavior in the ferromagnetic phase is crucial.

In the following, the ferromagnon contribution to the single-particle and transport relaxation rate in a metallic ferromagnets is calculated and it will be shown that it is indeed an exponential behavior of the form shown in Eq. (2.1). We also recover the Ueda-Moriya T^2 result, albeit only in a sizable preasymptotic temperature window. The reason for the exponential "activation-barrier"-like behavior is the fact

that, in a ferromagnet, the Goldstone modes are purely transverse and therefore only couple to electrons in different Stoner bands. In other words, the effective electron-electron interaction, mediated by ferromagnon exchange, is a purely inter-Stoner-band scattering, hence leading to an activated process. This is in contrast with helimagnets and antiferromagnets, wherein the effective electron-electron interaction has an intra-Stoner-band coupling term, which leads to a power law. This coupling vanishes in the ferromagnetic limit as the characteristic wavenumber of the magnetic order goes to zero. These results are valid for all metallic ferromagnets, irrespective of the origin of magnetism. The magnetism could be caused by the conduction electrons themselves, such systems are referred to as "itinerant ferromagnets", or by localized electrons in a different band, referred to as "localized-moment ferromagnets". The model considered for the necessary calculations is very general and only relies on basic symmetry arguments.

Model: Magnon-mediated Electron-electron Interaction

Effective Action

We start with an action $S_0[\bar{\psi}, \psi]$ for the conduction electrons in terms of the fermionic spinor fields $\bar{\psi} = (\bar{\psi}_\uparrow, \bar{\psi}_\downarrow)$ and $\psi = (\psi_\uparrow, \psi_\downarrow)$. The suffixes $(\uparrow, \downarrow) \equiv (+, -) = \sigma$ are the spin projection indices of the fermions. In terms of $\bar{\psi}$ and ψ, the electronic spin density is expressed as

$$\boldsymbol{n}_s(x) = \sum_{\sigma,\sigma'} \bar{\psi}_\sigma(x) \boldsymbol{\sigma}_{\sigma,\sigma'} \psi_{\sigma'}(x), \tag{2.2}$$

with $\boldsymbol{\sigma} = (\sigma_1, \sigma_2, \sigma_3)$ the Pauli matrices and $x = (\boldsymbol{x}, \tau)$ corresponding to the real-space position $\boldsymbol{x}$ and the imaginary-time variable τ. We now assume that the conduction

electrons are subjected to a magnetization $\boldsymbol{M}(x)$, whose origin is not relevant for the following calculations. This magnetization will act as an effective magnetic field that the conduction electrons couple to, via a Zeeman term. Then, the action is

$$S[\bar{\psi},\psi] = S_0[\bar{\psi},\psi] + \Gamma_t \int dx\, \boldsymbol{M}(x).\boldsymbol{n}_s(x). \tag{2.3}$$

Γ_t is a coupling constant, with the dimensions of energy times volume, or inverse density of states. The ferromagnet is assumed to order in the 3−direction. Therefore, $\langle M_i(x)\rangle = \delta_{i,3}m$, with m, the value of the spontaneous magnetization. Now, in Eq. (2.3), $\boldsymbol{M}$ is replaced by its average to obtain

$$S_\lambda[\bar{\psi},\psi] = S_0[\bar{\psi},\psi] + \lambda \int dx\, n_{s,3}(x), \tag{2.4a}$$

where $\lambda = \Gamma_t m$. Then, the partition function for the electrons is given by

$$Z_\lambda = \int D[\bar{\psi},\psi]\, e^{S_\lambda[\bar{\psi},\psi]}. \tag{2.4b}$$

We note that the Zeeman term splits the conduction band into two subbands, one for each spin projection. Henceforth, λ will be referred to as the Stoner gap. In Eq. (2.4a), the fluctuations of the magnetization were neglected, in a mean-field approximation. Considering the fluctuations of the magnetization $\delta\boldsymbol{M}$,

$$S[\bar{\psi},\psi] = S_\lambda[\bar{\psi},\psi] + \Gamma_t \int dx\, \delta\boldsymbol{M}(x).\boldsymbol{n}_s(x). \tag{2.5a}$$

Along with the additional term in above, we must include an action that describes the dynamics of $\delta\boldsymbol{M}$. This extra term in the action must correspond to the fluctuations

of the physical magnetization and therefore, must contain the ferromagnons. To Gaussian order, this term reads

$$S_{\text{fluct}}[\delta \boldsymbol{M}] = -\frac{1}{2}\int dx\, dy\, \delta M_{s,i}(x)\, \chi_{ij}^{-1}(x,y)\, \delta M_{s,j}(y), \tag{2.5b}$$

where $\chi_{ij}(x,y)$ is the physical magnetic susceptibility. In the ordered phase of a ferromagnet, the transverse components of χ_{ij}, which in this case are $i,j=1,2$ with the assumed choice of the magnetization direction, correspond to the ferromagnons, the Goldstone modes of the ordered phase. Therefore, these components of χ_{ij} must be singular in the limit of small frequencies and wave numbers. By adding Eqs. (2.5a) and (2.5b) and integrating out the fluctuations $\delta \boldsymbol{M}$ using a Gaussian integral, an effective action purely in terms of the electronic fields is obtained.

$$S_{\text{eff}}[\bar{\psi},\psi] = S_{\lambda}[\bar{\psi},\psi] + S_{\text{ex}}[\bar{\psi},\psi], \tag{2.6a}$$

where

$$S_{\text{ex}}[\bar{\psi},\psi] = \frac{\Gamma_t^2}{2}\int dx\, dy\, \delta n_{s,i}(x)\, \chi_{ij}(x,y)\, \delta n_{s,j}(y) \tag{2.6b}$$

describes the effective electron-electron interaction mediated by magnetization fluctuations. If only the transverse components ($i,j=1,2$) of χ_{ij} are considered, then S_{ex} corresponds to a ferromagnon-mediated effective electron-electron interaction.

To proceed with the calculations, we specify S_0 and χ_{ij}. In general, S_0 describes interacting conduction-band electrons. However, for the purpose of evaluating the ferromagnon-exchange contribution to the relaxation rates, the electron-electron interactions that do not involve any ferromagnon exchange are of no qualitative

importance and are neglected. Therefore, we work with an action S_0 that corresponds to non-interacting electrons in a band.

In Fourier space,

$$S_0[\bar{\psi}, \psi] = \sum_k \sum_\sigma \left[i\omega_n - \xi_{\boldsymbol{k}} \right] \bar{\psi}_\sigma(k)\, \psi_\sigma(k), \tag{2.7a}$$

where $k \equiv (\boldsymbol{k}, i\omega_n)$, $\omega_n = 2\pi T(n + 1/2), n \in \mathbb{Z}$. $\boldsymbol{k}$ is the Fourier space momentum and ω_n is a fermionic Matsubara frequency. $\xi_{\boldsymbol{k}} = \epsilon_{\boldsymbol{k}} - \mu$, where μ is the chemical potential and $\epsilon_{\boldsymbol{k}}$ is the energy-momentum relation for the electrons in the band under consideration. Then, S_λ

$$S_\lambda[\bar{\psi}, \psi] = \sum_k \sum_\sigma \left[i\omega_n - \omega_\sigma(\boldsymbol{k}) \right] \bar{\psi}_\sigma(k)\, \psi_\sigma(k) \tag{2.7b}$$

with

$$\omega_\pm(\boldsymbol{k}) = \xi_{\boldsymbol{k}} \mp \lambda. \tag{2.7c}$$

We see that the Zeeman coupling of the conduction electrons to the average magnetization splits the conduction band into two Stoner bands for the two spin projections as shown in Fig. 4, with their Fermi surfaces given by the equation,

$$\omega_\sigma(\boldsymbol{p}) \Big|_{\boldsymbol{p} \in \mathrm{FS}_\sigma} = 0. \tag{2.8}$$

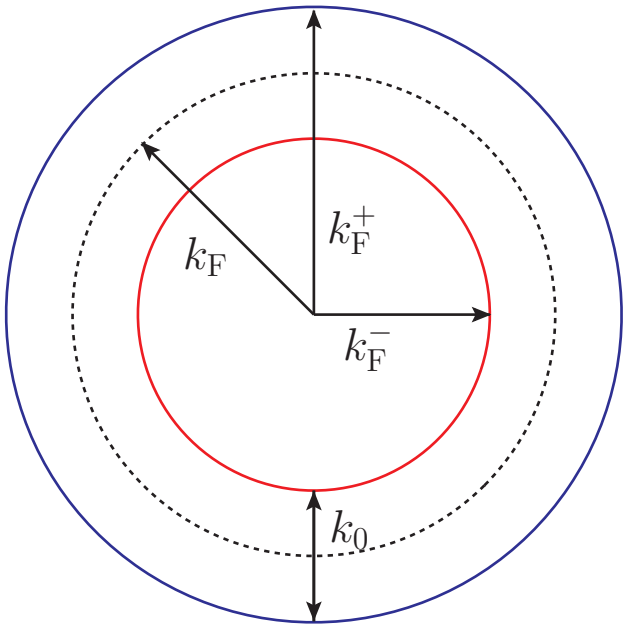

FIGURE 4. Splitting of the conduction band Fermi surface. Here, $k_0 = k_{\mathrm{F}}^{+} - k_{\mathrm{F}}^{-}$. The blue and red Fermi surfaces represent the up-spin and down-spin electrons, respectively.

For future reference, we define at the $\sigma-$ Fermi surface, the density of states N_{F}^{σ} and the corresponding Fermi wave number k_{F}^{σ}. In a parabolic band, where $\epsilon_{\boldsymbol{k}} = \boldsymbol{k}^2/2m_{\mathrm{e}}$,

$$k_{\mathrm{F}}^{\pm} = k_{\mathrm{F}}\sqrt{1 \pm \lambda/\epsilon_{\mathrm{F}}}, \qquad\qquad N_{\mathrm{F}}^{\pm} = k_{\mathrm{F}}^{\pm} m_{\mathrm{e}}/2\pi^2. \tag{2.9}$$

The Green functions for the electrons in the two Stoner bands are

$$G_{\lambda,\sigma}(p) = \frac{1}{i\omega_n - \omega_\sigma(\boldsymbol{p})}. \tag{2.10}$$

In an isotropic ferromagnet where the crystal-field effects or spin-orbit coupling are neglected, the Goldstone modes accompanying the spontaneously broken symmetry in spin space, the ferromagnons, are purely massless.

A ferromagnon of momentum $\boldsymbol{k}$ has a resonance frequency given by the dispersion relation

$$\omega_0(\boldsymbol{k}) = D(\lambda)\boldsymbol{k}^2, \tag{2.11}$$

where $D(\lambda)$ is the spin-stiffness coefficient and vanishes as $\lambda \to 0$. It is given by a magnetic energy scale divided by a microscopic wave-number scale squared, on the order of the Fermi wave number. The transverse magnetic susceptibility can be written down in terms of simple poles that describe circularly polarized ferromagnons,

$$\chi_{\pm}(\boldsymbol{k}, i\Omega_m) = \frac{K(\lambda)}{(2N_{\mathrm{F}}\Gamma_t)^2}\frac{1}{\omega_0(\boldsymbol{k}) \pm i\Omega_m} \tag{2.12}$$

where $\Omega_m = 2\pi m T, m \in \mathbb{Z}$, a bosonic Matsubara frequency. The factor $K(\lambda)$ is dimensionally an inverse volume. The coefficients $K(\lambda)$ and $D(\lambda)$ both are model-dependent. However, the above expression has this particular form in any isotropic ferromagnet, irrespective of the origin of magnetism. In $k \equiv (\boldsymbol{k}, i\Omega_m)$ space, we write down the transverse susceptibility tensor $\chi_{\mathrm{T}}(k)$ in terms of $\chi_{\pm}(k)$ using the symmetry arguments: $\chi^{ii}_{\mathrm{T}}(k) = \chi^{ii}_{\mathrm{T}}(-k)$ and $\chi^{ij}_{\mathrm{T}}(k) = \chi^{ji}_{\mathrm{T}}(-k) = -\chi^{ij}_{\mathrm{T}}(-k)$.

$$\chi_{\mathrm{T}}(k) = \frac{1}{2}\begin{pmatrix} \chi_+(k) + \chi_-(k) & i[\chi_+(k) - \chi_-(k)] \\ -i[\chi_+(k) - \chi_-(k)] & \chi_+(k) + \chi_-(k) \end{pmatrix} \tag{2.13a}$$

which, for small $\boldsymbol{k}$ and Ω_m, reads as

$$\chi_{\mathrm{T}}(k) = \frac{K(\lambda)}{(2N_{\mathrm{F}}\Gamma_t)^2}\frac{1}{\omega_0(\boldsymbol{k})^2 - (i\Omega_m)^2}\begin{pmatrix} D(\lambda)\boldsymbol{k}^2 & -i(i\Omega_m) \\ i(i\Omega_m) & D(\lambda)\boldsymbol{k}^2 \end{pmatrix}. \tag{2.13b}$$

Using Eq. (2.13a), the magnon exchange interaction, Eq. (2.6b), is now

$$S_{\rm ex}[\bar{\psi},\psi] = \frac{1}{2}\sum_{\sigma,\sigma'}\int_k \delta n_{\sigma\sigma'}(k)\mathcal{V}_{\sigma'\sigma}(k)\delta n_{\sigma'\sigma}(-k), \tag{2.14a}$$

where $\int_k \equiv (1/V)\sum_{\boldsymbol{k}} T\sum_{i\Omega_m}$, and the effective potential $\mathcal{V}$ is

$$\mathcal{V}_{\sigma'\sigma}(k) = V_{\sigma'\sigma}(k) + V_{\sigma\sigma'}(-k), \qquad V_{\sigma\sigma'}(k) = (1-\delta_{\sigma\sigma'})\,\Gamma_t^2\,\chi_{\sigma'}(k). \tag{2.14b}$$

Diagrammatically, this is shown in Fig. 5.

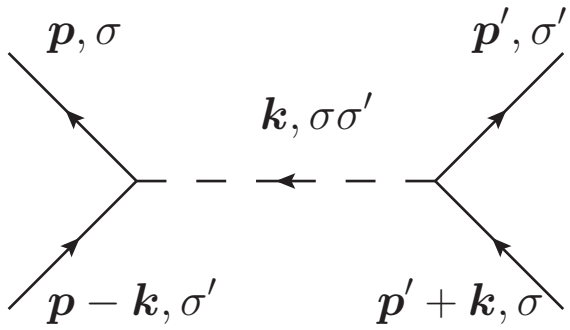

FIGURE 5. Effective electron-electron interaction mediated via magnon exchange. The dashed line represents the effective potential $\mathcal{V}_{\sigma\sigma'}(k)$

From Fig. 5, we notice that the ferromagnons couple only electrons with opposite spin projections. Therefore, a ferromagnon-exchange mediated effective electron-electron scattering is a purely inter-Stoner-band scattering process. This is the crucial point that is in contrast to the helimagnetic case, where the effective electron-electron interaction has an intra-Stoner-band scattering contribution and comes with a prefactor that is proportional to the square of the helical pitch wave number [26].

Stoner Model for Itinerant Ferromagnetism

In the previous discussion, a conduction band of electrons subject to a non-zero magnetization of unspecified origin was considered. Now, we examine the case of itinerant ferromagnetism, where the conduction electrons themselves are responsible for the magnetism. Using the formalism introduced in the preceding discussion, we have the fermionic action

$$S[\bar{\psi},\psi] = S_0[\bar{\psi},\psi] + \frac{\Gamma_t}{2}\int dx\, \boldsymbol{n}_s(x).\boldsymbol{n}_s(x) \tag{2.15}$$

where the second term now represents the spin-triplet interaction between the conduction electrons, which is known to be responsible for magnetism. Γ_t is the spin-triplet interaction amplitude. S_0 is the same as the one defined in Eq. (2.7a). Again, all other electronic interactions that do not contribute to magnetism, have been neglected as they will not qualitatively affect the forthcoming results. In the ordered state of an itinerant ferromagnet, $\langle n_{s,i}\rangle = \delta_{i3}\lambda/\Gamma_t$, assuming the system orders along the $3-$ direction. A simple mean-field approximation can be made by replacing one of the spin density fields in the second term of Eq. (2.15) by its expectation value. Concretely,

$$\boldsymbol{n}_s^2 \approx 2\langle \boldsymbol{n}_s\rangle.\boldsymbol{n}_s - \langle \boldsymbol{n}_s\rangle^2. \tag{2.16}$$

Upto an irrelevant constant term, we have

$$S_\lambda[\bar{\psi},\psi] = S_0[\bar{\psi},\psi] + \lambda\int dx\, n_{s,3}(x). \tag{2.17}$$

The mean-field approximation used to obtain S_λ assumed $\langle n_{s,i}\rangle = \delta_{i3}\lambda/\Gamma_t$. To ensure that this approximation is self consistent, we require the following:

$$\begin{aligned}\lambda = \Gamma_t \langle n_{s,3}(x)\rangle_\lambda &\equiv \frac{\Gamma_t}{Z_\lambda}\int D[\bar{\psi},\psi]\, n_{s,3}(x)\, e^{S_\lambda[\bar{\psi},\psi]} \\ &= \Gamma_t \frac{d}{d\lambda}\ln Z_\lambda. \end{aligned} \tag{2.18}$$

Note that the average $\langle \ldots \rangle_\lambda$ implies that the average is determined by S_λ itself, as stipulated by the usual self-consistent mean-field requirement. As before, a parabolic band is assumed and the non-interaction Green function corresponding to S_0 given by

$$G_0(\boldsymbol{k}, i\omega_n) = \frac{1}{i\omega_n - \xi_{\boldsymbol{k}}} \tag{2.19}$$

with the same $\xi_{\boldsymbol{k}}$ defined previously. Eq. (2.18) then becomes

$$1 = -2\Gamma_t \int_p \frac{1}{G_0^{-2}(p) - \lambda^2}. \tag{2.20}$$

The condition for a nonzero solution for λ, which implies a nonzero magnetization, is $2N_{\mathrm{F}}\Gamma_t > 1$. This condition is the famous Stoner criterion for itinerant ferromagnetism [4]. Explicitly, after performing the integral in above, we find

$$\lambda = 2N_{\mathrm{F}}\Gamma_t \frac{\epsilon_{\mathrm{F}}}{3}\left[(1+\lambda/\epsilon_{\mathrm{F}})^{3/2} - (1-\lambda/\epsilon_{\mathrm{F}})^{3/2}\right]. \tag{2.21}$$

The action S_λ does not contain any ferromagnetic fluctuations. However, it is useful for calculating the effective action. We designate S_λ as the "reference ensemble". The spin susceptibility of the reference ensemble is defined as

$$\chi_{\lambda,ij}(x,y) = \langle \delta n_{s,i}(x)\delta n_{s,j}(y)\rangle_{S_\lambda}. \tag{2.22}$$

In terms of the reference-ensemble Green function

$$G_\lambda(k) = \frac{G_0^{-1}(k)}{G_0^{-2}(k) - \lambda^2}\,\sigma_0 - \frac{\lambda}{G_0^{-2}(k) - \lambda^2}\,\sigma_3, \tag{2.23}$$

χ_λ is

$$\chi_{\lambda,ij}(x,y) = -\mathrm{tr}\,[\sigma_i\, G_\lambda(x,y)\,\sigma_j\, G_\lambda(y,x)]. \tag{2.24}$$

The trace is performed over the spin degrees of freedom. Upon tracing and performing a Fourier transform, we find

$$\chi_{\lambda,ij}(k) = \begin{pmatrix} f_1(k) & f_2(k) & 0 \\ -f_2(k) & f_1(k) & 0 \\ 0 & 0 & f_3(k) \end{pmatrix} \tag{2.25}$$

where

$$f_1(k) = -2\int_p \frac{G_0^{-1}(p)\,G_0^{-1}(p-k) - \lambda^2}{[G_0^{-2}(p) - \lambda^2][G_0^{-2}(p-k) - \lambda^2]}, \tag{2.26a}$$

$$f_2(k) = -2i\lambda\int_p \frac{G_0^{-1}(p) - G_0^{-1}(p-k)}{[G_0^{-2}(p) - \lambda^2][G_0^{-2}(p-k) - \lambda^2]}, \tag{2.26b}$$

$$f_3(k) = -2\int_p \frac{G_0^{-1}(p)\,G_0^{-1}(p-k) + \lambda^2}{[G_0^{-2}(p) - \lambda^2][G_0^{-2}(p-k) - \lambda^2]}. \tag{2.26c}$$

It is useful to note that

$$f_1(k=0) = 1/\Gamma_t, \qquad\qquad f_2(k=0) = 0. \tag{2.27}$$

The first equality follows from Eq. (2.20).

It should be noted that the reference ensemble does not have the magnons that are the Goldstone modes of the the spontaneously broken symmetry in the ordered

phase. We require a theory of fluctuations, like S_{fluct} in the previous discussion, that is consistent with the treatment of the static magnetization to describe the magnons. However, having obtained the reference-ensemble spin susceptibility, a Gaussian action for the magnetization fluctuations, which in this case are $\delta \boldsymbol{n}_s(x)$, can be written down in terms of χ_λ.

$$\mathcal{A}_{\lambda,\text{fluct}}[\delta \boldsymbol{n}_s(x)] = -\frac{1}{2} \int dx\, dy\, \delta n_{s,i}(x)\, \chi^{-1}_{\lambda,ij}(x,y)\, \delta n_{s,j}(y) \tag{2.28a}$$

such that,

$$\chi_{\lambda,ij}(x,y) = \int D[\delta \boldsymbol{n}_s]\, \delta n_{s,i}(x)\, \delta n_{s,j}(y)\, e^{-\mathcal{A}_{\lambda,\text{fluct}}[\delta \boldsymbol{n}_s]}. \tag{2.28b}$$

There is another term that is quadratic in $\delta \boldsymbol{n}_s$, that has not been considered until now. This term comes from the original spin-triplet interaction term in Eq. (2.15). Adding this term to Eq. (2.28b), the complete Gaussian fluctuation action is

$$\mathcal{A}_{\text{fluct}}[\delta \boldsymbol{n}_s(x)] = -\frac{1}{2} \int dx\, dy\, \delta n_{s,i}(x)\, \chi^{-1}_{ij}(x,y)\, \delta n_{s,j}(y), \tag{2.29a}$$

where χ is now the physical spin susceptibility, which is related to the reference ensemble spin susceptibility χ_λ by

$$\chi^{-1}_{ij}(x,y) = \chi^{-1}_{\lambda,ij}(x,y) - \delta_{ij}\, \delta(x-y)\, \Gamma_t. \tag{2.29b}$$

$\mathcal{A}_{\text{fluct}}[\delta \boldsymbol{n}_s]$ is a specific case of the general $S_{\text{fluct}}[\delta \boldsymbol{M}]$ that was written down in Eq. (2.5b).

Considering only the transverse (T) components$(i,j=1,2)$ of χ_{ij}, in $k\equiv(\boldsymbol{k},i\Omega_m)$ space,

$$\chi_{\mathrm{T}}^{-1}(\boldsymbol{k},i\omega_m)=\begin{pmatrix} f_1(\boldsymbol{k},i\Omega_m)/N(\boldsymbol{k},i\Omega_m)-\Gamma_t & -f_2(\boldsymbol{k},i\Omega_m)/N(\boldsymbol{k},i\Omega_m) \\ f_2(\boldsymbol{k},i\Omega_m)/N(\boldsymbol{k},i\Omega_m) & f_1(\boldsymbol{k},i\Omega_m)/N(\boldsymbol{k},i\Omega_m)-\Gamma_t \end{pmatrix} \tag{2.30a}$$

with

$$N(\boldsymbol{k},i\Omega_m)=[f_1(\boldsymbol{k},i\Omega_m)]^2+[f_2(\boldsymbol{k},i\Omega_m)]^2. \tag{2.30b}$$

From Eq. (2.27), it is clear that, at zero frequency and wave number, χ_{T}^{-1} has two zero eigenvalues. After performing the integrals in Eq. (2.26) using standard Matsubara frequency summation techniques, and keeping terms up to linear order in $i\Omega_m$ and second order in $\boldsymbol{k}$, Eq. (2.30a) is

$$\chi_{\mathrm{T}}^{-1}(\boldsymbol{k},i\Omega_m)=\frac{(2N_{\mathrm{F}}\Gamma_t)^2}{2N_{\mathrm{F}}}\begin{pmatrix} \hat{\boldsymbol{k}}^2 f_{\boldsymbol{k}}(\lambda)/3 & 2i(i\hat{\Omega}_m)f_\Omega(\lambda)\epsilon_{\mathrm{F}}/\lambda \\ -2i(i\hat{\Omega}_m)f_\Omega(\lambda)\epsilon_{\mathrm{F}}/\lambda & \hat{\boldsymbol{k}}^2 f_{\boldsymbol{k}}(\lambda)/3 \end{pmatrix}, \tag{2.31a}$$

with the normalized frequency-momentum $\hat{\boldsymbol{k}}=\boldsymbol{k}/2k_{\mathrm{F}}$ and $\hat{\Omega}_m=\Omega_m/4\epsilon_{\mathrm{F}}$. The functions $f_{\boldsymbol{k}}(\lambda)$ and $f_\Omega(\lambda)$ are

$$f_{\boldsymbol{k}}(\lambda) = -\frac{4\epsilon_{\mathrm{F}}^3}{5\lambda^3}\left[\left(1-\frac{3\lambda}{2\epsilon_{\mathrm{F}}}\right)\left(1+\frac{\lambda}{\epsilon_{\mathrm{F}}}\right)^{3/2}-\left(1+\frac{3\lambda}{2\epsilon_{\mathrm{F}}}\right)\left(1-\frac{\lambda}{\epsilon_{\mathrm{F}}}\right)^{3/2}\right], \tag{2.31b}$$

$$f_\Omega(\lambda) = \frac{\epsilon_{\mathrm{F}}}{3\lambda}\left[\left(1+\frac{\lambda}{\epsilon_{\mathrm{F}}}\right)^{3/2}-\left(1-\frac{\lambda}{\epsilon_{\mathrm{F}}}\right)^{3/2}\right]. \tag{2.31c}$$

Typically, the Stoner gap λ is small compared to the Fermi energy ϵ_{F}. Therefore, in the limit of weak ferromagnets, where $2N_{\mathrm{F}}\Gamma_t\approx 1$ and $\lambda/\epsilon_{\mathrm{F}}\ll 1$,

$$f_{\boldsymbol{k}}(\lambda\to 0)=f_\Omega(\lambda\to 0)=1+O(\lambda^2). \tag{2.32}$$

In this limit, after inverting χ_{T}^{-1} in Eq. (2.31a) and comparing it with the general transverse susceptibility written down in Eq. (2.13b), we find [24]

$$D(\lambda) = \frac{\lambda}{6k_{\mathrm{F}}^2}, \qquad\qquad K(\lambda) = 4N_{\mathrm{F}}\lambda. \tag{2.33}$$

It is useful to identify some relevant energy scales and their relation to experimentally observable quantities. The following quantities are defined for the simple case of one conduction band. One obvious fundamental magnetic energy scale is the Stoner gap, λ, which is also closely related to the exchange splitting $\delta E_{\mathrm{ex}} = 2\lambda$ [32]. The latter can be measured by photoemission experiments and can also be obtained from band structure calculations. Due to the fact that magnon-exchange between the conduction electrons is a purely inter-Stoner-band process, the smallest wave number that can be transferred by means of magnon-exchange is $k_0 = \delta E_{\mathrm{ex}}/v_{\mathrm{F}}$. Specifically, for a parabolic band, this corresponds to $k_0 = k_{\mathrm{F}}^{+} - k_{\mathrm{F}}^{-}$, as shown in Fig. 4. Therefore, the smallest energy that can be transferred by magnon exchange is

$$T_0 = Dk_0^2 \approx \frac{1}{4}Dk_{\mathrm{F}}^2\left(\frac{\delta E_{\mathrm{ex}}}{\epsilon_{\mathrm{F}}}\right)^2. \tag{2.34}$$

The largest momentum transfer is given by $k_1 = k_{\mathrm{F}}^{+} + k_{\mathrm{F}}^{-} \approx 2k_{\mathrm{F}}$. This corresponds to the energy scale,

$$T_1 = 4Dk_{\mathrm{F}}^2 \tag{2.35}$$

which is expected to be close to the exchange splitting. In Stoner theory, $T_1 = 2\lambda/3 = \delta E_{\mathrm{ex}}/3$. There is also the microscopic energy scale given by the Fermi energy, ϵ_{F}.

We thus have a hierarchy of energy scales, $T_0 \ll T_1 \ll \epsilon_{\mathrm{F}}$. Additionally, the ratio of energy scales T_0/T_1 is given in terms of the Stoner gap and the microscopic energy,

$$\frac{T_0}{T_1} \approx \frac{1}{4}\Big(\frac{\lambda}{\epsilon_{\mathrm{F}}}\Big)^2. \tag{2.36a}$$

In terms of electron number density, n_e and the magnetization m, the above relation becomes

$$\frac{T_0}{T_1} \approx \frac{1}{9}\Big(\frac{m}{n_e}\Big)^2. \tag{2.36b}$$

Single-particle Relaxation Rate

Having obtained the effective electronic action, the single-particle inelastic relaxation rate due to the exchange of magnons can now be calculated. The single-particle relaxation rate is directly related to the electronic self-energy Σ, which is defined such that the full Green function $\mathcal{G}$ of the electron, with the interactions taken into account, is given by a Dyson equation:

$$\mathcal{G}_\sigma^{-1}(p) = G_{\lambda,\sigma}^{-1}(p) - \Sigma_\sigma(p), \tag{2.37}$$

$G_{\lambda,\sigma}(p)$ is defined in Eq. (2.10).

To linear order in the effective potential, Eq. (2.14) gives two contributions to the spin-dependent self-energy Σ_σ, as shown in Fig. 6.

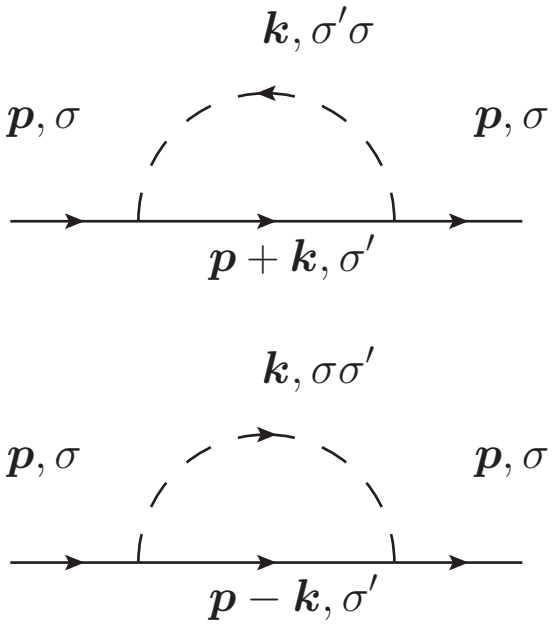

FIGURE 6. Self-energy contributions $\Sigma_\sigma(p)$ for the σ-spin Green function

Therefore, the self-energy Σ_σ can be calculated as

$$\begin{aligned} \Sigma_\sigma(p) &= \int_k \sum_{\sigma'} \mathcal{V}_{\sigma\sigma'}(k)\, G_{\lambda,\sigma'}(p+k) \\ &= 2\Gamma_t^2 \int_k \chi_\sigma(k)\, G_{\lambda,-\sigma}(p+k). \end{aligned} \tag{2.38}$$

The single-particle relaxation rate Γ for a quasiparticle with spin-σ, averaged over the σ-Fermi surface is related to the self-energy Σ_σ as

$$\Gamma_\sigma(\epsilon) = -\frac{1}{N_{\mathrm{F}}^\sigma V} \sum_{\boldsymbol{p}} \delta(\omega_\sigma(\boldsymbol{p}))\, \Sigma''(\boldsymbol{p}, \epsilon), \tag{2.39}$$

where $\Sigma''(\boldsymbol{p}, \epsilon) = \mathrm{Im}\, \Sigma(\boldsymbol{p}, i\omega_n \to \epsilon + i0)$ is the spectrum of the self-energy. The Matsubara frequency $i\omega_n$ has been analytically continued to a real frequency ϵ, following the standard procedure in finite temperature Quantum Field Theory

techniques. The factor $\delta(\omega_\sigma(\boldsymbol{p}))$ pins the momentum $\boldsymbol{p}$ to the σ-Fermi surface and the factor $1/(N_{\rm F}^\sigma V)$ is the appropriate normalization factor for the Fermi surface average.

Now, from Eq. (2.38),

$$\Sigma_\sigma(\boldsymbol{p}, i\omega_n) = \frac{T}{V}\sum_{\boldsymbol{k}}\sum_{i\Omega_m} \mathcal{V}_{\sigma\sigma'}(\boldsymbol{k}, i\Omega_m)\, G_{\lambda,\sigma'}(\boldsymbol{p}+\boldsymbol{k}, i\omega_n + i\Omega_m). \tag{2.40a}$$

We now use the spectral representations for the effective potential $\mathcal{V}$ and the Green function $G_{\lambda,\sigma}$,

$$\begin{aligned} \mathcal{V}_{\sigma\sigma'}(\boldsymbol{k}, i\Omega_m) &= \int_{-\infty}^{\infty} \frac{du}{2\pi}\, \frac{\mathcal{V}''_{\sigma\sigma'}(\boldsymbol{k}, u)}{i\Omega_m - u}, \\ \mathcal{V}''_{\sigma\sigma'}(\boldsymbol{k}, u) &= -2\,\mathrm{Im}\,\mathcal{V}_{\sigma\sigma'}(\boldsymbol{k}, i\Omega_m \to u + i0). \end{aligned} \tag{2.40b}$$

where $\bar{\mathcal{V}}''$ is the spectrum of the effective potential, and

$$\begin{aligned} G_{\lambda,\sigma'}(\boldsymbol{k}, i\omega_n) &= \int_{-\infty}^{\infty} \frac{dv}{2\pi}\, \frac{A''_{\sigma'}(\boldsymbol{k}, v)}{i\omega_n - v}, \\ A''_{\sigma'}(\boldsymbol{k}, v) &= -2\,\mathrm{Im}\, G_{\lambda,\sigma'}(\boldsymbol{k}, i\omega_n \to v + i0) = 2\pi\,\delta[v - \omega_{\sigma'}(\boldsymbol{k})] \end{aligned} \tag{2.40c}$$

where, $A''_{\sigma'}$ is the spectrum of the Green function $G_{\lambda,\sigma'}$. Then,

$$\Sigma_\sigma(\boldsymbol{p}, i\omega_n) = \frac{T}{V}\sum_{\boldsymbol{k}}\sum_{i\Omega_m} \int_{-\infty}^{\infty} du \int_{-\infty}^{\infty} dv\, \frac{\mathcal{V}''_{\sigma\sigma'}(\boldsymbol{k}, u)}{i\Omega_m - u}\, \frac{A''_{\sigma'}(\boldsymbol{p}+\boldsymbol{k}, v)}{i\omega_n + i\Omega_m - v}. \tag{2.40d}$$

Using the Matsubara summation identity,

$$-T\sum_{i\Omega_m} \frac{1}{i\Omega_m - u}\, \frac{1}{i\omega_n + i\Omega_m - v} = \frac{n_B(u) + n_F(v)}{i\omega_n + u - v} \tag{2.40e}$$

$$\Sigma_\sigma(\boldsymbol{p}, i\omega_n) = -\frac{1}{V}\sum_{\boldsymbol{k}} \int_{-\infty}^{\infty} \frac{du}{2\pi} \int_{-\infty}^{\infty} dv\, [n_B(u) + n_F(v)]\, \frac{\mathcal{V}''_{\sigma\sigma'}(\boldsymbol{k}, u)\, \delta[v - \omega_{\sigma'}(\boldsymbol{p}+\boldsymbol{k})]}{i\omega_n + u - v}. \tag{2.40f}$$

Then, Eq. (2.39) yields

$$\begin{aligned} \Gamma_\sigma(\epsilon) &= N_{\rm F}^{-\sigma} \int du\, [n_B(u) + n_F(u+\epsilon)] \sum_{\sigma'} \bar{\mathcal{V}}''_{\sigma\sigma'}(u) \\ &= 2\Gamma_t^2 N_{\rm F}^{-\sigma} \int_{-\infty}^{\infty} du\, [n_B(u) + n_F(u+\epsilon)]\, \bar{\chi}''_\sigma(u), \end{aligned} \tag{2.41a}$$

where $n_B(u) = 1/(e^{u/T} - 1)$ and $n_F(u) = 1/(e^{u/T} + 1)$ are the Bose and Fermi distribution functions respectively, and

$$\bar{\mathcal{V}}''_{\sigma\sigma'}(u) = \frac{1}{N_{\rm F}^{\sigma} N_{\rm F}^{\sigma'} V^2} \sum_{\boldsymbol{k},\boldsymbol{p}} \delta[\omega_\sigma(\boldsymbol{k})]\, \delta[\omega_{\sigma'}(\boldsymbol{p})]\, \mathcal{V}''_{\sigma\sigma'}(\boldsymbol{k}-\boldsymbol{p}, u). \tag{2.41b}$$

Similarly,

$$\bar{\chi}''_\sigma(u) = \frac{1}{N_{\rm F}^{\sigma} N_{\rm F}^{\sigma'} V^2} \sum_{\boldsymbol{k},\boldsymbol{p}} \delta[\omega_\sigma(\boldsymbol{k})]\, \delta[\omega_{\sigma'}(\boldsymbol{p})]\, \chi''_\sigma(\boldsymbol{k}-\boldsymbol{p}, u). \tag{2.41c}$$

Recalling Eq. (2.12), we have

$$\chi''_\pm(\boldsymbol{k}, u) = \frac{\mp K(\lambda)\pi}{(2N_{\rm F}\Gamma_t)^2}\, \delta[\omega_0(\boldsymbol{k}) \mp u]. \tag{2.41d}$$

It is useful to note that the single-particle relaxation rates, Γ_σ, have the symmetry relation

$$N_{\rm F}^{+}\, \Gamma_+(\epsilon) = N_{\rm F}^{-}\, \Gamma_-(-\epsilon). \tag{2.41e}$$

Because the wave vectors $\boldsymbol{k}$ and $\boldsymbol{p}$ are pinned to different Fermi surfaces, a consequence of pure inter-Stoner-band scattering contribution to the self energy, the spectrum

$\bar{\chi}''_\sigma(u)$ is nonzero only in a range of frequencies, $T_0 \leq |u| \leq T_1$. On the energy shell $\epsilon = 0$, the relaxation rate on the σ-Fermi surface is

$$\begin{aligned}\Gamma_\sigma(\epsilon=0) = \frac{1}{2\tau_\sigma} &= \frac{\pi K}{2N_{\rm F}^\sigma T_1}\, T \int_{T_0/T}^{T_1/T} \frac{dx}{\sinh(x)} \\ &= \frac{\pi K}{N_{\rm F}^\sigma T_1} \begin{cases} T e^{-T_0/T} & \text{if } T \ll T_0 \\ \frac{1}{2} T \ln(T/T_0) & \text{if } T_0 \ll T \ll T_1 \\ \frac{1}{2} T \ln(T_1/T_0) & \text{if } T \gg T_1 \end{cases}. \end{aligned} \tag{2.42}$$

Therefore, the ferromagnon contribution to the thermal resistivity $\rho_{\rm th} = 1/\kappa$ is

$$\rho_{\rm th} = \frac{6}{v_{\rm F}^2 c_V} \frac{\pi K}{N_{\rm F} T_1} \begin{cases} T e^{-T_0/T} & \text{if} \quad T \ll T_0 \\ \frac{1}{2} T \ln(T/T_0) & \text{if} \quad T_0 \ll T \ll T_1 \\ \frac{1}{2} T \ln(T_1/T_0) & \text{if} \quad T \gg T_1 \end{cases}. \tag{2.43}$$

Transport Relaxation Rate

In the following, the transport relaxation rate, which determines the electrical resistivity, or equivalently the electrical conductivity is calculated. Consider the Kubo formula for the electrical conductivity tensor [33],

$$\sigma_{ij}(i\Omega) = \frac{i}{i\Omega} \left[\pi_{ij}(i\Omega) - \pi_{ij}(i\Omega = 0)\right] \tag{2.44a}$$

where

$$\pi_{ij}(i\Omega) = -e^2\, T \sum_{n_1, n_2} \frac{1}{V} \sum_{\boldsymbol{k},\boldsymbol{p}} v_i(\boldsymbol{k})\, v_j(\boldsymbol{p})\, \langle \bar{\psi}_{n_1,\sigma}(\boldsymbol{k})\, \psi_{n_1+n,\sigma}(\boldsymbol{k})\, \bar{\psi}_{n_2,\sigma'}(\boldsymbol{p})\, \psi_{n_2-n,\sigma'}(\boldsymbol{p}) \rangle. \tag{2.44b}$$

π_{ij} is the current-current polarization function. This correlation function describes the linear response of the system to an applied electric field. Here, $\boldsymbol{v}(\boldsymbol{k}) = \partial\epsilon_{\boldsymbol{k}}/\partial\boldsymbol{k}$. Assuming a parabolic band, $\boldsymbol{v}(\boldsymbol{k}) = \boldsymbol{k}/m_{\rm e}$. The average $\langle \ldots \rangle$ is to be calculated using the effective action in Eq. (2.6). In terms of the interacting Green function defined in Eq. (2.37), Eq. (2.44b) becomes

$$\pi_{ij}(i\Omega) = -i\, e^2\, T \sum_{i\omega} \frac{1}{V} \sum_{\boldsymbol{p},\sigma} \frac{p^i}{m_{\rm e}}\, \mathcal{G}_\sigma(\boldsymbol{p}, i\omega)\, \mathcal{G}_\sigma(\boldsymbol{p}, i\omega - i\Omega)\, \Gamma^j_\sigma(\boldsymbol{p}; i\omega, i\omega - i\Omega). \qquad (2.45)$$

where $\boldsymbol{\Gamma}$ is a vertex function. Diagrammatically, π_{ij} is represented by Fig. 7.

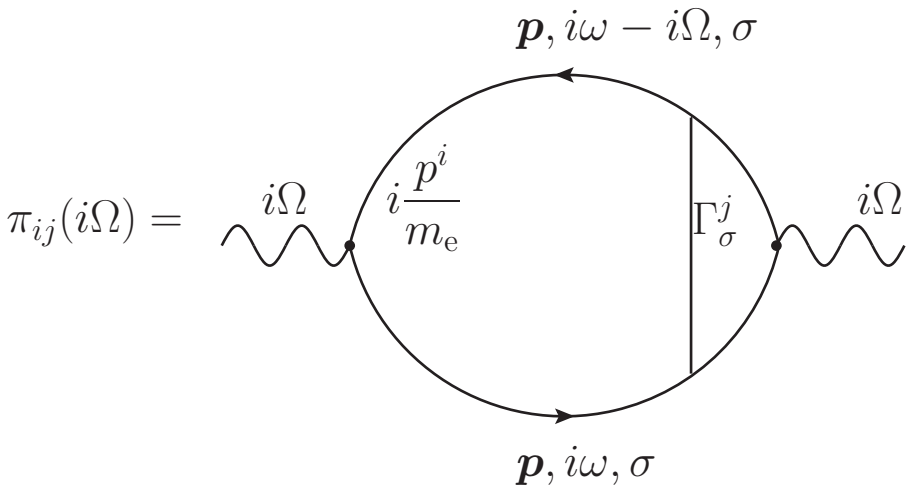

FIGURE 7. Diagrammatic representation of the current-current correlation function, which describes the linear response of the system to an applied external electric field

The vertex function $\boldsymbol{\Gamma}$ effectively gives more weight to large-angle scattering of electrons, as these processes contribute more to the transport relaxation rate. It is important that the interacting Green functions $\mathcal{G}$ which contain the self-energy Σ, are used. Also of importance is that the vertex $\boldsymbol{\Gamma}$ and the self-energy Σ are calculated in a mutually consistent way [34]. Thus, for the self-energy formula used in Eq.

(2.38) which is linear in the effective potential V, $\mathbf{\Gamma}$ is calculated using the ladder approximation,

$$\mathbf{\Gamma}_\sigma(\boldsymbol{p}; i\omega, i\omega - i\Omega) = i\frac{\boldsymbol{p}}{m_\mathrm{e}} + \frac{T}{V}\sum_{\boldsymbol{k},i\Omega'}\sum_{\sigma'}\mathcal{V}_{\sigma\sigma'}(\boldsymbol{k}-\boldsymbol{p}, i\Omega') \times \mathcal{G}_{\sigma'}(\boldsymbol{k}, i\omega + i\Omega')\,\mathcal{G}_{\sigma'}(\boldsymbol{k}, i\omega - i\Omega + i\Omega')\mathbf{\Gamma}_{\sigma'}(\boldsymbol{k}; i\omega + i\Omega', i\omega - i\Omega + i\Omega'). \tag{2.46}$$

The diagrammatic representation of Eq. (2.46) is given by Fig. 8.

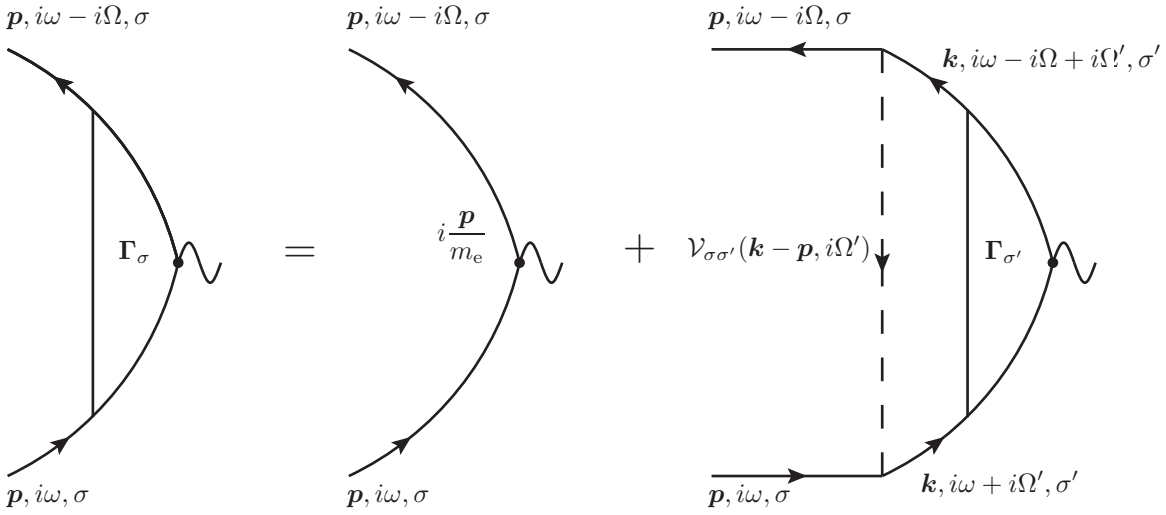

FIGURE 8. Ladder approximation for the vertex function $\mathbf{\Gamma}$

The vector vertex function $\mathbf{\Gamma}(\boldsymbol{p}; i\omega, i\omega - i\Omega)$ has to be parallel to $\boldsymbol{p}$. Therefore, using the ansatz $\mathbf{\Gamma}(\boldsymbol{p}; i\omega, i\omega - i\Omega) = i(\boldsymbol{p}/m_\mathrm{e})\gamma(\boldsymbol{p}; i\omega, i\omega - i\Omega)$, a scalar vertex function can be defined. Then Eq. (2.46) becomes

$$\gamma_\sigma(\boldsymbol{p}; i\omega, i\omega - i\Omega) = 1 + \frac{T}{V}\sum_{\boldsymbol{k},i\Omega'}\sum_{\sigma'}\frac{\boldsymbol{p}.\boldsymbol{k}}{\boldsymbol{p}^2}\,\mathcal{V}_{\sigma\sigma'}(\boldsymbol{k}-\boldsymbol{p}, i\Omega') \times \mathcal{G}_{\sigma'}(\boldsymbol{k}, i\omega + i\Omega')\,\mathcal{G}_{\sigma'}(\boldsymbol{k}, i\omega - i\Omega + i\Omega')\mathbf{\Gamma}_{\sigma'}(\boldsymbol{k}; i\omega + i\Omega', i\omega - i\Omega + i\Omega'). \tag{2.47}$$

The polarization and the conductivity tensors are diagonal. Therefore, Eq. (2.44b) becomes

$$\begin{aligned}\pi_{ij}(i\Omega) &= \delta_{ij}\, e^2\, T \sum_{i\omega} \frac{1}{V} \sum_{\boldsymbol{p},\sigma} \frac{\boldsymbol{p}^2}{m_{\rm e}^2}\, \mathcal{G}_\sigma(\boldsymbol{p}, i\omega)\, \mathcal{G}_\sigma(\boldsymbol{p}, i\omega - i\Omega)\, \gamma_\sigma(\boldsymbol{p}; i\omega, i\omega - i\Omega) \\ &= \delta_{ij}\, \frac{e^2}{m_{\rm e}^2}\, \frac{1}{V} \sum_{\boldsymbol{p},\sigma} \boldsymbol{p}^2\, S_\sigma(\boldsymbol{p}, i\Omega), \end{aligned} \tag{2.48a}$$

where

$$S_\sigma(\boldsymbol{p}, i\Omega) = T \sum_{i\omega} \mathcal{G}_\sigma(\boldsymbol{p}, i\omega)\, \mathcal{G}_\sigma(\boldsymbol{p}, i\omega - i\Omega)\, \gamma_\sigma(\boldsymbol{p}; i\omega, i\omega - i\Omega). \tag{2.48b}$$

To calculate the Matsubara frequency sum, the following contour integral is considered:

$$\begin{aligned} S_\sigma(\boldsymbol{p}, i\Omega) = -\int_{-\infty}^{\infty} \frac{d\varepsilon}{2\pi i}\, n_F(\varepsilon) \\ \times \Bigg\{ \mathcal{G}_\sigma(\boldsymbol{p}, \varepsilon + i\Omega) \Big[G^\sigma_{\rm ret}(\boldsymbol{p}, \varepsilon)\, \gamma_\sigma(\boldsymbol{p}, \varepsilon + i0, \varepsilon + i\Omega) - G^\sigma_{\rm adv}(\boldsymbol{p}, \varepsilon)\, \gamma_\sigma(\boldsymbol{p}, \varepsilon - i0, \varepsilon + i\Omega) \Big] \\ + \mathcal{G}_\sigma(\boldsymbol{p}, \varepsilon - i\Omega) \Big[G^\sigma_{\rm ret}(\boldsymbol{p}, \varepsilon)\, \gamma_\sigma(\boldsymbol{p}, \varepsilon - i\Omega, \varepsilon + i0) - G^\sigma_{\rm adv}(\boldsymbol{p}, \varepsilon)\, \gamma_\sigma(\boldsymbol{p}, \varepsilon - i\Omega, \varepsilon - i0) \Big] \Bigg\}. \end{aligned} \tag{2.48c}$$

Here, $G_{\rm ret}$ and $G_{\rm adv}$ are retarded and advanced Green functions, respectively. They are related to $\mathcal{G}$ by

$$G_{\rm ret}(\boldsymbol{p}, \varepsilon) = \mathcal{G}(\boldsymbol{p}, i\omega_n \to \varepsilon + i0), \qquad G_{\rm adv}(\boldsymbol{p}, \varepsilon) = \mathcal{G}(\boldsymbol{p}, i\omega_n \to \varepsilon - i0). \tag{2.48d}$$

From Eq. (2.44a), the dc conductivity is given by

$$\begin{aligned}\sigma &= \lim_{\Omega\to 0} \mathrm{Re}\,\sigma(i\Omega \to \Omega + i0) \\ &= \frac{e^2}{m_{\mathrm{e}}^2}\frac{1}{V}\sum_{\boldsymbol{p},\sigma}\boldsymbol{p}^2 \lim_{\Omega\to 0}\frac{\mathrm{Im}\left[S_\sigma(\boldsymbol{p}, i\Omega\to\Omega+i0) - S_\sigma(\boldsymbol{p}, i\Omega = 0)\right]}{\Omega}. \end{aligned} \tag{2.48e}$$

Eq. (2.48) yields

$$\sigma = \frac{e^2}{3\pi m_{\mathrm{e}}^2}\int_{-\infty}^{\infty} d\epsilon \Big[-\frac{\partial n_F(\epsilon)}{d\epsilon}\Big]\frac{1}{V}\sum_{\boldsymbol{p},\sigma}\boldsymbol{p}^2 \Big[|\mathcal{G}_\sigma(\boldsymbol{p},\epsilon+i0)|^2\,\gamma_\sigma(\boldsymbol{p};\epsilon+i0,\epsilon-i0) - \mathrm{Re}\Big[\mathcal{G}_\sigma(\boldsymbol{p},\epsilon+i0)\Big]^2\gamma_\sigma(\boldsymbol{p};\epsilon+i0,\epsilon+i0)\Big]$$

$$\sigma = \frac{e^2}{3\pi m_{\mathrm{e}}^2}\int_{-\infty}^{\infty} \frac{d\epsilon}{4T}\frac{1}{\cosh^2(\epsilon/2T)}\frac{1}{V}\sum_{\boldsymbol{p},\sigma}\boldsymbol{p}^2 \Big[|\mathcal{G}_\sigma(\boldsymbol{p},\epsilon+i0)|^2\,\gamma_\sigma(\boldsymbol{p};\epsilon+i0,\epsilon-i0) - \mathrm{Re}\Big[\mathcal{G}_\sigma(\boldsymbol{p},\epsilon+i0)\Big]^2\gamma_\sigma(\boldsymbol{p};\epsilon+i0,\epsilon+i0)\Big]. \tag{2.48f}$$

The momentum sum in the above expression is evaluated using the Abrikosov-Gorkov-Dzhyaloshinksii approximation, in which the radial part of the momentum integral is performed by means of a contour integral over the interval $\xi_{\boldsymbol{k}} \in (-\infty, \infty)$ [35]. The real part of the self-energy Σ_σ in $\mathcal{G}_\sigma$ only renormalizes the Fermi energy. The imaginary part of the self-energy, from which the single-particle relaxation rate was calculated in the previous section, vanishes at low temperatures, as can be seen from Eq. (2.42). Therefore, the AGD approximation can be carried out in the limit of vanishing self-energy. In this limit, the leading contribution to Eq. (2.48f) comes from the first term, where the frequency arguments of the two Green functions lie

on different sides of the real axis. Therefore, the second term in Eq. (2.48f) will be neglected. Then,

$$\sigma = \frac{e^2}{3\pi m_{\rm e}^2} \int_{-\infty}^{\infty} \frac{d\epsilon}{4T} \frac{1}{\cosh^2(\epsilon/2T)} \frac{1}{V} \sum_{\boldsymbol{p},\sigma} \boldsymbol{p}^2 \left|\mathcal{G}_\sigma(\boldsymbol{p}, \epsilon + i0)\right|^2 \gamma_\sigma(\boldsymbol{p}; \epsilon + i0, \epsilon - i0). \quad (2.48g)$$

In the aforementioned limit of a vanishing self-energy, the dominant contribution from the momentum integral comes from the momenta that obey $\omega_\sigma(\boldsymbol{p}) = \epsilon$. This is guaranteed by the pole of the Green function. Note that the energy ϵ scales as T. Therefore, for leading T dependence, all ϵ dependencies that do not appear as ϵ/T can be neglected. With these approximations, the conductivity is now given by

$$\sigma = \frac{e^2}{2m_{\rm e}} \int_{-\infty}^{\infty} \frac{d\epsilon}{4T} \frac{1}{\cosh^2(\epsilon/2T)} \sum_\sigma n_\sigma \frac{\Lambda_\sigma(\epsilon)}{\Gamma_\sigma(\epsilon)}, \quad (2.49a)$$

where n_σ is the density of σ-spin electrons. Γ_σ is the single-particle relaxation rate defined in Eq. (2.41). The quantity Λ_σ is defined as

$$\Lambda_\sigma(\epsilon) = \frac{1}{N_{\rm F}^\sigma V} \sum_{\boldsymbol{p}} \delta[\omega_\sigma(\boldsymbol{p})] \, \gamma_\sigma(\boldsymbol{p}; \epsilon + i0, \epsilon - i0). \quad (2.49b)$$

Using Eq. (II), $\Lambda_\sigma(\epsilon)$ obeys the following integral equation,

$$\Lambda_\sigma(\epsilon) = 1 + \sum_{\sigma'} N_{\rm F}^{\sigma'} \int du \, W_{\sigma\sigma'}(u) \left[n_B(u) + n_F(u+\epsilon)\right] \frac{\Lambda_{\sigma'}(u+\epsilon)}{\Gamma_{\sigma'}(u+\epsilon)}, \quad (2.50a)$$

with

$$W_{\sigma\sigma'}(u) = \frac{1}{N_{\rm F}^\sigma N_{\rm F}^{\sigma'} V^2} \sum_{\boldsymbol{p},\boldsymbol{k}} \sum_{\sigma' \neq \sigma} \delta[\omega_{\sigma'}(\boldsymbol{k})] \, \delta[\omega_\sigma(\boldsymbol{p})] \, \mathcal{V}''_{\sigma\sigma'}(\boldsymbol{k} - \boldsymbol{p}, u) \frac{\boldsymbol{k}.\boldsymbol{p}}{\boldsymbol{p}^2}. \quad (2.50b)$$

Again, $\mathcal{V}''_{\sigma\sigma'}$ is the spectrum of the effective potential.

Using the fact that $\boldsymbol{k}$ and $\boldsymbol{p}$ are pinned to different Fermi surfaces by the corresponding δ factors in above, the resulting identity,

$$\boldsymbol{k}.\boldsymbol{p} = k_{\mathrm{F}}^2 \left[1 - \frac{\omega_0(\boldsymbol{k}-\boldsymbol{p})}{2Dk_{\mathrm{F}}^2}\right]$$

can be used to express $W_{\sigma\sigma'}$ as

$$W_{\sigma\sigma'}(u) = \left(\frac{k_{\mathrm{F}}}{k_{\mathrm{F}}^{\sigma}}\right)^2 \left[\bar{\mathcal{V}}''_{\sigma\sigma'}(u) - \bar{\mathcal{V}}''^{,(2)}_{\sigma\sigma'}(u)\right] \tag{2.51a}$$

with $\bar{\mathcal{V}}''_{\sigma\sigma'}(u)$ defined in Eq. (2.41b) and

$$\bar{\mathcal{V}}''^{,(2)}_{\sigma\sigma'}(u) = \frac{1}{N_{\mathrm{F}}^{\sigma} N_{\mathrm{F}}^{\sigma'} V^2} \sum_{\boldsymbol{k},\boldsymbol{p}} \delta[\omega_{\sigma}(\boldsymbol{k})]\, \delta[\omega_{\sigma'}(\boldsymbol{p})]\, \mathcal{V}''_{\sigma\sigma'}(\boldsymbol{k}-\boldsymbol{p}, u)\, \frac{\omega_0(\boldsymbol{k}-\boldsymbol{p})}{2Dk_{\mathrm{F}}^2}. \tag{2.51b}$$

According to the spectrum of $\mathcal{V}_{\sigma\sigma'}$, which is related to the one in Eq. (2.41d), the ferromagnon energy $\omega_0(\boldsymbol{k}-\boldsymbol{p})$ in Eq. (2.51b) is equal to $\pm u$. Therefore, $\bar{\mathcal{V}}''^{,(2)}_{\sigma\sigma'}(u)$ has an additional factor of u relative to $\bar{\mathcal{V}}''_{\sigma\sigma'}(u)$. Hence, the analog of $\Gamma_{\sigma}(\epsilon)$ in Eq. (2.41a) can be defined as

$$\Gamma^{(2)}_{\sigma}(\epsilon) = N_{\mathrm{F}}^{-\sigma} \int du\, [n_B(u) + n_F(u+\epsilon)] \sum_{\sigma'} \bar{\mathcal{V}}''^{,(2)}_{\sigma\sigma'}(u). \tag{2.52}$$

Then, Eq. (2.50a) becomes

$$\Lambda_{\sigma}(\epsilon) = 1 + \left(\frac{k_{\mathrm{F}}}{k_{\mathrm{F}}^{\sigma}}\right)^2 \int du \sum_{\sigma'} N_{\mathrm{F}}^{\sigma'} \left[\bar{\mathcal{V}}''_{\sigma\sigma'}(u) - \bar{\mathcal{V}}''^{,(2)}_{\sigma\sigma'}(u)\right] [n_B(u) + n_F(u+\epsilon)]\, \frac{\Lambda_{\sigma'}(u+\epsilon)}{\Gamma_{\sigma'}(u+\epsilon)}. \tag{2.53}$$

The usual procedure to solve this integral equation is to make an uncontrolled approximation that replaces $\Lambda(u+\epsilon)/\Gamma(u+\epsilon)$ in Eq. (2.53) with $\Lambda(\epsilon)/\Gamma(\epsilon)$, thus turning an integral equation into an algebraic equation [33]. However, it was pointed

out in [36] that Eq. (2.53) is a Fredholm equation of the second kind. This integral equation can be solved asymptotically exactly, and it was shown that the temperature dependence given by the exact solution and the one obtained from the simple approximation are qualitatively the same, only their prefactors are different. Therefore, using the simple approximation, Eq. (2.53) turns into a system of two coupled algebraic equations for $\Lambda_\pm(\epsilon)$. As before, ϵ is set to 0 in Eq. (2.49a), since this will only affect the prefactor of the temperature dependence of the conductivity. Using $\Lambda_\sigma \equiv \Lambda_\sigma(\epsilon = 0)$ and $\Gamma_\sigma \equiv \Gamma_\sigma(\epsilon = 0)$, the equations for Λ_σ are

$$\begin{aligned} \Lambda_+ &= 1 + \left(\frac{k_\mathrm{F}}{k_\mathrm{F}^+}\right)^2 \left[\Gamma_+ - \Gamma_+^{(2)}\right] \frac{\Lambda_-}{\Gamma_-}, \\ \Lambda_- &= 1 + \left(\frac{k_\mathrm{F}}{k_\mathrm{F}^-}\right)^2 \left[\Gamma_- - \Gamma_-^{(2)}\right] \frac{\Lambda_+}{\Gamma_+}. \end{aligned} \tag{2.54}$$

$\Gamma_\sigma(\epsilon = 0)$ is given by Eq. (2.42). $\Gamma_\sigma^{(2)}$ is obtained from an analogous integral with an additional factor of frequency in the integrand.

$$\begin{aligned} \Gamma_\sigma^{(2)} = &= \frac{\pi K}{N_\mathrm{F}^\sigma} \frac{T^2}{T_1^2} \int_{T_0/T}^{T_1/T} dx \, \frac{x}{\sinh(x)} \\ &= \frac{\pi K}{N_\mathrm{F}^\sigma} \frac{T}{T_1} \begin{cases} \dfrac{2T_0}{T_1}\left(1 + \dfrac{T}{T_0}\right) e^{-T_0/T} & \text{if } T \ll T_0 \\ \dfrac{\pi^2}{4} \dfrac{T}{T_0} & \text{if } T_0 \ll T \ll T_1 \\ 1 & \text{if } T \gg T_1 \end{cases} . \end{aligned} \tag{2.55}$$

For $T \ll T_0$, we notice that $\Gamma^{(2)}$ is proportional to Γ:

$$\Gamma^{(2)} = \frac{2T_0}{T_1}\left(1 + \frac{T}{T_0}\right)\Gamma. \tag{2.56}$$

Neglecting $\lambda/\epsilon_{\rm F} \ll 1$ wherever it is not of qualitative importance, and using Eqs. (2.42), (2.41e) and (2.55), the solution of Eqs. (2.54) is

$$\frac{\Lambda_\pm}{\Gamma_\pm} = \frac{\Gamma_+ + \Gamma_- - \Gamma_\pm^{(2)}}{-4\frac{T_0}{T_1}\Gamma_+\Gamma_- + \Gamma_+\Gamma_-^{(2)} + \Gamma_-\Gamma_+^{(2)} - \Gamma_+^{(2)}\Gamma_-^{(2)}}. \tag{2.57}$$

Using Eq. (2.57) in Eq. (2.49a), the transport relaxation time $\tau_{\rm tr}$, defined via a Drude formula $\sigma = (n_e e^2/m_{\rm e})\tau_{\rm tr}$, is given by

$$\tau_{\rm tr} = \frac{\Gamma - \frac{\Gamma^{(2)}}{2}}{-4\frac{T_0}{T_1}(\Gamma)^2 + 2\Gamma\Gamma^{(2)} - (\Gamma^{(2)})^2}. \tag{2.58}$$

Here, $\Gamma \approx \Gamma_+ \approx \Gamma_-$ and $\Gamma^{(2)} \approx \Gamma_+^{(2)} \approx \Gamma_-^{(2)}$, which are obtained from Eqs. (2.42) and (2.55), respectively, with $N_{\rm F}^\sigma$ replaced with $N_{\rm F}$. These approximations give small corrections of $O(\lambda/\epsilon_{\rm F})$ that only change the prefactor of the temperature dependence of the transport relaxation time.

Finally, the ferromagnon-exchange contribution to the electrical resistivity $\rho_{\rm el} = 1/\sigma$ is

$$\rho_{\rm el} = \frac{m_{\rm e}}{n_e e^2}\frac{\pi K}{N_{\rm F} T_1}\begin{cases} \dfrac{4}{T_1}T^2\, e^{-T_0/T} & \text{if} \quad T \ll T_0 \\ \dfrac{\pi^2}{2T_1}T^2 & \text{if} \quad T_0 \ll T \ll T_1 \\ T & \text{if} \quad T \gg T_1 \end{cases}. \tag{2.59}$$

Validity of the Effective Action

In this section, the validity of the ferromagnon-exchange mediated effective electronic interaction obtained in Eq. (2.6b) is discussed. To briefly summarize how the effective electronic interaction was obtained, it was assumed that the conduction electrons are subject to a magnetization and magnetic fluctuations of unspecified

origin. The dynamics of these fluctuations are governed by the physical magnetic susceptibility. Then, these fluctuations were integrated out, leaving behind an action purely in terms of the electronic fields. It is important to note that the feedback of the electrons on the magnetic fluctuations has already been built into the effective action, by means of the Zeeman coupling of the electronic spin density to magnetization fluctuations. Therefore, it would be erroneous to use the effective action to renormalize the susceptibility, either directly or indirectly.

However, for the purposes of calculating electronic relaxation rates, it is safe to use the effective potential, Eq. (2.14b), up to first order in $\mathcal{V}$ perturbatively. For localized-moment ferromagnets, where the magnetism is due to localized electrons in a different band, the validity of this procedure is more obvious compared to the case of itinerant ferromagnets. But, the coupling of the spin density to the magnetization fluctuations, produced by other electrons either in the same band or a different band, remains the same. Therefore, the above arguments must follow through similarly in the itinerant case. To further illustrate this point, we will now obtain well-established results for the electronic relaxation rates due to Coulomb interaction and due to phonons, using the presented procedure to generate the effective action.

We start with a band of noninteracting electrons with action S_0, with a statically screened Coulomb interaction given by

$$S_{\rm int}[\bar{\psi},\psi] = \int_k \delta n(k)\, v_{\rm sc}(\boldsymbol{k})\, \delta n(-k). \tag{2.60}$$

The screened Coulomb interaction is $v_{\rm sc}(\boldsymbol{k}) = 4\pi e^2/(\boldsymbol{k}^2+\kappa^2)$, with κ the screening wave number. $n(k)$ is the Fourier transform of the number density field, given in terms of the fermion fields by $n(x) = \bar{\psi}(x)\psi(x)$. In the magnetic case, we had

to assume a nonzero magnetization and define a reference ensemble with action S_λ. Here, the finite average number density of electrons is already built in via the chemical potential μ in S_0. Therefore, in this case, S_0 itself is the reference ensemble. Mirroring the steps in the magnetic case, one of the δn fields is replaced by δN, a number density fluctuation. We can interpret δN as the density fluctuation created by all other electrons, in analogy with magnetization fluctuations in the case of an itinerant magnet. This yields, in real space and imaginary time,

$$S[\bar{\psi},\psi] = S_0[\bar{\psi},\psi] + \int dx\, dy\, \delta N(x)\, \delta(\tau_x - \tau_y)\, v_{\rm sc}(\boldsymbol{x}-\boldsymbol{y})\, \delta n(y). \tag{2.61}$$

Including a Gaussian action that governs the density fluctuations, similar to $S_{\rm fluct}[\delta \boldsymbol{M}]$

$$S_{\rm fluct}[\delta N] = -\frac{1}{2}\int dx\, dy\, \delta N(x)\, \chi^{-1}(x-y)\, \delta N(y), \tag{2.62}$$

where χ is the physical density susceptibility. Integrating out the δN fields by means of a Gaussian integral, we obtain

$$S_{\rm eff}[\bar{\psi},\psi] = S_0[\bar{\psi},\psi] + \frac{1}{2}\int_k \delta n(k)\, V(k)\, \delta n(-k) \tag{2.63a}$$

with the effective potential

$$V(k) = [v_{\rm sc}(k)]^2 \chi(k). \tag{2.63b}$$

Using this effective action, the single-particle relaxation rate is

$$\frac{1}{2\tau} = \Gamma(\epsilon=0) = 2N_{\rm F}\int_{-\infty}^{\infty} du\, \bar{V}''(u)\, \frac{1}{\sinh(u/T)}, \tag{2.64a}$$

$$\bar{V}''(u) = \frac{1}{(2N_{\rm F}V)^2}\sum_{\boldsymbol{k},\boldsymbol{p}} \delta(\xi_{\boldsymbol{k}})\, \delta(\xi_{\boldsymbol{p}})\, V''(\boldsymbol{k}-\boldsymbol{p},u). \tag{2.64b}$$

From Eq. (2.63b), the spectrum of the effective potential V is given by the spectrum of the physical density susceptibility χ, which to the lowest order in the Coulomb interaction is nothing but the Lindhard susceptibility χ_0. The spectrum of χ_0 is

$$\chi_0''(\boldsymbol{k},u) = \frac{\pi N_{\rm F} u}{v_{\rm F}|\boldsymbol{k}|}, \qquad \text{for } |u| < \frac{2k_{\rm F}|\boldsymbol{k}| - \boldsymbol{k}^2}{2m_{\rm e}}. \tag{2.65}$$

Therefore, at low temperatures, we get the well-known Fermi-liquid result for the relaxation rate,

$$\frac{1}{2\tau_{\text{e-e}}} = \frac{\pi}{4}\frac{T^2}{\epsilon_{\rm F}}. \tag{2.66}$$

Hence, we conclude that the procedure followed to derive the effective electronic action gives the correct result in case of Coulomb scattering of electrons.

If δN represents ionic density fluctuations, they couple to δn in the same way as in Eq. (2.61), via a statically screened Coulomb interaction. In this case, the susceptibility χ describes ionic density fluctuations, which are the phonons. The calculations for the previous case follow through in the same way, except that the spectrum of effective potential, if we consider longitudinal phonons, is [37]

$$\bar{V}''(\boldsymbol{k},u) = [v_{\rm sc}(\boldsymbol{k})]^2\chi''(\boldsymbol{k},u), \qquad \chi''(\boldsymbol{k},u) = \pi\,\rho^2\,\kappa\,u^2\,\delta\Big[u^2 - \omega_{\rm L}^2(\boldsymbol{k})\Big], \tag{2.67}$$

with $\omega_{\rm L}(\boldsymbol{k}) = c|\boldsymbol{k}|$, the longitudinal phonon frequency. ρ is the ionic number density, c is the longitudinal speed of sound, and $\kappa = -(\partial V/\partial p)/V$, with V the system volume and p the pressure, the compressibility. This electron-phonon interaction in metals leads to the single-particle relaxation rate

$$\frac{1}{\tau_{\text{e-ph}}} = \frac{7\pi}{3}\,\zeta(3)\,\frac{\rho^2\kappa}{n_e m_{\rm e} c^2}\,T^3, \tag{2.68}$$

which is consistent with the established result [21]. This serves as a further justification of the validity of the magnon-exchange effective electronic action in the calculation of electronic relaxation rates.

Discussion and Conclusions

In summary, the ferromagnon exchange contribution to the thermal and electrical resistivity has been calculated, using a very general theory for the effective electronic interaction mediated by the ferromagnons. The theory only relies on symmetry arguments and is not sensitive to the origin of magnetization, be it localized electrons in a different band or the conduction electrons themselves. Eqs. (2.43) and (2.59) show that at asymptotically low temperatures, below a temperature scale T_0, both the thermal and the electrical resistivity due to the ferromagnons are exponentially small. The exponential dependence is a direct consequence of the conduction-band splitting in a metallic ferromagnet. The Ueda-Moriya T^2 behavior of the electrical resistivity is recovered in a pre-asymptotic temperature window. The thermal resistivity is proportional to T in the same window. This temperature window ranges from T_0 to a high temperature scale T_1, which is typically close to the exchange splitting. For $T \gg T_1$, both resistivities show a linear temperature dependence.

To elaborate on the physical reason for the exponential dependence of the relaxation rates at low temperatures, consider Fig. 4. The figure schematically shows the splitting of the conduction band Fermi surface into two for the two spin projections of the electrons. The ferromagnons couple only electrons with opposite spins. Therefore, the minimum momentum that can be transferred in this scattering process is $k_0 = k_{\rm F}^+ - k_{\rm F}^- \approx \Delta E_{\rm ex}/v_{\rm F}$. Now, the magnon dispersion relation is given by $\omega = Dk^2$, which implies that the smallest transferrable energy in the

scattering process is $T_0 = Dk_0^2$. Typically, the magnon stiffness coefficient D is itself roughly proportional to $\Delta E_{\rm ex}$. Hence, the temperature scale $T_0 \propto (\Delta E_{\rm ex})^3$. When the temperature $T \ll T_0$, the ferromagnon-exchange electron scattering process is greatly suppressed and thus, the relaxation rates show an activated behavior with an activation energy T_0. The largest momentum transfer in this scattering process is given by $k_1 = k_{\rm F}^+ + k_{\rm F}^- \approx 2k_{\rm F}$, which corresponds to a largest energy transfer of $T_1 = Dk_1^2 \approx \Delta E_{\rm ex}$. One may interpret T_1 as the fundamental magnetic energy scale, an analog of the Debye temperature Θ_D in case of electron-phonon coupling. However, there is no analog of T_0 in the electron-phonon problem, as the scattering process in that case is inter-band.

The primary difference between the results presented above and the Ueda-Moriya result [19] is that these authors neglected the exchange splitting of the conduction band in their calculation. Consequently, there was no minimum energy scale T_0 and the T^2 behavior of the transport relaxation rate, which is in fact only valid for temperatures larger than T_0, was obtained at low temperatures. It is worth noting that this discrepancy shows only in the ferromagnon contribution to the electrical resistivity. The contributions from the dissipative spin-excitations, somewhat similar to the Coulomb scattering case, remain unaffected by the exchange splitting and are proportional to T^2 even at asymptotically low temperatures.

In the following, numerical estimates of the values of T_0 and T_1 are discussed. To start with, a fictitious case of simple, single-conduction-band, metals with magnetic properties similar to the classic "high-temperature" ferromagnets Nickel, Cobalt and Iron are considered. The values of the exchange splitting in these materials are $\Delta E_{\rm ex} \approx 0.25, 1.0$ and 2.0 eV, respectively [32, 38]. These values are obtained from photoemission experiments. Neutron scattering experiments give values for the spin-

stiffness coefficient D, 364 for Ni, 500 for Co and 281 for Fe, in units of meV Å^2 [3]. Assuming a generic value $k_{\rm F} \approx 1\text{Å}^{-1}$ Fermi wave number and $\epsilon_{\rm F} \approx 10^5$ K for the Fermi energy, the temperature scales are, $T_1 \approx 10000 - 20000$ K for these materials, and $T_0 \approx 500$ mK for Ni, 10 K for Co and 30 K for Fe. For weak ferromagnets, such as MnSi or Ni_3Al, $D \approx 23.5$ meV Å^2 [39] and 70 meV Å^2 [40], respectively. The magnetic moments per formula unit is 0.4 μ_B for MnSi [41] and $0.17\mu_B$ for Ni_3Al [40], about two thirds and one third, respectively, that of Ni. Assuming a linear-correlation between the magnetic moment and exchange splitting based on observations [38], $\Delta E_{\rm ex} \approx 0.17$eV for MnSi and 0.07eV for Ni_3Al. Taking $k_{\rm F} \approx 1\text{Å}^{-1}$ and $\epsilon_{\rm F} \approx 10^5$ K, yields, $T_1 \approx 1000$ K and $T_0 \approx 20$ mK for Mnsi, and $T_1 \approx 2800$ K and $T_0 \approx 10$ mK for Ni_3Al.

Using the relation between K and λ as in Eq. (2.33) and the fact that $T_1 \approx \lambda$, the prefactor in Eq. (2.59) $\pi K/N_{\rm F}T_1$ is of order unity. Comparing this with the Fermi-liquid result Eq. (2.66), it seems that the ferromagnon T^2 contribution is larger than the Fermi-liquid T^2 contribution by roughly a factor of $\epsilon_{\rm F}/T_1 \approx 10$ in a single-band model. In reality however, the aforementioned materials are either transition metals, or compounds containing transition metals, with a complicated band structure and Fermi surfaces containing multiple sheets. Consequently, the electron-electron Coulomb scattering contribution to the electrical resistivity is likely much larger than implied by a single-band model. There have been suggestions that this scattering makes the largest contribution to the observed T^2 behavior at low temperatures [42]. This is due to the fact that in a realistic multi-band case, different band edges have different distances from the common chemical potential and thus, have different effective Fermi temperatures. Depending on whether the electron spin is flipped or not in the various scattering processes and whether or not these processes couple different

sheets of the Fermi surface, the various relaxation rate contributions may or may not be additive, leading to a complicated structure of the overall resistivity. In addition to ferromagnons and Coulomb scattering, dissipative spin excitations also contribute a T^2 term to the resistivity [19]. Hence, it turns out that the low-temperature transport rate in Fe, Ni, and Co is roughly 100 times larger than the estimate given by the single-band Fermi liquid result, Eq. (2.66), with a single Fermi temperature of 10^5 K [42]. The temperature scale T_1 is largely unaffected by the complicated band structure. It only depends on the spin-stiffness coefficient, which can be experimentally measured, and the largest possible momentum transfer, which in a good metal is on the order of $2\pi/a$, with a the lattice constant, and is roughly close to the value $2k_{\mathrm{F}}$ for a single spherical Fermi surface that yields the same electron density. Therefore, the estimates of T_1 are largely model independent. In conclusion, it turns out that the ferromagnon contribution to the electrical resistivity in Fe, Ni and Co at temperatures $T > T_0$ is about an order of magnitude less than the combined contribution from Coulomb scattering and dissipative magnetic excitations. Although in MnSi and Ni_3Al T_1 is much lower and the magnon scattering is accordingly stronger, the observed T^2 prefactors in the resistivity of these materials are orders of magnitude larger than the ones in Fe, Ni and Co. The ferromagnon contribution to the resistivity cannot possibly account for this.

The effect of the band structure on T_0 is more complicated. Various scattering processes involving electrons on different sheets of the Fermi surface are expected to be have different values of T_0. Therefore, with decreasing temperature, contributions to the ferromagnon-exchange part of the electronic scattering rate will sequentially freeze out as the temperature drops below a sequence of temperature scales T_0. The estimates of T_0 given previously are thus only rough estimates for the lowest of these

temperature scales. Estimating higher temperature scales requires a detailed analysis of the electronic band structure. The fact still remains that below the lowest T_0 the ferromagnon contribution to the relaxation rates will be exponentially small. Thus, the obvious candidates for the low-temperature T^2 behavior in metallic ferromagnets are Couloumb scattering and dissipative magnetic excitations. Experimentally, one would expect a distinct temperature dependence of the prefactor of the T^2 term in the electrical resistivity.

Additionally, in a material with complicated band structure, it could transpire that there may be points or lines in reciprocal space where the two Stoner bands cross. In such a case, the exponential suppression of the relaxation rates is expected to be weakened, but the nature of this weakening will be highly dependent on the nature of the crossing. Also, real materials always have some amount of quenched disorder. The interplay of the scattering process discussed in this chapter and quenched disorder is an interesting problem that is surely important for a quantitative understanding of real materials. A complete discussion of disorder effects is a separate problem on its own and will not be discussed here.

In the next chapter, we investigate the phenomenon of generic scale invariance in quantum magnets. More specifically, we calculate and compare the one-loop spin-wave contribution to the longitudinal order-parameter susceptibility in both quantum ferromagnets and antiferromagnets. We also make predictions for neutron-scattering experiments.

CHAPTER III

MAGNON-INDUCED LONG-RANGE CORRELATION FUNCTIONS IN QUANTUM MAGNETS

This work was published in volume 94 of the journal *Physical Review B* in October 2016. Dietrich Belitz and Theodore R. Kirkpatrick were the principal investigators for this work; Sripoorna Bharadwaj performed the calculations and produced the figures in this chapter.

Motivation

In the previous chapter, the magnon contribution to the electrical resistivity was calculated. Another important effect of these low-energy excitations is the long-ranged nature of certain correlation functions, which can be easily probed by neutron-scattering experiments. The magnons themselves can be directly observed via neutron scattering [16, 37]. However, these transverse order-parameter fluctuations (i.e. the Goldstone modes) also have profound indirect effects on other observables. An example of this is the divergence of the longitudinal spin susceptibility, χ_{L}, as $k \to 0$ in a classical Heisenberg ferromagnet or antiferromagnet. This divergence exists in the ordered phase for all spatial dimensions $2 < d < 4$ [43, 44]. The leading contribution to χ_{L} from the coupling of the longitudinal order-parameter fluctuations to the transverse ones takes the form of a convolution of two Goldstone modes,

$$\chi_{\mathrm{L}} \propto \int d\boldsymbol{p}\, \frac{1}{\boldsymbol{p}^2}\, \frac{1}{(\boldsymbol{p}-\boldsymbol{k})^2} \approx \int_{|\boldsymbol{k}|} d\boldsymbol{p}\, \frac{1}{\boldsymbol{p}^4} \propto \frac{1}{|\boldsymbol{k}|^{4-d}}. \tag{3.1}$$

The diagrammatic representation of above is as shown in Fig. 9. This result was originally derived for ferromagnets in perturbation theory and later shown to be asymptotically exact using renormalization-group (RG) methods [45]. It reflects the scale dimensions that characterize the stable RG fixed point describing the ordered phase. Eq. (3.1) holds for both classical ferromagnets and antiferromagnets. In the latter case, $\chi_{\rm L}$ is actually the longitudinal order-parameter susceptibility, which is the correlation function of the staggered magnetization rather than the physical spin susceptibility.

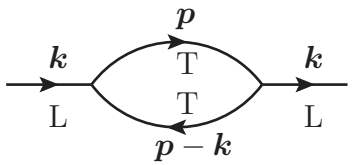

FIGURE 9. Diagrammatic representation of the coupling between the longitudinal and the transverse spin fluctuations in the classical case: A longitudinal (L) mode couples to two transverse (T) modes. The resulting contribution to the longitudinal susceptibility $\chi_{\rm L}$ has the form given in Eq. (3.1)

This divergence of $\chi_{\rm L}$, which in the absence of mode coupling with the Goldstone modes is a non-singular quantity, is an example of a nonanalyticity. This nonanalytic dependence of $\chi_{\rm L}$ on the wave number reflects long-range correlation functions in the system due to the massless magnons. In real space, for large distances r, $\chi_{\rm L}$ falls off as a power law, $\chi_{\rm L} \propto 1/r^{2d-4}$. This is an example of a more general phenomenon - soft or massless modes in the system inducing long-range correlations that are then reflected in the nonanalytic behavior in the limit of small frequencies and wave numbers. Existence of soft modes in entire phases implies nonanalytic behavior, usually in the form of power laws, over the entire phase. This phenomenon is known as generic

scale invariance [46]. Soft modes that exist only at isolated critical points are not related to this phenomenon. In a magnetic system, magnons are not necessarily the only massless modes in the system. There may be other soft modes that could couple to any given observable and compete with the magnons in producing long-range correlations or nonanalytic behavior. For instance, in disordered metals at zero temperature ($T = 0$), there are massless diffusive excitations known as "diffusons" and "Cooperons" that lead to nonanalyticities in observables known as weak-localization effects [47, 48].

The work presented in this chapter investigates the fate of the singular behavior of the classical longitudinal spin susceptibility, Eq. (3.1), in the limit $T \to 0$. In quantum statistical mechanics, the statics and the dynamics are intrinsically coupled. Therefore, at $T = 0$, the expression for $\chi_{\rm L}$ must include a frequency integration in addition to the wave-number integration, with the integrand being comprised of the dynamic Goldstone modes. Power counting arguments suggest that this additional frequency integration will weaken the classical singularity at $T = 0$. Specifically, for quantum antiferromagnets at $T = 0$, power counting suggests that Eq. (3.1) becomes

$$\chi_{\rm L} \sim \int_{|\boldsymbol{k}|} d\boldsymbol{p} \int_{\Omega} d\omega \frac{1}{(\boldsymbol{p}^2 + \omega^2)^2} \sim |\boldsymbol{k}|^{d-3} \sim |\Omega|^{d-3} \tag{3.2}$$

for $1 < d < 3$, with a logarithmic singularity in $d = 3$. The "$\sim$" symbol is meant to denote "scales as". An explicit calculation done later in this chapter agrees with this guess. For quantum ferromagnets, the expression obtained by replacing the denominator in Eq. (3.2) by $(\boldsymbol{p}^2+\omega)^2$, which yields a k^{d-2} or $|\Omega|^{(d-2)/2}$ behavior, is not correct. This can be seen from spin-wave theory, which expresses the spin operators by bosonic operators via a Holstein-Primakoff transformation [3]. In a ferromagnet, the longitudinal spin fluctuation is given in terms of the magnon-number operator

and thus, $\chi_{\rm L}$ is actually the magnon-number correlation function. There are no magnon number fluctuations at $T = 0$ and therefore, the contribution analogous to Eq. (3.2), is identically zero (i.e. scales like k^{d-2} with zero prefactor). In other words, in the ground state of a quantum ferromagnet the magnetization is at its maximum value. Hence, the ground-state energy has the same value as it does classically and cannot be decreased by quantum fluctuations. This argument clearly does not hold for a quantum antiferromagnet. The classical Neél state is not an eigenstate of the Hamiltonian, and the ground-state energy can be lowered below its classical value by quantum fluctuations. Detailed calculations are performed and discussed in this chapter, which will demonstrate the difference in the behavior of the $T = 0$ longitudinal order-parameter correlation function in quantum ferromagnets and quantum antiferromagnets. The calculations for both cases are performed using the nonlinear sigma model (NLσM), which provides a convenient description of the long-wavelength and low-frequency properties of the ordered phase of systems with spontaneously broken symmetry. This model is essentially an effective field theory that focuses on the Goldstone modes and integrates out all massive fluctuations in the simplest approximation that respects the symmetry. The divergence of $\chi_{\rm L}$ in a classical Heisenberg ferromagnet, Eq. (3.1), can be easily demonstrated using the classical $O(3)$-symmetric nonlinear sigma model [49]. Therefore, it is natural to consider a quantum NLσM to study the corresponding effect in quantum magnets. The results presented here were published as [50].

NLσM for Quantum Ferromagnets

Consider a quantum ferromagnet with a fluctuating magnetization $\boldsymbol{M}(x) = M_0(x)\hat{\boldsymbol{m}}(x)$, where $x = (\boldsymbol{x}, \tau)$ - $\boldsymbol{x}$ and τ being the real-space position and imaginary-

time, respectively. M_0 is the magnitude of the order parameter and the direction unit vector $\hat{\boldsymbol{m}}(x)$,

$$\hat{\boldsymbol{m}}(x) = (\pi_1(x), \pi_2(x), \sigma(x)) \tag{3.3a}$$

with

$$\hat{\boldsymbol{m}}^2(x) = \pi_1^2(x) + \pi_2^2(x) + \sigma^2(x) \equiv 1. \tag{3.3b}$$

In a NLσM description of a quantum ferromagnet, fluctuations of M_0 are neglected. Taking $M_0(x) \equiv M_0$, the partition function can be written as [51, 52]

$$Z = \int \mathcal{D}[\hat{\boldsymbol{m}}]\, \delta(\hat{\boldsymbol{m}}^2(x) - 1)\, e^{-\int dx\, \mathcal{L}_{\rm FM}[\hat{\boldsymbol{m}}]}. \tag{3.4a}$$

Here, $\int dx = \int_0^{1/T} d\tau \int_V d\boldsymbol{x}$, where T is the temperature and V is the system volume. The Lagrangian $\mathcal{L}_{\rm FM}$ is

$$\begin{aligned} \mathcal{L}_{\rm FM}[\hat{\boldsymbol{m}}] &= -\frac{\rho_s}{2}\, \hat{\boldsymbol{m}}(x).\boldsymbol{\nabla}^2 \hat{\boldsymbol{m}}(x) - M_0 \mu \boldsymbol{H}.\hat{\boldsymbol{m}}(x) \\ &\quad + \frac{iM_0}{1+\sigma(x)} \Big(\pi_1(x)\partial_\tau \pi_2(x) - \pi_2(x)\partial_\tau \pi_1(x) \Big), \end{aligned} \tag{3.4b}$$

where ρ_s is the spin-stiffness coefficient and is proportional to M_0^2, $\boldsymbol{H}$ is the external magnetic field and μ the Bohr magneton. In the right-hand side of Eq. (3.4b), the first two terms are the same as in a classical $O(3)$ NLσM [49]. The third term is a topological Wess-Zumino term or a Berry-phase term that describes the quantum dynamics [51, 52, 53, 54]. The Bloch spin precession is governed by this term. Note that Eq. (3.4b) has been written down, assuming that the ferromagnet order is along the z-direction.

Expanding the action in powers of the fields π_1 and π_2, the Fourier-space Gaussian action that governs the transverse fluctuations is as follows:

$$\mathcal{A}^{(2)}[\pi_1, \pi_2] = \frac{M_0}{2} \sum_k \sum_{i,j=1}^{2} \pi_1(k)\, \Gamma_{ij}(k)\, \pi_j(-k), \tag{3.5a}$$

Γ_{ij} represents the matrix elements of a 2×2 matrix

$$\Gamma(k) = \begin{pmatrix} D\,\boldsymbol{k}^2 \,+\, \mu H & -\Omega_n \\ \Omega_n & D\,\boldsymbol{k}^2 \,+\, \mu H \end{pmatrix} \tag{3.5b}$$

where $D = \rho_s/M_0$. Here $k = (\boldsymbol{k}, i\Omega_n)$ with $\boldsymbol{k}$ a wave vector and $\Omega_n = 2\pi T n$ (n integer) a bosonic Matsubara frequency. The external field is taken to be pointing in the z-direction $\boldsymbol{H} = (0, 0, H)$. The inverse of Γ yields the Gaussian transverse susceptibility matrix, i.e., the correlation function

$$M_0^2 \langle \pi_i(k) \pi_j(-k) \rangle = \chi_{\mathrm{T}}^{ij}(k), \tag{3.6a}$$

where

$$\chi_{\mathrm{T}}(k) = \frac{M_0}{(D\,\boldsymbol{k}^2 \,+\, \mu H)^2 + \Omega_n^2} \begin{pmatrix} D\,\boldsymbol{k}^2 \,+\, \mu H & \Omega_n \\ -\Omega_n & D\,\boldsymbol{k}^2 \,+\, \mu H \end{pmatrix}. \tag{3.6b}$$

The matrix Γ is non-Hermitian and the frequency couples the magnetization components M_x and M_y. This reflects the structure of the Bloch spin-precession term in Eq. (3.4b). This term also shows the quadratic dispersion relation of the ferromagnetic magnons, $i\Omega_n = \pm D\boldsymbol{k}^2$. The spin-wave stiffness coefficient D (not a diffusion coefficient) is linear in M_0 (since $\rho_s \propto M_0^2$). The eigenvalues of $\Gamma(k)$ are $\lambda_\pm(k)$ with

$$\lambda_\pm(k) = \lambda_\mp(-k) = D\boldsymbol{k}^2 \,+ \mu H \,\mp\, i\Omega_n. \tag{3.7a}$$

The left and right eigenvectors are

$$\begin{aligned} (u,v)_L &= (1,\mp i) \ , \\ (u,v)_R &= (1,\pm i) \ . \end{aligned} \tag{3.7b}$$

The Gaussian action can be diagonalized and written in terms of fields $\psi_L = (\psi_{L,+}, \psi_{L,-})$ and $\psi_R = (\psi_{R,+}, \psi_{R,-})$,

$$\mathcal{A}^{(2)}[\psi_L, \psi_R] = \frac{M_0}{2} \sum_k \sum_{\sigma=\pm} \psi_{L,\sigma}(k)\, \lambda_\sigma(k)\, \psi_{R,\sigma}(-k). \tag{3.8}$$

In terms of the ψ_L and ψ_R, the fields π_1 and π_2 are

$$\begin{aligned} \pi_1 &= \frac{1}{\sqrt{2}} (\psi_{L,+} - i\psi_{L,-}) = \frac{1}{\sqrt{2}} (\psi_{R,+} + i\psi_{R,-}) \ , \\ \pi_2 &= \frac{1}{\sqrt{2}} (-i\psi_{L,+} + \psi_{L,-}) = \frac{1}{\sqrt{2}} (i\psi_{R,+} + \psi_{R,-}) \ . \end{aligned} \tag{3.9}$$

We note that the four fields $\psi_{L,\sigma}, \psi_{R,\sigma}$ are not independent. Eq. (3.9) yields

$$\psi_{L,+} = i\psi_{R,-} \quad , \quad \psi_{L,-} = i\psi_{R,+}. \tag{3.10}$$

The above constraints restore the original number of degrees of freedom. Then, from Eq. (3.8), the Goldstone mode can be obtained.

$$g_\pm(k) = \langle \psi_{L,\pm}(k) \psi_{R,\pm}(-k) \rangle = 1/M_0\, \lambda_\pm(k). \tag{3.11}$$

This is massless in the absence of the symmetry breaking field H. Also, this equation only represents one Goldstone mode, since the two eigenvectors are not independent,

unlike the antiferromagnetic case, where there are two Goldstone modes [55]. Using the Eq. (3.10), the following nonzero correlation functions can be written down.

$$\begin{aligned} \langle \psi_{L,+}(k)\, \psi_{L,-}(-k) \rangle &= i/M_0\, \lambda_+(k)\ , \\ \langle \psi_{R,+}(k)\, \psi_{R,-}(-k) \rangle &= -i/M_0\, \lambda_+(-k). \end{aligned} \tag{3.12}$$

The normalized longitudinal magnetization fluctuations are given by $\delta\sigma(x) = \sigma(x) - \langle\sigma(x)\rangle$. Then, the normalized longitudinal susceptibility is given by the correlation function $\langle\delta\sigma(x)\delta\sigma(y)\rangle = \chi_{\rm L}(x-y)/M_0^2$. Utilizing the NL$\sigma$M constraint from Eq. (3.3b), the following expansion can be written down for this correlation function.

$$\langle\delta\sigma(x)\delta\sigma(y)\rangle = \frac{1}{4}\langle(\pi_1^2(x)+\pi_2^2(x))(\pi_1^2(y)+\pi_2^2(y))\rangle - \frac{1}{4}\langle(\pi_1^2(x)+\pi_2^2(x))\rangle^2 + \ldots . \tag{3.13a}$$

In terms of the fields ψ_L and ψ_R, the above expression becomes

$$\begin{aligned} \langle\delta\sigma(x)\delta\sigma(y)\rangle &= \frac{1}{4}\sum_{\sigma,\sigma'=\pm}\Big[\langle\psi_{L,\sigma}(x)\,\psi_{R,\sigma}(x)\,\psi_{L,\sigma'}(y)\,\psi_{R,\sigma'}(y)\rangle \\ &\quad -\langle\psi_{L,\sigma}(x)\,\psi_{R,\sigma}(x)\rangle\langle\psi_{L,\sigma'}(y)\,\psi_{R,\sigma'}(y)\rangle\Big] \end{aligned} \tag{3.13b}$$

Finally, the one-loop contribution to the longitudinal susceptibility $\chi_{\rm L}^{(1)}$, obtained by using Wick's theorem and the correlation functions in Eq. (3.12), is

$$\begin{aligned} \chi_{\rm L}^{(1)}(k) &= M_0^2\frac{T}{2V}\sum_p\sum_\sigma g_\sigma(p)\, g_\sigma(p-k) \\ &= \frac{T}{2V}\sum_p\sum_\sigma \frac{1}{\lambda_\sigma(p)\lambda_\sigma(p-k)}. \end{aligned} \tag{3.14}$$

Fig. 10 is the diagrammatic representation of this contribution.

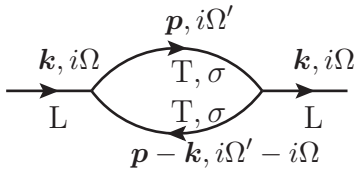

FIGURE 10. Diagrammatic representation of the coupling between longitudinal and transverse spin fluctuations in the quantum case

At $T = 0$, the frequency summation in Eq. (3.14) can be turned into an integral. Since the diagonalized Gaussian action in Eq. (3.8) only couples $\psi_{L,+}$ with $\psi_{R,+}$ and $\psi_{L,-}$ with $\psi_{R,-}$, the $T = 0$ frequency integral is such that both the poles of the integrand lie on the same side of the real axis. Therefore, at $T = 0$, the one-loop contribution to the longitudinal susceptibility vanishes, instead of being a nonzero k^{d-2} or $\Omega^{(d-2)/2}$ contribution. Hence, adding a frequency dependence to the classical expression has a much stronger effect than increasing the dimensionality by two, as the naive power counting argument suggests and at $T = 0$, it completely suppresses the effect. The absence of a nonanalyticity in the quantum case is a generic property of ferromagnets at $T = 0$ and can be readily traced back to the structure of the Bloch precession term in the action. This null result is neither an artifact of the NLσM nor the one-loop approximation. It is worth noting that this particular null result is specific to the 2-point correlation function of $\sigma(x)$.

The following correlation function is an example of a nonzero $T = 0$ one-loop contribution in a quantum ferromagnet.

$$\begin{aligned}\Psi(x-y) &= \frac{1}{4}\langle(\pi_1^2(x)-\pi_2^2(x))(\pi_1^2(y)-\pi_2^2(y))\rangle \\ &= \frac{1}{4}\sum_{\sigma,\sigma'=\pm}\sigma\sigma'\,\langle\psi_{L,\sigma}(x)\,\psi_{R,\sigma}(x)\,\psi_{L,\sigma'}(y)\,\psi_{R,\sigma'}(y)\rangle. \qquad (3.15)\end{aligned}$$

This correlation function is a physical, if hard to measure, correlation function. It describes the response to a "field" Δ that makes the exchange coupling J in a Heisenberg model anisotropic in the $x-y$ plane: $J_x = J + \Delta, J_y = J - \Delta$. After a Fourier transform, instead of Eq. (3.14), we obtain

$$\Psi(k) = \frac{T}{2V} \sum_p \sum_\sigma \frac{1}{\lambda_\sigma(p)\lambda_\sigma(k-p)}. \tag{3.16}$$

At $T = 0$, the frequency integral is now over a function that has poles on either side of the real axis and the correlation function behaves as simple power counting would suggest.

$$\begin{aligned} \Psi(\boldsymbol{k}, i\Omega_n = 0) &\propto \text{const.} + |\boldsymbol{k}|^{d-2}, \\ \Psi(\boldsymbol{k} = 0, i\Omega_n) &\propto \text{const.} + |\Omega_n|^{(d-2)/2}. \end{aligned} \tag{3.17}$$

In $d = 2$, there is a logarithmic singularity. This nonzero $T = 0$ contribution is in complete analogy to Eq. (3.2). This illustrates that the absence of a singular contribution to χ_{L} and the related fact that the maximally spin-polarized state is an exact eigenstate of the Heisenberg ferromagnet, is not due to the absence of quantum fluctuations. It is actually due to the fact that χ_{L} can be formulated as a correlation function of the magnon number. Quantum fluctuations do exist in the ground state of a ferromagnet and correlation functions like Ψ, that cannot be formulated entirely in terms of fluctuations of the magnon number, are affected by these quantum fluctuations. The same holds for the longitudinal susceptibility in an antiferromagnet.

Now, the $T > 0$ behavior of the one-loop contribution $\chi_{\rm L}^{(1)}$ in Eq. (3.14) will be analyzed. Performing the Matsubara frequency sum, we obtain

$$\chi_{\rm L}^{(1)}(k,H) = \frac{-1}{V}\sum_{\boldsymbol{p},\sigma} \frac{n(\omega_{\boldsymbol{p}}+\mu H) - n(\omega_{\boldsymbol{p}-\boldsymbol{k}}+\mu H)}{\omega_{\boldsymbol{p}} - \omega_{\boldsymbol{p}-\boldsymbol{k}} + \sigma i\Omega_n}, \tag{3.18}$$

where $n(x) = 1/(e^{x/T}-1)$ is the Bose distribution function. The units are such that $\hbar = k_B = 1$. $\omega_{\boldsymbol{p}} = D\boldsymbol{p}^2 = (\rho_s/M_0)\boldsymbol{p}^2$ is the ferromagnetic magnon frequency. To obtain the leading singular behavior as $\boldsymbol{k} \to 0$ for fixed T, the Bose function can be expanded, $n(x) \approx T/x$. Then, at zero external frequency, i.e. $k = (\boldsymbol{k}, i0)$ and zero external field, Eq. (3.18) becomes

$$\chi_{\rm L}^{(1)}(\boldsymbol{k}, H=0) \approx \left(\frac{M_0}{\rho_s}\right)^2 \frac{2T}{V}\sum_{\boldsymbol{p}} \frac{1}{\boldsymbol{p}^2(\boldsymbol{p}-\boldsymbol{k})^2}. \tag{3.19}$$

This leading contribution is necessarily linear in T and the wavenumber integral is a convolution of two classical Goldstone modes. In $d = 3$, the explicit expression for $\chi_{\rm L}^{(1)}$ is

$$\chi_{\rm L}^{(1)}(\boldsymbol{k}, H=0) = \frac{T}{4D^{3/2}\sqrt{\omega_{\boldsymbol{k}}}}\left[1 + O(\sqrt{\omega_{\boldsymbol{k}}/T})\right] \quad (d=3). \tag{3.20}$$

In generic dimensions $2 < d < 4$, the singularity is proportional to $T/|\boldsymbol{k}|^{4-d}$, with a d-dependent prefactor. For $d \leq 2$, the singular integral has a zero prefactor since $M_0 = 0$, which can be understood using the Mermin-Wagner theorem [30]. The above result is valid for $\mu H \ll \omega_{\boldsymbol{k}} \ll T$. This implies that the range of validity of Eq. (3.19) shrinks with decreasing temperature. In the asymptotic low-temperature limit in a vanishingly small field, i.e., for $\mu H \ll T \ll \omega_{\boldsymbol{k}}$,

$$\chi_{\rm L}^{(1)}(\boldsymbol{k}, H=0) = \frac{c_L}{\pi^2}\frac{T^{3/2}}{D^{3/2}\omega_{\boldsymbol{k}}}\left[1 + O(T/\omega_{\boldsymbol{k}})\right] \quad (d=3). \tag{3.21}$$

Here, $c_L = \sqrt{\pi/2}\,\zeta(3/2) \approx 2.395$, with ζ the Riemann zeta function. For $T < \omega_{\boldsymbol{k}}$, the $T/\sqrt{\omega_{\boldsymbol{k}}}$ singularity crosses over to $T^{3/2}/\omega_{\boldsymbol{k}}$. Also, as $T \to 0$, the prefactor of the singularity vanishes, which matches the $T = 0$ null result.

For $\omega_{\boldsymbol{k}} \ll \mu H \ll T$,

$$\chi_{\mathrm{L}}^{(1)}(\boldsymbol{k} \to 0, H) = \frac{T}{4\pi D^{3/2}(\mu H)^{1/2}} \left[1 + O(\sqrt{H/T})\right] \quad (d = 3). \tag{3.22}$$

For $T \ll \omega_{\boldsymbol{k}} \ll \mu H$, the leading behavior is

$$\chi_{\mathrm{L}}^{(1)}(\boldsymbol{k}, H) = \frac{1}{2\pi^{3/2}} \frac{T^{3/2}}{D^{3/2}\omega_{\boldsymbol{k}}} e^{-\mu H/T} \quad (d = 3). \tag{3.23}$$

Finally, for $\omega_{\boldsymbol{k}} \ll T \ll \mu H$, the result is proportional to $T^{1/2}e^{-\mu H/T}$ with no singular dependence on $\omega_{\boldsymbol{k}}$.

An important quantity in the context of neutron scattering experiments of ferromagnets is the dynamical structure factor. The longitudinal part of the dynamical structure factor $S_L(\boldsymbol{k}, \omega) = (2/(1 - e^{-\omega/T}))\chi_{\mathrm{L}}''(\boldsymbol{k}, \omega)$, with χ_{L}'' the spectrum of the longitudinal susceptibility χ_{L}. From Eq. (3.18), the one-loop contribution is [43]

$$S_L^{(1)}(\boldsymbol{k}, \omega) = \frac{1}{1 - e^{-\omega/T}} \frac{T}{4\pi D^{3/2}\sqrt{\omega_{\boldsymbol{k}}}} \ln\left(\frac{1 - e^{-(\omega+\omega_{\boldsymbol{k}})^2/4T\omega_{\boldsymbol{k}} - \mu H/T}}{1 - e^{-(\omega-\omega_{\boldsymbol{k}})^2/4T\omega_{\boldsymbol{k}} - \mu H/T}}\right). \tag{3.24}$$

For small $\boldsymbol{k}, \omega$ and H and fixed T, the leading behavior is

$$S_L^{(1)}(\boldsymbol{k}, \omega) \approx \frac{T^2}{4\pi D^{3/2}\omega\sqrt{\omega_{\boldsymbol{k}}}} \ln\left(\frac{(\omega + \omega_{\boldsymbol{k}})^2/4T\omega_{\boldsymbol{k}} + \mu H/T}{(\omega - \omega_{\boldsymbol{k}})^2/4T\omega_{\boldsymbol{k}} + \mu H/T}\right). \tag{3.25}$$

Eq. (3.25) is also obtained by taking the classical limit, $\hbar \to 0$ ($\mu/\hbar$ is independent of $\hbar$).

Figs. 11 and 12 show plots of a normalized version of $S_L^{(1)}$ as a function of the frequency ω, with $T, \omega_{\boldsymbol{k}}, H$ fixed.

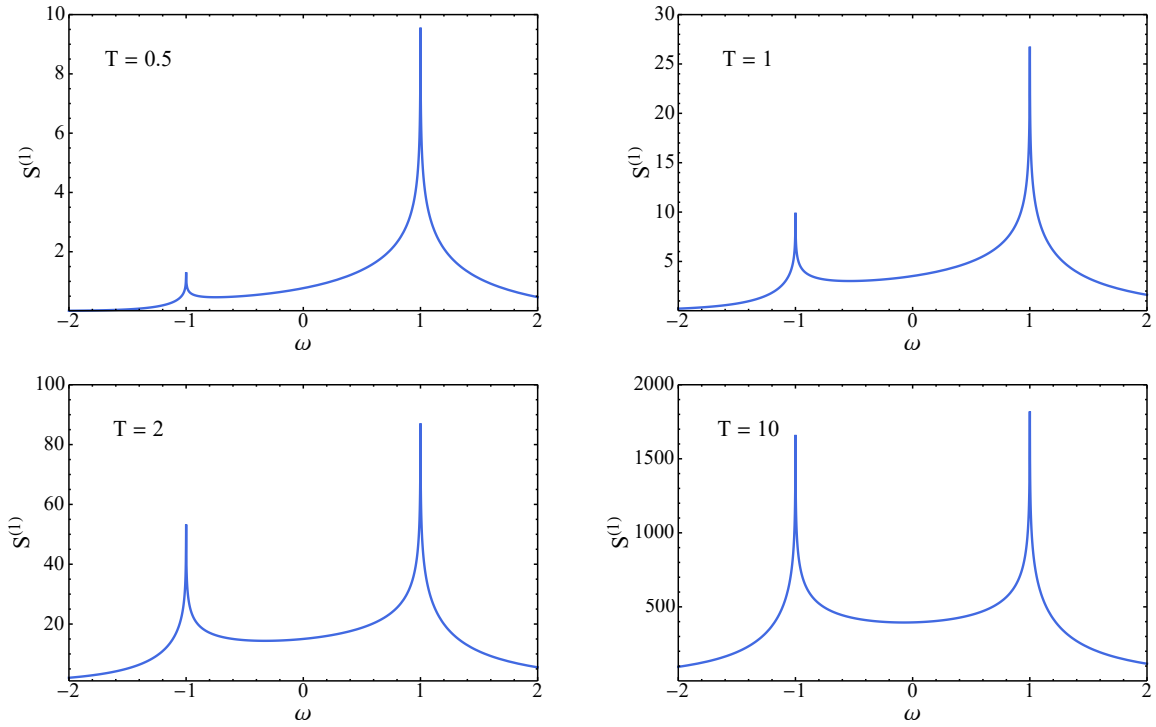

FIGURE 11. The one-loop contribution to the longitudinal part of the dynamical structure factor for a ferromagnet, Eq. (3.24), normalized by $\sqrt{\omega_{\boldsymbol{k}}}/4\pi D^{3/2}$, for $H = 0$ as a function of the frequency ω for various values of the temperature T. ω and T are measured in units of $\omega_{\boldsymbol{k}}$. On the scale shown, the result for $T/\omega_{\boldsymbol{k}} = 10$ is almost distinguishable from the classical result, Eq. (3.25)

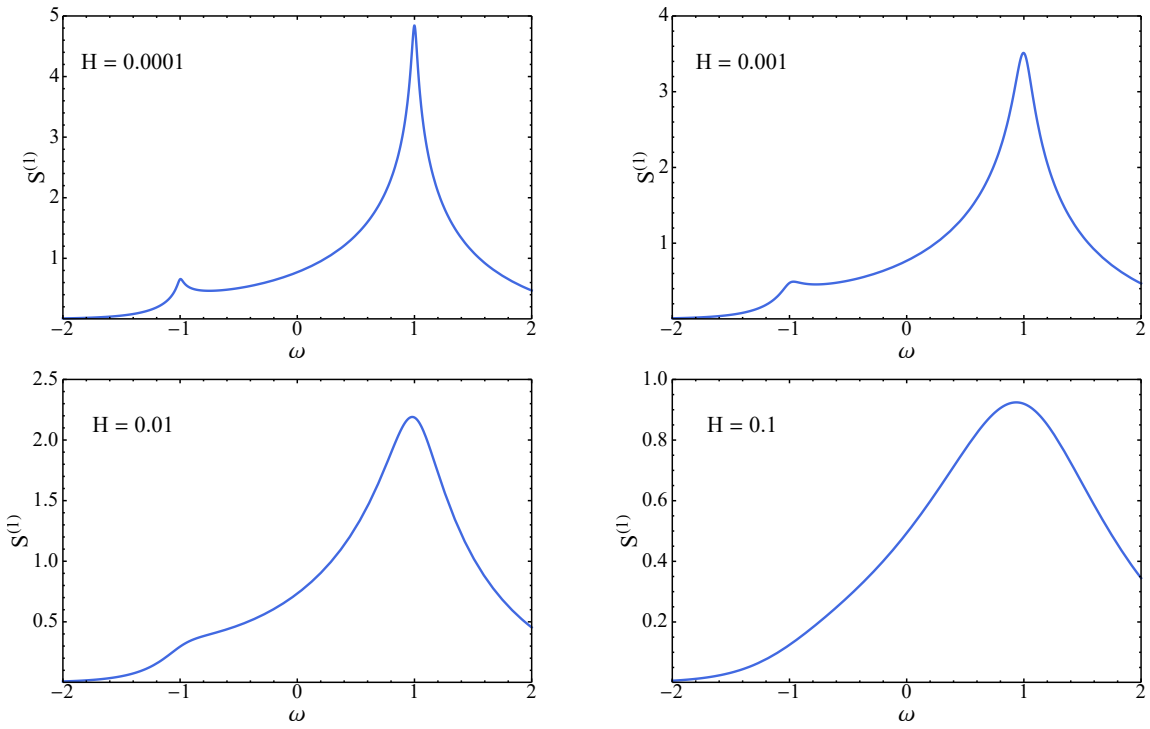

FIGURE 12. The one-loop contribution to the longitudinal part of the dynamical structure factor for a ferromagnet, Eq. (3.24), normalized as in Fig. 11, for $T/\omega_{\boldsymbol{k}}$ as a function of the frequency ω for various values of the magnetic field H. ω and H are measured in units of $\omega_{\boldsymbol{k}}$ and $\omega_{\boldsymbol{k}}/\mu$, respectively. Even a very weak magnetic field broadens the resonance feature.

The following are some of the notable features of the structure factor in Eq. (3.24).

1. There is a logarithmic singularity at $\omega = \pm\omega_{\boldsymbol{k}}$, the magnon frequency. This leads to a broad feature, even for undamped magnons, whose width is independent of the normalized temperature.

2. There is a marked decrease in the overall value of S_L with decreasing temperature.

3. S_L becomes strongly asymmetric at low temperature due to the detailed-balance factor.

4. A nonzero magnetic field removes the logarithmic singularity, and even a small magnetic field substantially broadens the resonance feature.

As an aside, the minus first frequency moment of the spectrum $\chi''_{\rm L}$ yields the static susceptibility: $\chi_{\rm L}(\boldsymbol{k}) = \int_{-\infty}^{\infty} d\omega\, \chi''_{\rm L}(\boldsymbol{k},\omega)/\pi\omega$. Performing the frequency integral recovers the results given in Eqs. (3.20)– (3.23).

NLσM for Quantum Antiferromagnets

The NLσM for quantum ferromagnets is as follows [51, 52]. The partition function is given by

$$Z = \int \mathcal{D}[\hat{\boldsymbol{n}}]\, \delta(\hat{\boldsymbol{n}}^2(x) - 1)\, e^{-\int dx\, \mathcal{L}_{\rm AFM}[\hat{\boldsymbol{n}}]} \tag{3.26a}$$

with the action density

$$\mathcal{L}_{\rm AFM}[\hat{\boldsymbol{n}}] = \frac{\rho_s}{2}\Big[-\hat{\boldsymbol{n}}(x).\boldsymbol{\nabla}^2\hat{\boldsymbol{n}}(x) + \frac{1}{c^2}(\partial_\tau \hat{\boldsymbol{n}}(x) - i\mu H \times \hat{\boldsymbol{n}}(x))^2\Big]. \tag{3.26b}$$

Here, $\hat{\boldsymbol{n}}(x)$ is the normalized staggered magnetization, ρ_s the spin stiffness, c is the spin-wave velocity and $\boldsymbol{H}$ is a homogeneous external magnetic field. As before, we can parameterize $\hat{\boldsymbol{n}}(x)$ as $\hat{\boldsymbol{n}}(x) \equiv (\pi_1(x), \pi_2(x), \sigma(x))$. The NL$\sigma$M constraint is given by

$$\hat{\boldsymbol{n}}^2(x) = \pi_1^2(x) + \pi_2^2(x) + \sigma^2(x) \equiv 1. \tag{3.27}$$

From Eq. (3.26a), it is clear that in the absence of an external field the dynamics are given by a $(\partial_\tau \hat{\boldsymbol{n}})^2$ term, in contrast to the linear dependence on ∂_τ in the

ferromagnetic case, Eq. (3.4b). Setting the external field $\boldsymbol{H} = 0$ and proceeding as in the ferromagnetic case, the Gaussian transverse fluctuation action diagonal in the π_1-π_2 basis is

$$\mathcal{A}^{(2)}[\pi_1, \pi_2] = \frac{\rho_s}{2c^2} \sum_k \sum_{i=1}^{2} \pi_i(k)\, \mu(k)\, \pi_i(-k) \tag{3.28a}$$

with an eigenvalue,

$$\mu(k) = \omega_{\boldsymbol{k}}^2 - (i\Omega_n)^2, \quad \omega_{\boldsymbol{k}} = c|\boldsymbol{k}|. \tag{3.28b}$$

$\omega_{\boldsymbol{k}}$ is the antiferromagnetic magnon frequency.

The one-loop contribution to the longitudinal order-parameter susceptibility is calculated, in a manner similar to the ferromagnetic case. It should be noted that in case of antiferromagnets, the longitudinal order-parameter susceptibility describes the response to a staggered field, rather than a homogeneous one. Taking $\chi_{\rm L}(x-y) = N_0^2 \langle \delta\sigma(x)\delta\sigma(y)\rangle$, the antiferromagnetic analog of Eq. (3.14) is

$$\chi_{\rm L}^{(1)}(k) = \left(\frac{N_0 c^2}{\rho_s}\right)^2 \frac{T}{V} \sum_p \frac{1}{\mu(p)\mu(p-k)}. \tag{3.29}$$

As in the ferromagnetic case, we first analyze Eq. (3.29) at $T = 0$. In contrast to Eq. (3.14), the frequency integration at $T = 0$ involves poles on either side of the real axis. This yields a nonzero result,

$$\chi_{\rm L}^{(1)}(\boldsymbol{k}, i\Omega_n = 0) = \left(\frac{N_0 c^2}{\rho_s}\right)^2 \frac{1}{2V} \sum_{\boldsymbol{p}} \frac{1}{\omega_{\boldsymbol{p}+\boldsymbol{k}/2}\, \omega_{\boldsymbol{p}-\boldsymbol{k}/2}} \times \frac{1}{\omega_{\boldsymbol{p}+\boldsymbol{k}/2} + \omega_{\boldsymbol{p}-\boldsymbol{k}/2}} \tag{3.30}$$

$$\chi_{\rm L}^{(1)}(\boldsymbol{k} = 0, i\Omega_n) = \left(\frac{N_0 c^2}{\rho_s}\right)^2 \frac{1}{V} \sum_{\boldsymbol{p}} \frac{1}{\omega_{\boldsymbol{p}}} \frac{1}{4\omega_{\boldsymbol{p}}^2 + \Omega_n^2}. \tag{3.31}$$

Performing the momentum integration in above yields results expected from naive power counting, Eq. (3.2). For $1 < d < 3$,

$$\begin{aligned} \chi_{\rm L}^{(1)}(\boldsymbol{k}, i\Omega_n = 0) &\propto |\boldsymbol{k}|^{d-3}, \\ \chi_{\rm L}^{(1)}(\boldsymbol{k} = 0, i\Omega_n) &\propto |\Omega_n|^{d-3}. \end{aligned} \tag{3.32}$$

The above derivation makes it clear that the difference in behavior of this correlation function for ferromagnets and antiferromagnets, respectively, is a direct consequence of the different spin dynamics in the two systems. In time space, a Ω_n^{d-3} low-frequency behavior corresponds to a $1/t^{d-2}$ long-time tail, as seen from Eq. (A.6).

In $d = 3$, the divergence is logarithmic. Keeping only the leading terms,

$$\chi_{\rm L}^{(1)}(\boldsymbol{k}, i0) = \frac{N_0^2 c}{8\pi^2 \rho_s^2} \log(\omega_0/\omega_{\boldsymbol{k}}), \tag{3.33a}$$

$$\chi_{\rm L}^{(1)}(\boldsymbol{k} = 0, i\Omega_n) = \frac{N_0^2 c}{8\pi^2 \rho_s^2} \log(\omega_0/|\Omega_n|), \tag{3.33b}$$

$$\chi_{\rm L}^{(1)}(\boldsymbol{k} = 0, i\Omega_n \to \Omega + i0) = \frac{N_0^2 c}{8\pi^2 \rho_s^2} \left[\log(\omega_0/|\Omega|) + i\,\frac{\pi}{2} \operatorname{sgn} \Omega \right]. \tag{3.33c}$$

where ω_0 is an ultraviolet cutoff frequency. In $d = 2$, the explicit result is

$$\chi_{\rm L}^{(1)}(\boldsymbol{k}, i0) = \frac{N_0^2 c^2}{8\rho_s^2} \frac{1}{\omega_{\boldsymbol{k}}}, \tag{3.34a}$$

$$\chi_{\rm L}^{(1)}(\boldsymbol{k} = 0, i\Omega_n) = \frac{N_0^2 c^2}{8\rho_s^2} \frac{1}{|\Omega_n|}, \tag{3.34b}$$

$$\chi_{\rm L}^{(1)}(\boldsymbol{k} = 0, i\Omega_n \to \Omega + i0) = \frac{N_0^2 c^2}{8\rho_s^2} \left[\frac{i}{\Omega} + \pi\, \delta(\Omega) \right]. \tag{3.34c}$$

In the following, the $T > 0$ behavior of the one-loop contribution from Eq. (3.29) is investigated. Performing the Matsubara frequency summation yields

$$\chi_{\rm L}^{(1)}(k) = \left(\frac{N_0 c^2}{\rho_s}\right)^2 \frac{-1}{2V} \sum_{\boldsymbol{p},\sigma} \frac{1}{\omega_{\boldsymbol{p}}} \frac{n(\omega_{\boldsymbol{p}}) - n(-\omega_{\boldsymbol{p}})}{(\omega_{\boldsymbol{p}} + \sigma i\Omega_n)^2 - \omega_{\boldsymbol{p}+\boldsymbol{k}}^2}. \tag{3.35}$$

The leading infrared behavior can be obtained by taking the small-momentum behavior of the integrand. To this end, the following approximation is used, $n(x) \approx T/x$. Then, at zero external frequency,

$$\chi_{\rm L}^{(1)}(\boldsymbol{k}, i0) \approx \left(\frac{N_0}{\rho_s}\right)^2 \frac{T}{V} \sum_{\boldsymbol{p}} \frac{1}{\boldsymbol{p}^2(\boldsymbol{p}-\boldsymbol{k})^2}. \tag{3.36}$$

Like the ferromagnetic case, Eq. (3.19), the above expression reproduces the classical result, Eq. (3.1). In $d = 3$,

$$\chi_{\rm L}^{(1)}(\boldsymbol{k}, i0) = \frac{N_0^2 c}{8\rho_s^2} \frac{T}{\omega_{\boldsymbol{k}}} \Big[1 + O\Big((\omega_{\boldsymbol{k}}/T)\, \log(\omega_0/\omega_{\boldsymbol{k}})\Big)\Big]. \tag{3.37}$$

The above expression is valid for $\omega_{\boldsymbol{k}} \ll T \ll \omega_0$.

Taking the $T \to 0$ limit of Eq. (3.35), when $n(\omega_{\boldsymbol{p}}) - n(-\omega_{\boldsymbol{p}}) \to 1$, the integrals of Eq. (3.30) are recovered. Specifically, Eq. (3.37) crosses over to Eq. (3.33a), for $T \ll \omega_{\boldsymbol{k}}$.

From Eq. (3.35), the one-loop contribution to the longitudinal part of the dynamical structure factor can be obtained. In three dimensions,

$$\begin{aligned} S_L^{(1)}(\boldsymbol{k},\omega) &= \frac{N_0^2 c}{4\pi\rho_s^2}\,\frac{T/\omega_{\boldsymbol{k}}}{1-e^{-\omega/T}}\,\ln\left(\frac{\sinh(|\omega_{\boldsymbol{k}}+\omega|/4T)}{\sinh(|\omega_{\boldsymbol{k}}-\omega|/4T)}\right) \\ &= \frac{N_0^2 c}{16\pi\rho_s^2}\,\frac{1}{1-e^{-\omega/T}}\left[\left|1+\frac{\omega}{\omega_{\boldsymbol{k}}}\right|-\left|1-\frac{\omega}{\omega_{\boldsymbol{k}}}\right|\right. \\ &\quad \left.+\frac{4T}{\omega_{\boldsymbol{k}}}\,\ln\left(\frac{1-e^{-|\omega_{\boldsymbol{k}}+\omega|/2T}}{1-e^{-|\omega_{\boldsymbol{k}}-\omega|/2T}}\right)\right]. \end{aligned} \tag{3.38}$$

In the second equation, the first term is a contribution that survives the $T \to 0$ limit and the second term is qualitatively very similar to the ferromagnetic longitudinal structure factor from Eq. (3.24). The first term represents the quantum fluctuations that are responsible for the singular behavior of $\chi_{\mathrm{L}}^{(1)}(\boldsymbol{k})$ at $T = 0$. The second term has the same logarithmic singularity at the magnon resonance frequency $\omega = \pm\omega_{\boldsymbol{k}}$ as the ferromagnetic case. This structure factor is plotted in Fig. 13.

The zero-temperature limit of Eq. (3.38) does not vanish as $\omega \to \infty$, instead it is constant. This statement is equivalent to the logarithmic divergence in the static susceptibility. This fact can be verified by calculating the minus first moment of the spectrum $\chi''_{\mathrm{L}}(\boldsymbol{k},\omega) = (1-e^{-\omega/T})S_L(\boldsymbol{k},\omega)/2$ in the $T \to 0$ limit, which recovers Eq. (3.33a).

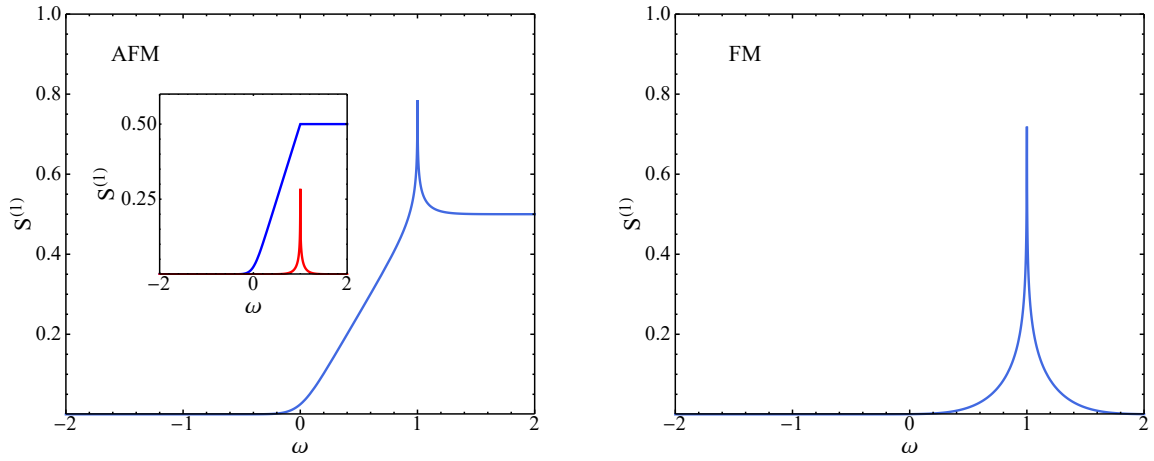

FIGURE 13. The one-loop contribution to the longitudinal part of the dynamical structure factor for an antiferromagnet (left panel) and a ferromagnet (right panel), normalized by $N_0^2 c/4\pi\rho_s^2$ and as Figs. 11 and 12, respectively, for $T/\omega_{\boldsymbol{k}} = 0.05$ as functions of the frequency ω measured in units of $\omega_{\boldsymbol{k}}$. The inset in the left panel separately shows the $T = 0$ contribution to the antiferromagnetic structure factor (blue curve) and the contribution that vanishes as $T \to 0$ (red curve). The structure factor shown in the main panel is the sum of these two contributions, as expressed in Eq. (3.38)

In the classical limit, Eq. (3.38) becomes

$$S_L^{(1)}(\boldsymbol{k},\omega) = \frac{N_0^2 c}{4\pi\rho_s^2}\,\frac{T^2}{\omega\omega_{\boldsymbol{k}}}\,\ln\left(\frac{\omega_{\boldsymbol{k}}+\omega}{\omega_{\boldsymbol{k}}-\omega}\right)^2, \tag{3.39}$$

analogous to Eq. (3.25).

In $d = 2$ at $T = 0$, the result is

$$S_L^{(1)}(\boldsymbol{k},\omega) = \frac{N_0^2 c^2}{4\rho_s^2}\,\Theta(\omega^2-\omega_{\boldsymbol{k}}^2)\,\frac{\Theta(\omega)}{\sqrt{\omega^2-\omega_{\boldsymbol{k}}^2}}. \tag{3.40}$$

Calculating the minus first frequency moment recovers Eq. (3.34a). For $T > 0$, there is no long range order in $d = 2$.

All the previous calculations were performed in the case of a vanishing external magnetic field. The following briefly describes the effects of a nonzero external field $\boldsymbol{H}$. The $(\boldsymbol{H} \times \hat{\boldsymbol{n}})^2$ term in the action, Eq. (3.26a), implies that in the ground state the order-parameter vector $\hat{n}$ is perpendicular to $\boldsymbol{H}$. Assuming $\boldsymbol{H} = (H, 0, 0)$ and parameterizing as in Eq. (3.27), the Gaussian action is

$$\mathcal{A}^{(2)}[\pi_1, \pi_2] = \frac{\rho_s}{2c^2} \sum_k \sum_{i=1}^{2} \pi_i(k)\, \mu_i(k)\, \pi_i(-k) \tag{3.41a}$$

where

$$\mu_1(k) = \mu(k) + (\mu H)^2 \quad , \quad \mu_2(k) = \mu(k), \tag{3.41b}$$

with $\mu(k)$ unchanged from the zero field case. Therefore, one of the two Goldstone modes in the zero field case acquires a mass and the other remains unchanged. Then, the nonzero field counterpart of Eq. (3.29) is

$$\chi_{\mathrm{L}}^{(1)}(k) = \left(\frac{N_0 c^2}{\rho_s}\right)^2 \frac{T}{V} \sum_p \sum_i \frac{1}{\mu_i(p)\mu_i(p-k)}. \tag{3.42}$$

Therefore, due to the presence of a massless mode, there is a singularity for $\boldsymbol{k} \to 0$ even for $H \neq 0$. At $T = 0$ in $d = 3$, to leading logarithmic accuracy,

$$\chi_{\mathrm{L}}^{(1)}(\boldsymbol{k}, i0) = \frac{N_0^2 c}{16\pi^2 \rho_s^2} \left[\log\left(\frac{\omega_0}{\omega_{\boldsymbol{k}}}\right) + \log\left(\frac{\omega_0}{\sqrt{\omega_{\boldsymbol{k}}^2 + (2\mu H)^2}}\right)\right]. \tag{3.43}$$

The corresponding result in $d = 2$ is

$$\chi_{\rm L}^{(1)}(\boldsymbol{k}, i0) = \frac{N_0^2 c^2}{16\rho_s^2}\,\frac{1}{\omega_{\boldsymbol{k}}}\left[1 + \frac{2}{\pi^2}\,g(\omega_{\boldsymbol{k}}/\sqrt{\omega_{\boldsymbol{k}}^2 + (2\mu H)^2})\right], \tag{3.44a}$$

$$g(x) = \int_{-1}^{1} d\eta\,\frac{\ln(1+x\eta)}{\eta\sqrt{1-\eta^2}} = \begin{cases} \pi^2/2 & \text{for } x = 1 \\ \pi x & \text{for } x \to 0 \end{cases}. \tag{3.44b}$$

For $\mu H \ll \omega_{\boldsymbol{k}}$, Eq. (3.34a) is recovered. For $\mu H \gg \omega_{\boldsymbol{k}}$, $\chi_{\rm L}^{(1)}(\boldsymbol{k}, i0) \propto 1/H$. Corresponding results are obtained for $\chi_{\rm L}^{(1)}$ as a function of the frequency.

Effects of Damped Ferromagnetic Magnons

In the preceding discussion, the effects of damping on the magnons have been neglected. This section determines the effects of magnon damping on the longitudinal susceptibility and the longitudinal dynamical structure factor in ferromagnets. To this end, the effects of damping on the ferromagnetic Goldstone mode need to be determined. Using the standard time-dependent Ginzburg-Landau theory for a ferromagnet [14, 56, 57], we have an equation of motion

$$\partial_t \boldsymbol{M}(\boldsymbol{x}, t) = \boldsymbol{M}(\boldsymbol{x}, t) \times \frac{\delta S}{\delta \boldsymbol{M}(\boldsymbol{x})}\bigg|_{\boldsymbol{M}(\boldsymbol{x},t)} - \int d\boldsymbol{y}\,\Gamma(\boldsymbol{x} - \boldsymbol{y})\frac{\delta S}{\delta \boldsymbol{M}(\boldsymbol{y})}\bigg|_{\boldsymbol{M}(\boldsymbol{y},t)}. \tag{3.45a}$$

Here, $\Gamma(\boldsymbol{x})$ is a damping operator and S a suitable action for the static magnetization $\boldsymbol{M}(\boldsymbol{x})$, say the Landau-Ginzburg functional of Eq. (1.2). To linear order in $\boldsymbol{M}$,

$$\frac{\delta S}{\delta \boldsymbol{M}(\boldsymbol{x})} = -\frac{\rho_s}{M_0^2}\,\boldsymbol{\nabla}^2 \boldsymbol{M}(\boldsymbol{x}) - \mu \boldsymbol{H}. \tag{3.45b}$$

The notation used for the prefactor of the gradient-squared term is the same as the one used in the ferromagnetic NLσM.

Using Eq. (3.45), the linear response of the transverse magnetization components to the external field $\boldsymbol{H}$, i.e., the transverse magnetic susceptibility $\chi_{\rm T}$, is calculated:

$$\begin{aligned}\chi_{\rm T}(k) &= \frac{M_0}{(D\,\boldsymbol{k}^2 + \mu H)^2 + (\Omega_n + \mathrm{sgn}\,(\Omega_n)\Gamma_{\boldsymbol{k}}\boldsymbol{k}^2)^2} \\ &\quad \times \begin{pmatrix} D\,\boldsymbol{k}^2 + \mu H & \Omega_n + \mathrm{sgn}\,(\Omega_n)\Gamma_{\boldsymbol{k}}\boldsymbol{k}^2 \\ -(\Omega_n + \mathrm{sgn}\,(\Omega_n)\Gamma_{\boldsymbol{k}}\boldsymbol{k}^2) & D\,\boldsymbol{k}^2 + \mu H \end{pmatrix}. \end{aligned} \tag{3.46}$$

The above result is Eq. (3.6b) with the substitution $\Omega_n \to \Omega_n + \mathrm{sgn}\,(\Omega_n)\Gamma_{\boldsymbol{k}}\boldsymbol{k}^2$. Here, $\Gamma_{\boldsymbol{k}}$ is the Fourier transform of $\Gamma(\boldsymbol{x})$.

An interesting aspect of ferromagnetic magnons is that these excitations cannot be overdamped, irrespective of the magnitude of the damping coefficient. This is because the poles of $\chi_{\rm T}(\boldsymbol{k}, z)$, with z the complex frequency, always have a real part given by $\pm D\boldsymbol{k}^2$, independent of $\Gamma_{\boldsymbol{k}}$. This is in contrast to a damped harmonic oscillator, where the resonance frequency has no real part if the damping coefficient is larger than a threshold value, and also to sound waves in fluids [37], antiferromagnetic magnons and helimagnons in helical magnets [26] - all of which have the same structure as a damped harmonic oscillator.

The one-loop contribution to the longitudinal susceptibility by the damped spin-waves is still given by Eq. (3.14), but with $\lambda_\pm$ replaced by

$$\lambda_\pm(\boldsymbol{k}, i\Omega_n) = D\boldsymbol{k}^2 + \mu H \mp i\Omega_n \mp i\Gamma_{\boldsymbol{k}}\boldsymbol{k}^2 \mathrm{sgn}\,(\Omega_n). \tag{3.47}$$

The sgn (Ω_n) in the damping term follows from causality requirements. The damping coefficient is written as an expansion in the long-wavelength limit,

$$\Gamma_{\boldsymbol{k}\to 0} = \gamma_0 + \gamma_2 \boldsymbol{k}^2. \tag{3.48}$$

The above expansion separates two physically distinct cases [57]:

1. A nonconserved order parameter, i.e., $\dfrac{d}{dt}\boldsymbol{M}^{\text{total}} \neq 0$, in which case $\gamma_0 > 0$. This is realized, for example, by magnetic impurities [58, 59].

2. A conserved order parameter, i.e., $\dfrac{d}{dt}\boldsymbol{M}^{\text{total}} = 0$, in which case $\gamma_0 = 0$. This is realized by, e.g., damping by electron-magnon and/or magnon-magnon interactions at $T > 0$ [60] or by nonmagnetic quenched disorder at any temperature, including $T = 0$ [59, 61, 62].

In the following, the integrals in Eq. (3.14), with $\lambda_\pm$ as defined in Eq. (3.47) and $H = 0$, are performed.

Nonconserved Order Parameter

For a nonconserved order parameter, $\Gamma_{\boldsymbol{p}} = \gamma_0$. For $d = 3$ and at $T = 0$, keeping only the leading terms,

$$\chi_{\text{L}}^{(1)}(\boldsymbol{k} \to 0, i0) = \text{const.} - \frac{1}{32\pi}\,\frac{\gamma_0/\sqrt{D}}{\gamma_0^2 + D^2}\,\sqrt{\omega_{\boldsymbol{k}}}. \tag{3.49a}$$

Since $\omega_{\boldsymbol{k}} = D\boldsymbol{k}^2$, $\chi_{\rm L}^{(1)}(\boldsymbol{k})$ has a $|\boldsymbol{k}|$ nonanalyticity at $T = 0$ for $d = 3$, with the prefactor of the nonanalyticity that vanishes as $\gamma_0 \to 0$. Similarly,

$$\begin{aligned}
\chi_{\rm L}^{(1)}(\boldsymbol{k}=0, i\Omega_n) &= \frac{2}{\pi V}\,\sum_{\boldsymbol{p}} \Gamma_{\boldsymbol{p}}\,\boldsymbol{p}^2 \int_{\omega_{\boldsymbol{p}}^2}^{\infty} dx\, \frac{1}{x + (\Gamma_{\boldsymbol{p}}\,\boldsymbol{p}^2)^2}\, \frac{1}{x + (\Gamma_{\boldsymbol{p}}\,\boldsymbol{p}^2 + \Omega_n)^2} \\
&= \frac{2}{\pi V}\,\sum_{\boldsymbol{p}} \Gamma_{\boldsymbol{p}}\,\boldsymbol{p}^2\, \frac{1}{\Omega_n^2 + 2\Omega_n \Gamma_{\boldsymbol{p}}\,\boldsymbol{p}^2}\, \ln\left(1 + \frac{\Omega_n^2 + 2\Omega_n \Gamma_{\boldsymbol{p}}\,\boldsymbol{p}^2}{\omega_{\boldsymbol{p}}^2 + (\Gamma_{\boldsymbol{p}}\,\boldsymbol{p}^2)^2}\right) \\
&= \frac{2}{\pi} \int_0^1 d\alpha\, \frac{1}{V} \sum_{\boldsymbol{p}} \frac{\Gamma_{\boldsymbol{p}}\,\boldsymbol{p}^2}{\alpha\Omega_n^2 + 2\alpha\Omega_n \Gamma_{\boldsymbol{p}}\,\boldsymbol{p}^2 + \omega_{\boldsymbol{p}}^2 + (\Gamma_{\boldsymbol{p}}\,\boldsymbol{p}^2)^2}. \qquad (3.49b)
\end{aligned}$$

In the last line, the logarithm has been expressed in terms of an auxiliary integral. After splitting off the constant contribution at $\Omega_n = 0$ in $d = 3$, and scaling out the frequency,

$$\begin{aligned}
\chi_{\rm L}^{(1)}(\boldsymbol{k}=0, i\Omega_n) &= \text{const.} - \frac{\gamma_0}{\pi^3 D^{5/2}}\, f(\gamma_0/D)\, |\Omega_n|^{1/2}, \qquad (3.49c) \\
\chi_{\rm L}^{(1)}(\boldsymbol{k}=0, i\Omega_n \to \Omega + i0) &= \text{const.} - \\
&\qquad \frac{\gamma_0}{\sqrt{2}\pi^3 D^{5/2}}\, f(\gamma_0/D)[1 - i\,\mathrm{sgn}\,(\Omega)]|\Omega|^{1/2}. \qquad (3.49d)
\end{aligned}$$

The function f is given by

$$\begin{aligned}
f(x) &= \frac{1}{(1+x^2)^2} \int_0^1 d\alpha\, \alpha \int_0^\infty dy\, \frac{1 + 2xy^2}{y^4 + 2y^2\alpha x/(1+x^2) + \alpha/(1+x^2)} \\
&= \frac{\pi}{6\sqrt{2}}\, \frac{1}{x^{5/2}(1+x^2)^{3/2}} \Big\{ \Big[3 + 7x^2 - 2x\sqrt{1+x^2}\Big]\, \sqrt{x^2 + x\sqrt{1+x^2}} \\
&\qquad\qquad -3(1+x^2)^{3/2} \sinh^{-1}(\sqrt{x}/(1+x^2)^{1/4}) \Big\}.
\end{aligned}$$

For small γ_0/D,

$$f(\frac{\gamma_0}{D} \to 0) = \frac{\sqrt{2}\pi}{5} + \frac{3\pi}{7\sqrt{2}}\, \frac{\gamma_0}{D} + O(\frac{\gamma_0^2}{D^2}). \qquad (3.49e)$$

In $d = 2$, there is a logarithmic singularity. This can be seen easily by looking at the last line of Eq. (3.49b) and power counting. Explicitly,

$$\chi_{\rm L}^{(1)}(\boldsymbol{k} \to 0, i0) = \frac{1}{2\pi^2} \frac{\gamma_0}{\gamma_0^2 + D^2} \ln(\omega_0/\omega_{\boldsymbol{k}}), \tag{3.50a}$$

$$\chi_{\rm L}^{(1)}(\boldsymbol{k} = 0, i\Omega_n) = \frac{1}{2\pi^2} \frac{\gamma_0}{\gamma_0^2 + D^2} \ln(\omega_0/|\Omega_n|), \tag{3.50b}$$

$$\chi_{\rm L}^{(1)}(\boldsymbol{k} = 0, i\Omega_n \to \Omega + i0) = \frac{1}{2\pi^2} \frac{\gamma_0}{\gamma_0^2 + D^2} \left[\ln(\omega_0/|\Omega|) + i \frac{\pi}{2} \operatorname{sgn} \Omega \right]. \tag{3.50c}$$

Conserved Order Parameter

For a conserved order parameter, $\Gamma_{\boldsymbol{p}} = \gamma_2 \boldsymbol{p}^2$. Using this in Eq. (3.49b) and to linear order in γ_2, we get the following results.

For $d = 3$,

$$\chi_{\rm L}^{(1)}(\boldsymbol{k} \to 0, i0) = \text{const.} + \frac{\gamma_2}{64\pi D^{7/2}} \omega_{\boldsymbol{k}}^{3/2} + O(\boldsymbol{k}^2), \tag{3.51a}$$

$$\chi_{\rm L}^{(1)}(\boldsymbol{k} = 0, i\Omega_n) = \text{const.} - \frac{\sqrt{2}\,\gamma_2}{7\pi^2 D^{7/2}} |\Omega_n|^{3/2}, \tag{3.51b}$$

$$\chi_{\rm L}^{(1)}(\boldsymbol{k} = 0, i\Omega_n \to \Omega + i0) = \text{const.} + \frac{\gamma_2}{7\pi^2 D^{7/2}} [1 + i \operatorname{sgn}(\Omega)] |\Omega|^{3/2}. \tag{3.51c}$$

In $d = 2$, the leading singularity is

$$\chi_{\rm L}^{(1)}(\boldsymbol{k} \to 0, i0) = \text{const.} - \frac{\gamma_2}{48\pi^2 D^3} \omega_{\boldsymbol{k}} \ln(\omega_0/\omega_{\boldsymbol{k}}), \tag{3.52a}$$

$$\chi_{\rm L}^{(1)}(\boldsymbol{k} = 0, i\Omega_n) = \text{const.} - \frac{\gamma_2}{6\pi D^3} |\Omega_n|, \tag{3.52b}$$

$$\chi_{\rm L}^{(1)}(\boldsymbol{k} = 0, i\Omega_n \to \Omega + i0) = \text{const.} + \frac{i\gamma_2}{6\pi D^3} \Omega. \tag{3.52c}$$

The nonanalyticities obtained are weaker in comparison with the nonconserved order parameter case.

To summarize, in ferromagnets with undamped magnons, the nonanalytic frequency and wave-number dependence of the one-loop contribution to the longitudinal susceptibility is absent at zero temperature. This is due to the absence of fluctuations that couple to the longitudinal magnetization fluctuations. However, when damped magnons were considered, certain nonanalyticities were found. This is a consequence of additional fluctuations introduced by the disorder in the system. Furthermore, magnetic disorder which couples directly to the order parameter, has a stronger effect than nonmagnetic disorder and thus results in a stronger singularity.

Renormalization-group Interpretation of the Results

In the following, we confirm all of the aforementioned ferromagnetic results using scaling arguments and renormalization-group considerations. It will be demonstrated that the exponents of the nonanalyticties obtained when damping is considered, are asymptotically exact.

The following is a schematic Gaussian action, with a damping term included according to the prescription $\Omega_n \to \Omega_n + \mathrm{sgn}\,(\Omega_n)\Gamma_{\boldsymbol{k}}\boldsymbol{k}^2$. This schematic action is in a notation that shows only what is necessary for power counting and is as follows:

$$\mathcal{A}^{(2)} = \int dx\, \pi(x)\left[D\partial_x^2 + \partial_\tau + H + \gamma_n \partial_x^{n+2}\right]\pi(x), \tag{3.53}$$

where $\pi(x)$ is the transverse magnetization fluctuations. Here, $n = 0$ and $n = 2$ correspond to cases of a nonconserved and conserved order parameter, respectively. Any additional terms in the action fall into two classes:

1. Gaussian with additional gradients, with the leading terms of the form

$$\delta\mathcal{A}^{(2)} = \int dx\, \partial_x^4 \pi^2(x), \tag{3.54a}$$

   or equivalent in terms of scale dimensions.

2. Higher order in π, with leading terms of the form

$$\delta\mathcal{A}^{(4)} = \int dx\, \partial_x^2 \pi^4(x), \tag{3.54b}$$

   or equivalent.

We now sketch a renormalization-group analysis of this action. Using the scheme pioneered by Shang-Keng Ma [14], scale dimensions are assigned to lengths and imaginary times, respectively: $[L] = -1, [\tau] = -2$. Then, there is a stable Gaussian fixed point where π has a scale dimension $[\pi(x)] = d/2$. In Fourier space, this corresponds to $[\pi(k)] = -1$. Thus, $\langle \pi(k)\pi(-k)\rangle \sim 1/\boldsymbol{k}^2 \sim 1/\Omega_n$. This scaling behavior describes the magnons and the Gaussian fixed point describes the ordered phase where the symmetry is broken. The field H is relevant with respect to this fixed point with a scale dimension $[H] = 2$. For a nonconserved order parameter, the damping coefficient γ_0 is dimensionless, $[\gamma_0] = 0$, and the damping term is part of the fixed-point Hamiltonian. The free energy density f, the magnetization m, and the scaling part $\delta\chi_{\rm L}$ of the longitudinal susceptibility $\chi_{\rm L} = \partial m/\partial H$ then have scale dimensions $[f] = d - 2, [m] = d$, and $[\delta\chi_{\rm L}] = d - 2$, respectively. Then we can write down the homogeneity law

$$\delta\chi_{\rm L}(\boldsymbol{k}, i\Omega_n) = b^{2-d}\, F_\chi(\boldsymbol{k}b, i\Omega_n b^2, \gamma_0), \tag{3.55}$$

with b an arbitrary length rescaling factor and F_χ a scaling function. This function has the property $F_\chi(x, y, \gamma_0 \to 0) = O(\gamma_0)$. This yields the scaling behavior

$$\delta\chi_{\mathrm{L}}(\boldsymbol{k}, i\Omega_n) \sim \gamma_0 |\boldsymbol{k}|^{d-2} \sim \gamma_0 |\Omega_n|^{(d-2)/2}, \tag{3.56}$$

which agrees with the explicit calculations. The leading correction terms to the fixed-point action are irrelevant by power counting, with scale dimensions -2 for the operator in Eq. (3.54a) and $-d$ for the one in Eq. (3.54b), respectively. This implies that the one-loop results obtained in the previous section are exact as far as the exponents are concerned. Higher order terms in the loop expansion will change the prefactor of the nonanalyticity, but not the power.

In the case of conserved order parameter dynamics, the damping term is not part of the fixed-point action. It is an irrelevant operator with a scale dimension $[\gamma_2] = -2$, which is the same as the operator in Eq. (3.54a). The homogeneity equation for $\delta\chi_{\mathrm{L}}$ is now

$$\delta\chi_{\mathrm{L}}(\boldsymbol{k}, i\Omega_n) = b^{2-d} F_\chi(\boldsymbol{k}b, i\Omega_n b^2, \gamma_2 b^{-2}). \tag{3.57a}$$

Other irrelevant operators are not shown. Even though γ_2 is irrelevant, the scaling function still vanishes for $\gamma_2 = 0$. Therefore, to linear order in γ_2,

$$\delta\chi_{\mathrm{L}}(\boldsymbol{k}, i\Omega_n) = b^{-d} \gamma_2 \tilde{F}_\chi(\boldsymbol{k}b, i\Omega_n b^2) \tag{3.57b}$$

with $\tilde{F}_\chi$ another scaling function. This yields

$$\delta\chi_{\mathrm{L}}(\boldsymbol{k}, i\Omega_n) \sim \gamma_2 |\boldsymbol{k}|^{d} \sim \gamma_2 |\Omega_n|^{d/2}, \tag{3.58}$$

which agrees with the calculations.

Conclusions

In summary, the coupling of the magnons in quantum ferromagnets and antiferromagnets to other correlation functions, in particular the longitudinal susceptibility and the longitudinal part of the dynamical structure factor, have been investigated. In the case of ferromagnets with undamped magnons, the magnon contribution to the longitudinal susceptibility vanishes at $T = 0$. In $d = 3$, and in the absence of an external magnetic field, an interpolating expression that correctly describes the leading behavior for both $T > \omega_{\boldsymbol{k}}$ and $T < \omega_{\boldsymbol{k}}$ is

$$\chi_{\mathrm{L}}^{(1)}(\boldsymbol{k}, H = 0) = \frac{T}{4D^{3/2}\sqrt{\omega_{\boldsymbol{k}}}} \frac{1}{1 + (\pi^2/c_L)\sqrt{\omega_{\boldsymbol{k}}/T}}, \tag{3.59}$$

where $\omega_{\boldsymbol{k}} = D\boldsymbol{k}^2$ is the ferromagnetic magnon frequency and c_L is a constant. For $T > \omega_{\boldsymbol{k}}$, the classical $1/|\boldsymbol{k}|$ is obtained. For $T < \omega_{\boldsymbol{k}}$, χ_{L} vanishes as $T^{3/2}$. For a quantum antiferromagnet, the corresponding interpolating expression is

$$\chi_{\mathrm{L}}^{(1)}(\boldsymbol{k}, i0) = \frac{N_0^2 c}{8\rho_s^2} \frac{T}{\omega_{\boldsymbol{k}}} \Big[1 + (\omega_{\boldsymbol{k}}/\pi^2 T) \log(\omega_0/\omega_{\boldsymbol{k}})\Big]. \tag{3.60}$$

Here, $\omega_{\boldsymbol{k}} = c|\boldsymbol{k}|$ is the antiferromagnetic magnon frequency. This reflects the expected scaling behavior: $1/|\boldsymbol{k}|$ for high temperatures, and $\ln|\boldsymbol{k}|$ for low temperatures. Similarly, the longitudinal structure factor vanishes at $T = 0$ in the ferromagnetic case, whereas in the antiferromagnetic case, there is a nonzero contribution even at $T = 0$. Quenched disorder introduces additional fluctuations, which lead to magnon damping and qualitatively change the ferromagnetic results. Magnetic impurities, which lead to a nonconserved order parameter, result in a longitudinal susceptibility that scales as $|\boldsymbol{k}|^{d-2}$, where the zero exponent in $d = 2$ signifies logarithmic divergence.

Nonmagnetic disorder leads to a weaker scaling, $|\boldsymbol{k}|^d$. For $T > 0$, the longitudinal dynamical structure factor has a logarithmic singularity at the magnon frequency in both ferromagnets and antiferromagnets.

The classical singularity of χ_{L} in the ferromagnetic case as a function of an external field has been observed experimentally [63]. The theoretical prediction is that in the limit of low temperatures, $T \ll \mu H$, χ_{L} becomes exponentially small. The logarithmic singularity at the magnon resonance frequency is a remarkable feature in the longitudinal dynamical structure factor. In a clean system at low temperature, the magnon damping is very weak and the spectrum of the transverse dynamical susceptibility has very narrow magnon peaks. The longitudinal susceptibility, or the structure factor, by contrast, shows an intrinsically broad feature at the magnon frequency. The prediction is that even a small magnetic field substantially broadens and suppresses this logarithmic singularity.

In the following, we interpret the differing results of ferromagnets and antiferromagnets using entanglement entropy arguments. The entanglement entropy gives a global measurement of fluctuations in a system. It is defined as the von Neumann entropy of a subsystem of linear size L. At zero temperature, the entropy vanishes in the thermodynamic limit, and for $L \to \infty$, it grows more slowly than the volume L^d. In systems that do not contain a Fermi surface, the leading contribution is in general given by an "area-law" term that grows as L^{d-1} [64]; this term is due to short-range entanglement and has a non-universal prefactor. The leading universal contribution, which is a measure of long-range fluctuations, in systems with Goldstone modes grows as $\ln L$. This is true for both quantum ferromagnets [65, 66], and antiferromagnets [67, 68, 69] for $d = 2, 3$. But, the area-law term is missing in the ferromagnetic case [66]. This is another indication that the fluctuations exist in the

ferromagnetic ground state, although they may or may not be probed by a specific correlation function. In metallic magnets, and more generally in systems with a Fermi surface, there is an area-law term with a multiplicative logarithm that is due to long-range fluctuations in the fermionic degrees of freedom. This is one of many indications of the fundamental differences between metallic and insulating magnets.

Finally, we recall Eq. (3.34a), which predicts that in a $T = 0$ antiferromagnet in $d = 2$, $\chi^{(1)}_{\rm L}(\boldsymbol{k} = 0, i\Omega_n) \propto 1/|\Omega_n|$. In real-time, this nonanalyticity signifies a constant long-time behavior, Eq. (A.19). The following is a comment on the physical meaning of this constant long-time behavior. Let $T_{\rm max}$ be the maximum time scale, which can be say, the total duration of the experiment, or L divided by the relevant characteristic velocity. $\chi_{\rm L}$ then depends on two times, t_1 and t_2. As long as t_1, t_2 and $|t_1 - t_2|$ all are small compared to $T_{\rm max}$, $\chi_{\rm L}$ will not decay as $|t_1 - t_2|$ increases. In position space, by contrast, $\chi_{\rm L}$ does decay, but only as a power: The $1/|\boldsymbol{k}|$ divergence in the 2-d quantum antiferromagnet is the same as the one in a 3-d classical magnet, and implies that in the real space the correlation function decays as $1/r$. This result is an example of an effect that can be even stronger: In classical non-equilibrium fluids, and in Fermi liquids even in equilibrium, there are correlation functions that increase with increasing length or time-scales in a well-defined sense[70, 71, 72].

An important point worth repeating is that the behavior of the longitudinal susceptibility, namely it vanishing at $T = 0$ in the undamped ferromagnetic case, is not generic, but rather restricted to a class of correlation functions that can be expressed entirely in terms of magnon number fluctuations. Other correlation functions do show the expected $\omega^{(d-2)/2}$ frequency scaling. An example of a correlation function belonging to the same class as the longitudinal susceptibility is the dynamical electrical conductivity in a metallic quantum ferromagnet. They both share the same

scaling behavior. This implies that the undamped magnons do not lead to an $\omega^{(d-2)/2}$ frequency dependence of the conductivity at $T = 0$, or a $\ln \omega$ singularity in $d = 2$. This is in contrast to the results from a previous work [20], which agrees only with the latter conclusion, because there was a sign error in the calculations. The detailed calculations of the conductivity are presented in the next chapter.

CHAPTER IV

AN EFFECTIVE FIELD THEORY APPROACH TO ITINERANT FERROMAGNETS

This work contains unpublished co-authored material. Dietrich Belitz and Theodore R. Kirkpatrick were the principal investigators for this work; Sripoorna Bharadwaj performed the calculations and produced the figures in this chapter. The calculations presented here are, in large parts, a reproduction of the calculations in [20]. However, there was a sign error in the original reference and this chapter reports the correct results.

Motivation

In the previous chapter, the magnon contributions to the longitudinal order-parameter susceptibility in quantum ferromagnets and antiferromagnets were calculated. The nonlinear sigma model provided a general theoretical framework for those calculations. The origin of the magnetization was not relevant in that discussion. In quantum ferromagnets, when undamped magnons were considered, their contribution to the longitudinal susceptibility vanished at $T = 0$. This was interpreted as a consequence of the longitudinal magnetization fluctuations being purely determined by the magnon-number fluctuations. In general, correlation functions that can be expressed entirely in terms of the magnon-number fluctuations all share this property of vanishing $T = 0$ contribution. A correlation function that can not be formulated as a correlation function of the magnon number, see Eqn. (3.15), was also considered and a singular nonzero $T = 0$ contribution was found. In

the conclusions section of the preceding chapter, we mentioned in passing that the dynamical electrical conductivity in a metallic quantum ferromagnet is a correlation function that belongs to the same class as the longitudinal susceptibility. The aim of the work presented in this chapter is to perform the conductivity calculations and explicitly prove this claim. For this purpose, the quantum ferromagnetic NLσM of the previous chapter is not suitable because it only describes the behavior of the magnetization, not the conduction electrons. Therefore, the Stoner model for itinerant ferromagnets introduced in Chapter II is considered.

An effective field theory is developed in terms of the quaternionic fields Q, which are bilinear products of the fermionic fields ψ and $\bar{\psi}$. This theory was used previously to describe a disordered Fermi liquid [45, 73]. It turns out that this theory also has a saddle-point solution, a "Stoner saddle-point", that corresponds to a ferromagnet - both with and without quenched disorder [20]. The magnonic soft modes are identified in this theory. The contributions of these soft modes to various observables like the longitudinal susceptibility, dynamical electrical conductivity and density of states are calculated by expanding about the saddle point to Gaussian order. These calculations are performed at the one-loop order within a loop expansion method that does not assume the electron-electron interaction to be a small parameter. This technique is fundamentally different from the perturbative schemes based on many-body diagrammatic theory. The power and generality of the loop-expansion method allows for a renormalization-group analysis that shows that the one-loop results represent the exact leading nonanalyticities.

Q-matrix Formalism

Action in terms of Composite Variables

We start with an action for the electrons in terms of the Grassmann valued fermionic fields $\bar{\psi}$ and ψ, which includes the spin-triplet interaction responsible for ferromagnetism,

$$S[\bar{\psi},\psi] = S_0[\bar{\psi},\psi] + \frac{\Gamma_t}{2}\int dx\ \boldsymbol{n}_{\rm s}(x).\boldsymbol{n}_{\rm s}(x). \tag{4.1}$$

where S_0 represents the free fermion action, $x = (\boldsymbol{x},\tau)$ denotes the real-space position $\boldsymbol{x}$ and imaginary-time variable τ. $n^i_{\rm s}(x) = \sum_{\alpha,\beta}\bar{\psi}_\alpha(x)\sigma^i_{\alpha,\beta}\psi_\beta(x)$ corresponds to the electronic spin-density. $\sigma^{1,2,3}$ are the Pauli matrices. The fields ψ and $\bar{\psi}$ carries a Matsubara frequency index n and a spin index $\sigma = (\uparrow,\downarrow) \equiv (+,-)$. Fermionic Matsubara frequencies are denoted by $\omega_n = 2\pi T(n+1/2)$ and bosonic Matsubara frequencies by $\Omega_n = 2\pi T n$. The units are such that $\hbar = 1$ and $k_B = 1$. The second term in Eq. (4.1) represents the spin-triplet interaction.

We are interested in the effects of spin waves in an itinerant ferromagnet. These spin waves involve fluctuations of the electronic spin density $\boldsymbol{n}_{\rm s}$, which is a bilinear product of ψ and $\bar{\psi}$. Hence, it is useful to transform to a field theory in terms of composite variables. We introduce a matrix of bilinear products of the fermion fields,

$$B_{12} = \frac{i}{2}\begin{pmatrix} -\psi_{1\uparrow}\bar{\psi}_{2\uparrow} & -\psi_{1\uparrow}\bar{\psi}_{2\downarrow} & -\psi_{1\uparrow}\psi_{2\downarrow} & \psi_{1\uparrow}\psi_{2\uparrow} \\ -\psi_{1\downarrow}\bar{\psi}_{2\uparrow} & -\psi_{1\downarrow}\bar{\psi}_{2\downarrow} & -\psi_{1\downarrow}\psi_{2\downarrow} & \psi_{1\downarrow}\psi_{2\uparrow} \\ \bar{\psi}_{1\downarrow}\bar{\psi}_{2\uparrow} & \bar{\psi}_{1\downarrow}\bar{\psi}_{2\downarrow} & \bar{\psi}_{1\downarrow}\psi_{2\downarrow} & -\psi_{1\downarrow}\psi_{2\uparrow} \\ -\bar{\psi}_{1\uparrow}\bar{\psi}_{2\uparrow} & -\bar{\psi}_{1\uparrow}\bar{\psi}_{2\downarrow} & -\bar{\psi}_{1\uparrow}\psi_{2\downarrow} & \bar{\psi}_{1\uparrow}\psi_{2\uparrow} \end{pmatrix} \cong Q_{12}. \tag{4.2}$$

All the fields in Eq. (4.2) are taken at position $\boldsymbol{x}$ and $(1,2) \equiv (n_1,n_2)$ denotes the fermionic Matsubara frequencies. The elements of B commute with each other and

therefore are isomorphic to complex-valued (classical) fields Q. Consequently, the adjoint operation on a product of fermion fields is equivalent to complex conjugation of the classical fields. We can then rewrite the partition function by constraining B to Q using a functional δ function. This delta function can be enforced by means of a functional integral over an auxiliary or ghost complex valued field $\tilde{\Lambda}$, which plays the role of a Lagrange multiplier. Then, the fermionic fields can be integrated out to give an effective action entirely in terms of the classical matrix fields Q and $\tilde{\Lambda}$.

$$\begin{aligned} Z &= \int D[\bar{\psi},\psi]\, e^{S[\bar{\psi},\psi]} \int D[Q]\, \delta[Q-B] \\ &= \int D[\bar{\psi},\psi]\, e^{S[\bar{\psi},\psi]} \int D[Q]\, D[\tilde{\Lambda}]\, e^{\mathrm{tr}[\tilde{\Lambda}(Q-B)]} \\ &\equiv \int D[Q]\, D[\tilde{\Lambda}]\, e^{\mathcal{A}[Q,\tilde{\Lambda}]}. \end{aligned} \tag{4.3}$$

The matrix elements of both Q and $\tilde{\Lambda}$ are spin-quaternions, i.e. elements of $\mathcal{Q}\times\mathcal{Q}$, with $\mathcal{Q}$ the quaternion field. It is clear from Eq. (4.2) that expectation values of the Q matrix elements yield single particle Green functions and Q-Q correlations describe four-fermion correlation functions. To perform calculations involving the matrix field Q, it is useful to expand this 4×4 matrix field in a spin-quaternion basis,

$$Q_{12}(\boldsymbol{x}) = \sum_{r,i=0}^{3} (\tau_r \otimes s_i)\, {}^{i}_{r}Q_{12}(\boldsymbol{x}). \tag{4.4}$$

The same applies for $\tilde{\Lambda}$ as well. Here, $\tau_0 = s_0$ is the 2×2 unit matrix, and $\tau_j = -s_j = -i\,\sigma_j, (j=1,2,3)$, with $\sigma_{1,2,3}$ the Pauli matrices.

From Eq. (4.2), we note that $i = 1,2,3$ correspond to the spin-triplet and $r = 0,3$ describes the particle-hole channel ($\bar{\psi}\psi$ and $\psi\bar{\psi}$). Spin-singlet is given by $i = 0$, while $r = 1,2$ describes the particle-particle channel ($\psi\psi$ and $\bar{\psi}\bar{\psi}$).

In the spin-quaternion basis, the Q matrices have the following symmetry properties,

$$ {}^{0}_{r}Q_{12} = (-1)^{r}\ {}^{0}_{r}Q_{21} \qquad (r = 0, 3) \tag{4.5a} $$

$$ {}^{i}_{r}Q_{12} = (-1)^{r+1}\ {}^{i}_{r}Q_{21} \qquad (r = 0, 3; i = 1, 2, 3) \tag{4.5b} $$

$$ {}^{0}_{r}Q_{12} = {}^{0}_{r}Q_{21} \qquad (r = 1, 2) \tag{4.5c} $$

$$ {}^{i}_{r}Q_{12} = -\ {}^{i}_{r}Q_{21} \qquad (r = 1, 2; i = 1, 2, 3) \tag{4.5d} $$

$$ {}^{i}_{r}Q^{*}_{12} = -\ {}^{i}_{r}Q_{-n_1-1,-n_2-1} \tag{4.5e} $$

where $*$ denotes complex conjugation.

In Eq. (4.3), the 'tr' is a trace over all discrete indices that are not explicitly shown. The action $\mathcal{A}$ is the following.

$$ \mathcal{A}[Q, \tilde{\Lambda}] = \frac{1}{2}\mathrm{Tr}\log(G_0^{-1} - i\tilde{\Lambda}) + \int d\boldsymbol{x}\ \mathrm{tr}(\tilde{\Lambda}(\boldsymbol{x})Q(\boldsymbol{x})) + \mathcal{A}_{\mathrm{int}}. \tag{4.6a} $$

Here,

$$ G_0^{-1} = -\partial_\tau + \partial_{\boldsymbol{x}}^2/2m_{\mathrm{e}} + \mu \tag{4.6b} $$

is the inverse free electron Green operator, ∂_τ and $\partial_{\boldsymbol{x}}$ being the derivatives with respect to imaginary time and position, respectively. m_{e} is the electon mass and μ is the chemical potential. 'Tr' denotes trace over all degrees of freedom, including the continuous position variable. $\mathcal{A}_{\mathrm{int}}$ corresponds to the interacting part of the action and is given by

$$ \begin{aligned} \mathcal{A}_{\mathrm{int}} \;=\; & \frac{T\,\Gamma_t}{2}\int d\boldsymbol{x} \sum_{r=0,3}(-1)^r \sum_{n_1,n_2,m}\sum_{i=1}^{3}[\mathrm{tr}((\tau_r \otimes s_i)Q_{n_1,n_1+m}(\boldsymbol{x}))] \\ & \times\ [\mathrm{tr}((\tau_r \otimes s_i)Q_{n_2+m,n_2}(\boldsymbol{x}))]. \end{aligned} \tag{4.6c} $$

Stoner Saddle Point

The saddle point of the field theory Eq. (4.6) must represent an itinerant ferromagnet, with a spatially homogeneous ground state. Assuming the system orders along the 3-direction, the particle number density n and the magnetization M can be defined in terms of expectation values of Q fields in the spin-quaternion basis as

$$n = -4i\,T\sum_{n}\langle {}^{0}_{0}Q_{nn}(\boldsymbol{x})\rangle \tag{4.7a}$$

$$M = -4i\,\mu_B\,T\sum_{n}\langle {}^{3}_{3}Q_{nn}(\boldsymbol{x})\rangle, \tag{4.7b}$$

where μ_B is the Bohr magneton. The average $\langle\ldots\rangle$ is taken with respect to the full action Eq. (4.6).

Based on Eq. (4.7), the following ansatz for the saddle point can be used.

$${}^{i}_{r}Q_{12}|_{\mathrm{sp}} = \delta_{12}[\delta_{r0}\delta_{i0}G_{n_1} + \delta_{r3}\delta_{i3}F_{n_1}], \tag{4.8a}$$

$${}^{i}_{r}\tilde{\Lambda}_{12}|_{\mathrm{sp}} = \delta_{12}[-\delta_{r0}\delta_{i0}i\Sigma_{n_1} + \delta_{r3}\delta_{i3}i\Delta_{n}]. \tag{4.8b}$$

The saddle-point condition is

$$\left.\frac{\delta\mathcal{A}}{\delta Q}\right|_{Q_{\mathrm{sp}},\tilde{\Lambda}_{\mathrm{sp}}} = \left.\frac{\delta\mathcal{A}}{\delta\tilde{\Lambda}}\right|_{Q_{\mathrm{sp}},\tilde{\Lambda}_{\mathrm{sp}}} = 0. \tag{4.9}$$

This yields the following equations,

$$G_n = \frac{i}{2V}\sum_{\boldsymbol{k}} \frac{i\omega_n - \xi_{\boldsymbol{k}}}{(i\omega_n - \xi_{\boldsymbol{k}})^2 - \Delta_n^2} = \frac{i}{2V}\sum_{\boldsymbol{k}} \mathcal{G}_n(\boldsymbol{k}) \tag{4.10a}$$

$$F_n = -\frac{i}{2V}\sum_{\boldsymbol{k}} \frac{\Delta_n}{(i\omega_n - \xi_{\boldsymbol{k}})^2 - \Delta_n^2} = \frac{i}{2V}\sum_{\boldsymbol{k}} \mathcal{F}_n(\boldsymbol{k}) \tag{4.10b}$$

$$\Sigma_n = 0 \tag{4.10c}$$

$$\Delta_n = -4i\,\Gamma_t\, T\sum_m e^{i\omega_m 0} F_m = \Delta, \tag{4.10d}$$

with $\xi_{\boldsymbol{k}} = \boldsymbol{k}^2/2m_{\mathrm{e}} - \mu$ and $\Delta = \Gamma_t M/\mu_B$. The last equation in Eq. (4.10) leads to the familiar equation of state from Stoner theory:

$$1 = -2\Gamma_t\, T\sum_n \frac{1}{V}\sum_{\boldsymbol{k}} \frac{1}{(i\omega_n - \xi_{\boldsymbol{k}})^2 - \Delta^2}. \tag{4.11}$$

The above equation also recovers the Stoner criterion for the onset of magnetization. The threshold value of Γ_t is given by

$$2N_F\Gamma_t = 1, \tag{4.12}$$

where N_F is the density of states at the Fermi surface.

At this stage, a matrix saddle-point Green function can be defined as follows.

$$G_{\mathrm{sp}} = \left(G_0^{-1} - i\tilde{\Lambda}\right)^{-1}\Big|_{\mathrm{sp}} \tag{4.13a}$$

with

$$(G_{\mathrm{sp}})_{12} = \delta_{12}[\mathcal{G}_{n_1}(\tau_0 \otimes s_0) + \mathcal{F}_{n_1}(\tau_3 \otimes s_3)]. \tag{4.13b}$$

Expanding Q and $\tilde{\Lambda}$ about their saddle points as : $Q = Q_{\rm sp}+\delta Q$ and $\tilde{\Lambda} = \tilde{\Lambda}_{\rm sp}+\delta\tilde{\Lambda}$, the full action can be expressed in powers of δQ and $\delta\tilde{\Lambda}$. Keeping only the Gaussian order terms in the expansion gives $\mathcal{A} = \mathcal{A}_{\rm sp} + \mathcal{A}_{\rm G}$ with

$$\mathcal{A}_{\rm G} = \frac{1}{4}{\rm Tr}\Big(G_{\rm sp}\,\delta\tilde{\Lambda}\,G_{\rm sp}\,\delta\tilde{\Lambda}\Big) + {\rm Tr}(\delta\tilde{\Lambda}\,\delta Q) + \mathcal{A}_{\rm int}[\delta Q]. \tag{4.14}$$

After Fourier transforming the fields δQ and $\delta\tilde{\Lambda}$ as $\delta Q, \delta\tilde{\Lambda}(\boldsymbol{k}) = \int d\boldsymbol{x}\exp(i\boldsymbol{k}\,\boldsymbol{x})\,\delta Q, \delta\tilde{\Lambda}(\boldsymbol{x})$, the piece of Eq. (4.14) quadratic in $\delta\tilde{\Lambda}$ is

$$\mathcal{A}_{\rm quad}[\delta\tilde{\Lambda}] = \frac{1}{V}\sum_{\boldsymbol{k}}\sum_{1234}\sum_{r,s=\{0,3\}}\sum_{ij} {}^{i}_{r}(\delta\tilde{\Lambda})_{12}(\boldsymbol{k})\;{}^{ij}_{rs}A_{12,34}(\boldsymbol{k})\;{}^{j}_{s}(\delta\tilde{\Lambda})_{34}(-\boldsymbol{k}), \tag{4.15a}$$

with the matrix A defined as

$${}^{ij}_{rs}A_{12,34}(\boldsymbol{k}) = \delta_{13}\,\delta_{24}\,[\varphi^{00}_{n_1n_2}(\boldsymbol{k})\,m^{00}_{rs,ij}+\varphi^{03}_{n_1n_2}(\boldsymbol{k})\,m^{03}_{rs,ij}+\varphi^{30}_{n_1n_2}(\boldsymbol{k})\,m^{30}_{rs,ij}+\varphi^{33}_{n_1n_2}(\boldsymbol{k})\,m^{33}_{rs,ij}] \tag{4.15b}$$

where

$$\varphi^{ab}_{nm}(\boldsymbol{k}) = \frac{1}{V}\sum_{\boldsymbol{p}} G^{a}_{n}(\boldsymbol{p})\,G^{b}_{m}(\boldsymbol{p}+\boldsymbol{k}), \tag{4.15c}$$

with $a, b = 0, 3$, $G^0 = \mathcal{G}$ and $G^3 = \mathcal{F}$.

The m matrices are defined as

$$
\begin{aligned}
m^{00}_{rs,ij} &= \frac{1}{4}\mathrm{tr}(\tau_r\tau_s^\dagger)\mathrm{tr}(s_i s_j^\dagger) && \text{(4.15d)}\\
m^{03}_{rs,ij} &= \frac{1}{4}\mathrm{tr}(\tau_r\tau_3\tau_s^\dagger)\mathrm{tr}(s_i s_3 s_j^\dagger) && \text{(4.15e)}\\
m^{30}_{rs,ij} &= \frac{1}{4}\mathrm{tr}(\tau_3\tau_r\tau_s^\dagger)\mathrm{tr}(s_3 s_i s_j^\dagger) && \text{(4.15f)}\\
m^{33}_{rs,ij} &= \frac{1}{4}\mathrm{tr}(\tau_r\tau_s^\dagger)\begin{pmatrix}+\\-\\-\\+\end{pmatrix}_i \mathrm{tr}(s_i s_j^\dagger), && \text{(4.15g)}
\end{aligned}
$$

with $r,s=\{0,3\}$ and $\begin{pmatrix}+\\-\\-\\+\end{pmatrix}_i = \delta_{i0}-\delta_{i1}-\delta_{i2}+\delta_{i3}$. The matrix A has the following structure.

$$
A_{nm} = \begin{pmatrix}
X^+_{nm} & 0 & 0 & 0 & 0 & 0 & 0 & Y^+_{nm}\\
0 & X^-_{nm} & 0 & 0 & 0 & 0 & Y^-_{nm} & 0\\
0 & 0 & X^-_{nm} & 0 & 0 & -Y^-_{nm} & 0 & 0\\
0 & 0 & 0 & X^+_{nm} & -Y^+_{nm} & 0 & 0 & 0\\
0 & 0 & 0 & -Y^+_{nm} & X^+_{nm} & 0 & 0 & 0\\
0 & 0 & -Y^-_{nm} & 0 & 0 & X^-_{nm} & 0 & 0\\
0 & Y^-_{nm} & 0 & 0 & 0 & 0 & X^-_{nm} & 0\\
Y^+_{nm} & 0 & 0 & 0 & 0 & 0 & 0 & X^+_{nm}
\end{pmatrix} \qquad \text{(4.16a)}
$$

where, using φ^{ab}_{nm} as defined in Eq. (4.15c),

$$
\begin{aligned}
X^\pm_{nm} &= \varphi^{00}_{nm} \pm \varphi^{33}_{nm}\\
Y^\pm_{nm} &= \varphi^{03}_{nm} \pm \varphi^{30}_{nm} && \text{(4.16b)}
\end{aligned}
$$

Rescaling Q by a factor of 4, defining a new field $\bar{\Lambda}$ via

$$\delta\tilde{\Lambda}(\boldsymbol{k}) = 2A^{-1}(\delta\bar{\Lambda}(\boldsymbol{k}) - \delta Q(\boldsymbol{k})) \tag{4.17}$$

and using the above expression for $\delta\tilde{\Lambda}$ in Eq. (4.14), $\bar{\Lambda}$ and Q decouple. Then, $\delta\bar{\Lambda}$ can be integrated out, leaving behind a Gaussian action purely in terms of δQ.

$$\mathcal{A}_{\mathrm{G}}[\delta Q] = -\frac{4}{V}\sum_{\boldsymbol{k}}\sum_{1234}\sum_{r,s=\{0,3\}}\sum_{ij} {}^{i}_{r}(\delta Q)_{12}(\boldsymbol{k})\, {}^{ij}_{rs}\mathcal{M}_{12,34}(\boldsymbol{k})\, {}^{j}_{s}(\delta Q)_{34}(-\boldsymbol{k}) \tag{4.18a}$$

with

$${}^{ij}_{rs}\mathcal{M}_{12,34}(\boldsymbol{k}) = \delta_{13}\,\delta_{24}\,{}^{ij}_{rs}[(A_{12})^{-1}](\boldsymbol{k}) + 2\,T\,\Gamma_t\,\delta_{1-2,3-4}\,\delta_{rs}\,\delta_{ij}\,(1-\delta_{i0}). \tag{4.18b}$$

The matrix $\mathcal{M}$ is an 8×8 matrix, since $r, s = \{0, 3\}$ and $i, j = \{0, 1, 2, 3\}$. A^{-1} is the inverse of A defined in Eq. (4.15b). Using Eq. (4.18), the Gaussian Q propagators can be written down. At this stage, frequency restrictions on the Q matrix fields are enforced by only considering matrix elements Q_{12} with $n_1 \geq n_2$. This is done to remove any redundancies arising from the symmetry properties of Q, Eq. (4.5). We find

$$\langle {}^{i}_{r}(\delta Q)_{12}(\boldsymbol{k})\, {}^{j}_{s}(\delta Q)_{34}(-\boldsymbol{p})\rangle_{\mathrm{G}} = \delta_{\boldsymbol{k},\boldsymbol{p}}\frac{V}{16}\,{}^{ij}_{rs}I_{12}\,{}^{ij}_{rs}\mathcal{M}^{-1}_{12,34}(\boldsymbol{k}) \tag{4.19a}$$

with

$${}^{ij}_{rs}I_{12} = 1 + \delta_{12}[-1 + J^{ij}_{rs}], \tag{4.19b}$$

The matrix J is given by the following.

$$J^{ij}_{rs} = \frac{1}{4}\mathrm{tr}(\tau_r\tau_s\tau_3^\dagger)\,\delta_{r0}\left[\mathrm{tr}(s_i s_j s_3^\dagger) + \begin{pmatrix}+\\+\\+\\-\end{pmatrix}_i \mathrm{tr}(s_j s_i s_3^\dagger)\right]$$
$$+ \frac{1}{4}\mathrm{tr}(\tau_r\tau_s\tau_3^\dagger)\,\delta_{r3}\left[\mathrm{tr}(s_i s_j s_3^\dagger) - \begin{pmatrix}+\\+\\+\\-\end{pmatrix}_i \mathrm{tr}(s_j s_i s_3^\dagger)\right] + 2\,\delta_{rs}\,\delta_{ij}\,[\delta_{r0}\,\delta_{i0} + \delta_{r3}\,(1-\delta_{i0})] \tag{4.19c}$$

and

$$^{ij}_{rs}\mathcal{M}^{-1}_{12,34}(\boldsymbol{k}) = \delta_{13}\delta_{24}\,^{ij}_{rs}A_{n_1n_2}(\boldsymbol{k}) + \delta_{1-2,3-4}\,^{ij}_{rs}E_{n_1n_2,n_3,n_4}(\boldsymbol{k}) \tag{4.19d}$$

where the 8×8 matrix E, which is the interacting part of the propagator, is defined as

$$E_{n_1n_2,n_3n_4}(\boldsymbol{k}) = A_{n_1n_2}(\boldsymbol{k}).B.\left[\mathbb{I}_{8\times 8} - \sum_{n_5,n_6}\delta_{n_1-n_2,n_5-n_6}A_{n_5n_6}(\boldsymbol{k}).B\right]^{-1}.A_{n_3n_4}(\boldsymbol{k}), \tag{4.19e}$$

with

$$B = -2\,T\,\Gamma_t\,\delta_{rs}\,\delta_{ij}\,(1-\delta_{i0}). \tag{4.19f}$$

The elements of E that diverge as $\boldsymbol{k}\to 0$ and $n_1\to n_2$ correspond to the soft modes of the system. Taking $\left[\mathbb{I}_{8\times 8} - \sum_{n_5,n_6}\delta_{n_1-n_2,n_5-n_6}A_{n_5n_6}(\boldsymbol{k}).B\right]$, we identify which elements on the diagonal and the anti-diagonal go to zero in the $\boldsymbol{k}\to 0, n_1-n_2\to 0$ limit.

Using the following,

$$\varphi^{03}_{nn}(\boldsymbol{k}=0) - \varphi^{30}_{nn}(\boldsymbol{k}=0) = 0 \tag{4.20a}$$

and

$$1 + 2\,\Gamma_t\,T\sum_n [\varphi^{00}_{nn}(\boldsymbol{k}=0) - \varphi^{33}_{nn}(\boldsymbol{k}=0)] = 0, \tag{4.20b}$$

we find that ${}^{ij}_{rs}E$ is massless for $i,j = 1,2$. (It should be noted that Eq. (4.20b) is the same as Eq. (4.11).) These matrix elements are nothing but the magnetic Goldstone modes. In the limit $|\boldsymbol{k}|/k_{\rm F}, \Omega_n/\epsilon_{\rm F} \ll \Delta/\epsilon_{\rm F} \ll 1$, they take the following form.

$$g^{\pm}(\boldsymbol{k}, i\Omega_n) = \frac{d}{\pm i\Omega_n - c\boldsymbol{k}^2} \tag{4.21a}$$

with

$$c = \frac{\Delta}{6k_{\rm F}^2}, \qquad\qquad d = -\frac{\Delta}{2N_{\rm F}\Gamma_t}. \tag{4.21b}$$

Spin Waves and Longitudinal Susceptibility

One-loop Contribution

Having identified the spin-waves in the Gaussian order matrix field theory, we proceed to calculate the one-loop contribution of these soft modes to the longitudinal susceptibility $\chi_{\rm L}$. The aim here is to try and reproduce the results from Chapter III.

To perform this calculation, the following source term is added to Eq. (4.1).

$$S_j = -\sum_m \int d\boldsymbol{x}\, j_m(\boldsymbol{x}) \sum_n \sum_\sigma \sigma\, \bar{\psi}_{n,\sigma}(\boldsymbol{x})\, \psi_{n-m,\sigma}(\boldsymbol{x}). \tag{4.22a}$$

As before, the fermionic fields are integrated out by introducing the classical matrix fields Q and $\tilde{\Lambda}$. The source-dependent partition function is

$$Z[j] = \int D[Q]\, D[\tilde{\Lambda}]\, e^{\mathcal{A}[Q,\tilde{\Lambda},j]} \tag{4.22b}$$

with

$$\mathcal{A}[Q,\tilde{\Lambda},j] = \frac{1}{2}\mathrm{Tr}\log(G_0^{-1} + JL - i\tilde{\Lambda}) + \int d\boldsymbol{x}\ \mathrm{tr}(\tilde{\Lambda}(\boldsymbol{x})Q(\boldsymbol{x})) + \mathcal{A}_{\mathrm{int}}, \tag{4.22c}$$

where

$$(JL)_{12}(\boldsymbol{x}) = \frac{1}{2}\sum_m j_m(\boldsymbol{x}) L_{12,m} \tag{4.22d}$$

and

$$L_{12,m} = [(\tau_- \otimes \sigma_3)\, \delta_{n_1,n_2+m} - (\tau_+ \otimes \sigma_3)\, \delta_{n_2,n_1+m}], \qquad \tau_\pm = \tau_0 \pm i\tau_3. \tag{4.22e}$$

Then, $\chi_{\mathrm{L}}(\boldsymbol{k}, i\Omega_m)$ is given in terms of derivatives of $Z[j]$ as

$$\chi_{\mathrm{L}}(\boldsymbol{k}, i\Omega_m) = \frac{\partial^2}{\partial j_m(\boldsymbol{k}) \partial j_{-m}(-\boldsymbol{k})} \log Z[j]\bigg|_{j=0}. \tag{4.23}$$

Expanding the first term in Eq. (4.22c) in powers of j and $\delta\tilde{\Lambda}$, and utilizing Eq. (4.13), we find

$$\mathcal{A}[Q,\tilde{\Lambda},j] \supset \underbrace{-\frac{1}{4}\mathrm{Tr}(G_{\mathrm{sp}}JLG_{\mathrm{sp}}JL)}_{A_{(2,0)}} + \underbrace{-\frac{1}{2}\mathrm{Tr}(G_{\mathrm{sp}}JLG_{\mathrm{sp}}\delta\tilde{\Lambda}G_{\mathrm{sp}}\delta\tilde{\Lambda})}_{A_{(1,2)}}$$
$$\underbrace{\frac{3}{8}\Big[\mathrm{Tr}(G_{\mathrm{sp}}JLG_{\mathrm{sp}}\delta\tilde{\Lambda}G_{\mathrm{sp}}JLG_{\mathrm{sp}}\delta\tilde{\Lambda}) + \mathrm{Tr}(G_{\mathrm{sp}}JLG_{\mathrm{sp}}JLG_{\mathrm{sp}}\delta\tilde{\Lambda}G_{\mathrm{sp}}\delta\tilde{\Lambda})\Big]}_{A_{(2,2)}}$$
$$+ (\text{higher order terms}). \tag{4.24}$$

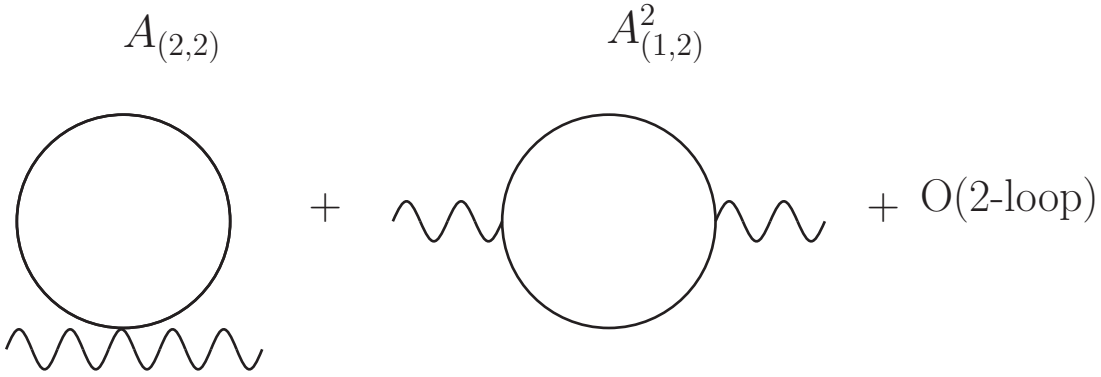

FIGURE 14. The solid lines represent $\delta\tilde{\Lambda}$ and the wavy lines represent JL

Fig. 14 is a diagrammatic representation of the terms $A_{(2,2)}$ and $A^2_{(1,2)}$. The higher order terms are neglected. Using Eq. (4.24) in Eq. (4.23),

$$\chi_{\mathrm{L}}(\boldsymbol{k}, i\Omega_m) = \frac{\partial^2}{\partial j_m(\boldsymbol{k})\partial j_{-m}(-\boldsymbol{k})}\bigg|_{j=0}\Big[\langle A_{(2,0)}\rangle_{\mathrm{G}} + \langle A_{(2,2)}\rangle_{\mathrm{G}} + \frac{1}{2}\langle A^2_{(1,2)}\rangle_{\mathrm{G}}\Big]. \tag{4.25}$$

The average $\langle\ldots\rangle_{\mathrm{G}}$ is taken with respect to the Gaussian action derived in the previous section. $\langle A_{(2,0)}\rangle_{\mathrm{G}}$ gives the tree-level longitudinal susceptibility. It does not involve any spin-wave contribution. The spin-wave contribution comes from the last two

terms in Eq. (4.25). However, it turns out that $\langle A_{(2,2)}\rangle_{\rm G}$ does not contribute at all at zero temperature. Therefore, the focus is on calculating $\frac{1}{2}\langle A^2_{(1,2)}\rangle_{\rm G}$. We start with writing out $A_{(1,2)}$ explicitly.

$$\begin{aligned} A_{(1,2)} &= -\frac{1}{2}\int d\boldsymbol{x}d\boldsymbol{y}d\boldsymbol{z}\,\mathrm{tr}\Big[G^{n_1n_2}_{\rm sp}(\boldsymbol{x}-\boldsymbol{y})JL^{n_2n_3}(\boldsymbol{y})G^{n_3n_4}_{\rm sp}(\boldsymbol{y}-\boldsymbol{z}) \\ &\quad\times\delta\tilde{\Lambda}^{n_4n_5}(\boldsymbol{z})\,G^{n_5n_6}_{\rm sp}(\boldsymbol{z}-\boldsymbol{x})\delta\tilde{\Lambda}^{n_6n_1}(\boldsymbol{x})\Big]. \end{aligned} \tag{4.26}$$

We are only concerned with the singular terms originating from the wavenumber and frequency dependence of soft modes. Therefore, we are justified in neglecting all non-singular $\boldsymbol{k}$ and Ω dependencies. Then,

$$A_{(1,2)} \approx \sqrt{\frac{T}{V}}\sum_{\boldsymbol{k},m} A_{(1,2)m}(\boldsymbol{k})\,j_m(\boldsymbol{k}) \tag{4.27a}$$

with

$$\begin{aligned} A_{(1,2)m}(\boldsymbol{k}) &= -\frac{1}{4}\sum_{n_1n_2}\sum_{rs,ij}\frac{1}{V}\sum_{\boldsymbol{p}}\sum_{\sigma=\pm}\sigma\,{}^{ij}_{rs}N^{-\sigma}_{n_1} \\ &\quad\times{}^{i}_{r}(\delta\tilde{\Lambda})_{n_1,n_1+n_2}(\boldsymbol{p})\,{}^{j}_{s}(\delta\tilde{\Lambda})_{n_1+n_2,n_1+\sigma m}(-\boldsymbol{p}-\boldsymbol{k}), \end{aligned} \tag{4.27b}$$

where

$$\begin{aligned} {}^{ij}_{rs}N^{-\sigma}_{n} &= \sum_{a,b,c=0,3}\mathrm{tr}(\tau_a\tau_{-\sigma}\tau_b\tau_r\tau_c\tau_s)\,\mathrm{tr}(s_a\sigma_3s_bs_is_cs_j)\underbrace{\int d\boldsymbol{x}d\boldsymbol{y}G^a_n(\boldsymbol{x})G^b_n(\boldsymbol{x}-\boldsymbol{y})G^c_n(\boldsymbol{y})}_{M^{abc}_n} \\ &= \sum_{a,b,c=0,3}\mathrm{tr}(\tau_a\tau_{-\sigma}\tau_b\tau_r\tau_c\tau_s)\,\mathrm{tr}(s_a\sigma_3s_bs_is_cs_j)M^{abc}_n \\ &= [(-1)^r\,\delta_{rs}+i\sigma\,(1-\delta_{rs})]\,[-4\sigma\,N^{(1)}_n\,\delta_{ij}+(\delta_{i2}\delta_{j1}-\delta_{i1}\delta_{j2})\,4i\,N^{(2)}_n]. \end{aligned} \tag{4.27c}$$

The factors $N^{(1)}$ and $N^{(2)}$ are defined as follows.

$$N_n^{(1)} = M_n^{003} - M_n^{030} - M_n^{300} + M_n^{333}$$
$$N_n^{(2)} = M_n^{000} - M_n^{033} - M_n^{303} + M_n^{330}. \tag{4.27d}$$

This yields

$$\begin{aligned}\chi_{\rm L}(\boldsymbol{k}, i\Omega_m)|_{\text{one-loop}} = \frac{T}{16V} \sum_{n_1,n_2,n_1',n_2'} \sum_{i,j,i',j'} \sum_{r,s,r',s'} \sum_{\sigma,\sigma'} \sigma\sigma' \, {}^{ij}_{rs}N^{-\sigma}_{n_1} \, {}^{i'j'}_{r's'}N^{-\sigma'}_{n_1'} \frac{1}{V^2} \\ \times \sum_{\boldsymbol{p},\boldsymbol{p}'} \Big[\langle {}^{i}_{r}(\delta\tilde{\Lambda})_{n_1,n_1+n_2}(\boldsymbol{p}) \, {}^{i'}_{r'}(\delta\tilde{\Lambda})_{n_1',n_1'+n_2'}(\boldsymbol{p}') \rangle_{\rm G} \\ \times \langle {}^{j}_{s}(\delta\tilde{\Lambda})_{n_1+n_2,n_1+\sigma m}(-\boldsymbol{p}-\boldsymbol{k}) \, {}^{j'}_{s'}(\delta\tilde{\Lambda})_{n_1'+n_2',n_1'-\sigma' m}(-\boldsymbol{p}'+\boldsymbol{k}) \rangle_{\rm G} \\ + \langle {}^{i}_{r}(\delta\tilde{\Lambda})_{n_1,n_1+n_2}(\boldsymbol{p}) \, {}^{j'}_{s'}(\delta\tilde{\Lambda})_{n_1'+n_2',n_1'-\sigma' m}(-\boldsymbol{p}'+\boldsymbol{k}) \rangle_{\rm G} \\ \times \langle {}^{j}_{s}(\delta\tilde{\Lambda})_{n_1+n_2,n_1+\sigma m}(-\boldsymbol{p}-\boldsymbol{k}) \, {}^{i'}_{r'}(\delta\tilde{\Lambda})_{n_1',n_1'+n_2'}(\boldsymbol{p}') \rangle_{\rm G} \Big].\end{aligned} \tag{4.28}$$

The $\delta\tilde{\Lambda}$ fluctuations contain the massive $\delta\bar{\Lambda}$ and the soft δQ fluctuations. In the saddle point approximation, the $\delta\bar{\Lambda}$ fluctuations can be integrated out by simply dropping them. Recalling Eq. (4.17), dropping $\delta\bar{\Lambda}$ amounts to doing the following.

$$\begin{aligned} {}^{ij}_{rs}N^{\sigma}_{n} &\implies 4\,{}^{ij}_{rs}N^{\sigma}_{n}/B_n^2 \\ \delta\tilde{\Lambda} &\implies \delta Q, \end{aligned} \tag{4.29a}$$

where

$$B_n = \frac{1}{V}\sum_{\boldsymbol{p}} [\mathcal{G}_n^2(\boldsymbol{p}) - \mathcal{F}_n^2(\boldsymbol{p})]. \tag{4.29b}$$

The above procedure is valid for $i,j=1,2$, which is the channel that corresponds to the soft modes. Thus,

$$\begin{aligned}\chi_{\rm L}(\boldsymbol{k},i\Omega_m)|_{\text{one-loop}} = \frac{T}{V}\sum_{n_1,n_2,n_1',n_2'}\sum_{i,j,i',j'}\sum_{r,s,r',s'}\sum_{\sigma,\sigma'}\sigma\sigma'\,\frac{{}^{ij}_{rs}N^{-\sigma}_{n_1}}{B_n^2}\,\frac{{}^{i'j'}_{r's'}N^{-\sigma'}_{n_1'}}{B_{n_1'}^2}\frac{1}{V^2}\\ \times\sum_{\boldsymbol{p},\boldsymbol{p}'}\Big[\langle{}^{i}_{r}(\delta Q)_{n_1,n_1+n_2}(\boldsymbol{p})\;{}^{i'}_{r'}(\delta Q)_{n_1',n_1'+n_2'}(\boldsymbol{p}')\rangle_{\rm G}\\ \times\langle{}^{j}_{s}(\delta Q)_{n_1+n_2,n_1+\sigma m}(-\boldsymbol{p}-\boldsymbol{k})\;{}^{j'}_{s'}(\delta Q)_{n_1'+n_2',n_1'-\sigma' m}(-\boldsymbol{p}'+\boldsymbol{k})\rangle_{\rm G}\\ +\langle{}^{i}_{r}(\delta Q)_{n_1,n_1+n_2}(\boldsymbol{p})\;{}^{j'}_{s'}(\delta Q)_{n_1'+n_2',n_1'-\sigma' m}(-\boldsymbol{p}'+\boldsymbol{k})\rangle_{\rm G}\\ \times\langle{}^{j}_{s}(\delta Q)_{n_1+n_2,n_1+\sigma m}(-\boldsymbol{p}-\boldsymbol{k})\;{}^{i'}_{r'}(\delta Q)_{n_1',n_1'+n_2'}(\boldsymbol{p}')\rangle_{\rm G}\Big].\end{aligned}\tag{4.30}$$

We thus need correlation functions of the form

$$\langle{}^{i}_{r}(\delta Q)_{n_1,n_1+n_2}(\boldsymbol{p})\;{}^{i'}_{r'}(\delta Q)_{n_1',n_1'+n_2'}(\boldsymbol{p}')\rangle_{\rm G} = V\,(2\pi)^d\,\delta(\boldsymbol{p}+\boldsymbol{p}')\,\mathcal{C}^{ij}_{rs}(n_1,n_1+n_2,\boldsymbol{p}|n_1',n_1'+n_2')\tag{4.31a}$$

with

$$\mathcal{C}^{ij}_{rs}(n_1,n_2,\boldsymbol{p}|n_3,n_4) = \frac{1}{16}\Big[\Theta(n_1-n_2)\Theta(n_3-n_4)\ {}^{ij}_{rs}\mathcal{M}^{-1}_{n_1n_2,n_3n_4}(\boldsymbol{p})$$
$$+\Theta(n_1-n_2)\Theta(n_4-n_3)(-1)^s \begin{pmatrix}+\\-\\-\\-\end{pmatrix}_j {}^{ij}_{rs}\mathcal{M}^{-1}_{n_1n_2,n_4n_3}(\boldsymbol{p})$$
$$+\Theta(n_2-n_1)\Theta(n_3-n_4)(-1)^r \begin{pmatrix}+\\-\\-\\-\end{pmatrix}_i {}^{ij}_{rs}\mathcal{M}^{-1}_{n_2n_1,n_3n_4}(\boldsymbol{p})$$
$$+\Theta(n_2-n_1)\Theta(n_4-n_3)(-1)^{r+s} \begin{pmatrix}+\\-\\-\\-\end{pmatrix}_i \begin{pmatrix}+\\-\\-\\-\end{pmatrix}_j {}^{ij}_{rs}\mathcal{M}^{-1}_{n_2n_1,n_3n_4}(\boldsymbol{p})\Big] \tag{4.31b}$$

The Θ functions in the above expression are a consequence of the frequency restriction enforced in the previous section to get around the redundancies due to the symmetry of $Q-$matrix elements.

The sums over $r, r', s, s', i, i', j, j'$ in Eq. (4.30) are performed. We restrict $i, j, i', j' = 1, 2$ because, as shown previously, the $i, j = 1, 2$ channel of the interacting

part of the propagator ${}^{ij}_{rs}E$ corresponds to the spin waves. This yields

$$\chi_{\rm L}(\boldsymbol{k}, i\Omega_m)|_{\text{one-loop}} = \frac{64T}{V} \sum_{n_1,n_2,n_1',n_2'} \sum_{\sigma,\sigma'} \sum_{\boldsymbol{p}} \frac{\sigma\sigma'}{B_{n_1}^2 B_{n_1'}^2}$$

$$\times \Bigg\{ [N_{n_1'}^{(1)} N_{n_1}^{(1)} \Big[(\sigma \mathcal{C}_{00}^{11} - \sigma' \mathcal{C}_{33}^{11})(\sigma' \mathcal{C}_{00}^{11} - \sigma \mathcal{C}_{33}^{11}) - (\sigma \mathcal{C}_{03}^{12} + \sigma' \mathcal{C}_{30}^{12})(\sigma \mathcal{C}_{30}^{12} + \sigma' \mathcal{C}_{03}^{12}) \Big] \tag{4.32}$$

$$- N_{n_1'}^{(1)} N_{n_1}^{(2)} \Big[(\sigma \mathcal{C}_{30}^{12} + \sigma' \mathcal{C}_{03}^{12})(\sigma' \mathcal{C}_{00}^{11} - \sigma C_{33}^{11}) - (\sigma \mathcal{C}_{00}^{11} - \sigma' \mathcal{C}_{33}^{11})(\sigma \mathcal{C}_{03}^{12} + \sigma' \mathcal{C}_{30}^{12}) \Big] \Bigg\},$$

wherein $\mathcal{C}$ in the first bracket is $\mathcal{C}(n_1, n_1+n_2, \boldsymbol{p}|n_1', n_1'+n_2')$ and in the second bracket is $\mathcal{C}(n_1+n_2, n_1+\sigma m, \boldsymbol{p}+\boldsymbol{k}|n_1'+n_2', n_1'-\sigma' m)$. In obtaining the above expression, approximations have been made that do not affect the leading nonanalytic terms. It turns out that the second term in Eq. (4.32) does not contribute to the leading nonanalytic frequency dependence. In terms of Eq. (4.21), we obtain

$$\chi_{\rm L}(\boldsymbol{k}, i\Omega_m)|_{\text{one-loop}} = \Gamma_t^2 a^2 \frac{T}{V} \sum_{\boldsymbol{p}} \sum_{n_2} \Theta(n_2)$$

$$\times \Big\{ g^+(\boldsymbol{p}, i\Omega_{n_2}) [g^+(\boldsymbol{p}+\boldsymbol{k}, i\Omega_{n_2} - i\Omega_m) + g^+(\boldsymbol{p}+\boldsymbol{k}, i\Omega_{n_2} + i\Omega_m)]$$

$$+ \text{complex conjugate} \Big\} \tag{4.33a}$$

where

$$a = T \sum_n [\varphi_{nn}^{00}(\boldsymbol{k}=0) - \varphi_{nn}^{33}(\boldsymbol{k}=0)] \frac{N_n^{(1)}}{B_n^2}. \tag{4.33b}$$

Finally,

$$\chi_{\rm L}(\boldsymbol{k}, i\Omega_m)|_{\text{one-loop}} = 2\Gamma_t^2 a^2 d^2 \frac{T}{V} \sum_{\boldsymbol{p}} \sum_{n_2} \frac{c^2|\boldsymbol{p}|^2|\boldsymbol{p}+\boldsymbol{k}|^2 - \Omega_{n_2}(\Omega_{n_2} - \Omega_m)}{(c^2\boldsymbol{p}^4 + \Omega_{n_2}^2)(c^2|\boldsymbol{p}+\boldsymbol{k}|^4 + (\Omega_{n_2} - \Omega_m)^2)}. \tag{4.34}$$

The above expression is mathematically equivalent to Eq. (3.14) from the previous chapter. Therefore, Eq. (4.34) evaluates to zero at $T = 0$ and there are no

nonanalyticities. This is due to the lack of fluctuations coupling to the longitudinal magnetization fluctuations.

Effects of Damping

In the preceding calculations, the damping of the magnons was ignored. In the following, the effects of damping, due to quenched disorder, are calculated explicitly by including the following term in the full action $\mathcal{A}[Q,\tilde{\Lambda}]$ from Eq. (4.6a):

$$\begin{aligned} \mathcal{A}'[Q,\tilde{\Lambda}] &= \mathcal{A}[Q,\tilde{\Lambda}] + \mathcal{A}_{\rm dis}[Q] \\ \mathcal{A}_{\rm dis}[Q] &= \frac{1}{\pi N_{\rm F}\tau}\int d\boldsymbol{x}\,{\rm tr}\left(Q(\boldsymbol{x})\right)^2, \end{aligned} \tag{4.35}$$

with $N_{\rm F}$ the density of states at the Fermi level in saddle point approximation and τ the single-particle scattering or relaxation time. The disorder term $\mathcal{A}_{\rm dis}$ corresponds to nonmagnetic impurities in the system.

As in the clean case earlier in this chapter, we make a saddle point ansatz like in Eq. (4.8) and obtain the saddle-point equations,

$$G_n = \frac{i}{2V}\sum_{\boldsymbol{k}}\frac{i\omega_n-\xi_{\boldsymbol{k}}-\Sigma_n}{(i\omega_n-\xi_{\boldsymbol{k}}-\Sigma_n)^2-\Delta_n^2} = \frac{i}{2V}\sum_{\boldsymbol{k}}\mathcal{G}_n(\boldsymbol{k}) \tag{4.36}$$

$$F_n = -\frac{i}{2V}\sum_{\boldsymbol{k}}\frac{\Delta_n}{(i\omega_n-\xi_{\boldsymbol{k}}-\Sigma_n)^2-\Delta_n^2} = \frac{i}{2V}\sum_{\boldsymbol{k}}\mathcal{F}_n(\boldsymbol{k}) \tag{4.37}$$

$$\Sigma_n = -\frac{2i}{\pi N_{\rm F}\tau}\,G_n \tag{4.38}$$

$$\Delta_n = \frac{2i}{\pi N_{\rm F}\tau}\,F_n - 4i\,\Gamma_t\,T\sum_m e^{i\omega_m 0}F_m. \tag{4.39}$$

These equations lead to an equation of state,

$$1 = -2\Gamma_t\,T\sum_n\frac{1}{V}\sum_{\boldsymbol{k}}\frac{1}{(i\omega_n-\xi_{\boldsymbol{k}}+\frac{i}{2\tau}{\rm sgn}\,\omega_n)^2-\Delta_n^2}. \tag{4.40}$$

This integral is independent of the disorder to the lowest order in $1/\tau$ and therefore is identical to the Stoner criterion in the clean case, Eq. (4.12). This is the magnetic equivalent of Anderson's theorem for superconductors [35].

Using this disordered saddle point, the Gaussian Q propagators can be calculated using the Replica trick and in a similar fashion to the clean case. Then, Eq. (4.18) in the presence of quenched disorder becomes

$$\mathcal{A}_{\mathrm{G}}[\delta Q] = -\frac{4}{V}\sum_{\boldsymbol{k}}\sum_{1234}\sum_{r,s=\{0,3\}}\sum_{ij} {}^{i}_{r}(\delta Q)_{12}(\boldsymbol{k})\, {}^{ij}_{rs}\mathcal{M}_{12,34}(\boldsymbol{k})\, {}^{j}_{s}(\delta Q)_{34}(-\boldsymbol{k}), \tag{4.41a}$$

with

$${}^{ij}_{rs}\mathcal{M}_{12,34}(\boldsymbol{k}) = \delta_{13}\,\delta_{24}\left[{}^{ij}_{rs}(A_{12})^{-1}(\boldsymbol{k}) - \mathbb{1}/(\pi N_{\mathrm{F}}\tau)\,\delta_{rs}\,\delta_{ij}\right] + 2\,T\,\Gamma_t\,\delta_{1-2,3-4}\,\delta_{rs}\,\delta_{ij}\,(1-\delta_{i0}). \tag{4.41b}$$

Proceeding as in the clean case, the structure of the magnetic Goldstone modes can be determined. We find

$$\begin{aligned} g^{\pm}(\boldsymbol{k}, i\Omega_n) &= \frac{1}{1 + 2\Gamma_t\, T\sum_m \mathcal{E}^{\pm}_{m,n+m}(\boldsymbol{k})} \\ \mathcal{E}^{\pm}_{nm}(\boldsymbol{k}) &= \frac{X^{-}_{nm}(\boldsymbol{k}) \pm Y^{-}_{nm}(\boldsymbol{k})}{1 - (X^{-}_{nm}(\boldsymbol{k}) \pm Y^{-}_{nm}(\boldsymbol{k}))/(\pi N_{\mathrm{F}}\tau)}, \end{aligned} \tag{4.42a}$$

with X^{-} and Y^{-} as defined in Eq. (4.16b).

In the limit $|\boldsymbol{k}|/k_{\mathrm{F}}, \Omega_n/\epsilon_{\mathrm{F}} \ll \Delta/\epsilon_{\mathrm{F}} \ll 1$, we find

$$g^{\pm}(\boldsymbol{k}, i\Omega_n) = \frac{d(\frac{1}{\tau})}{\pm i\Omega_n - c(\frac{1}{\tau})\boldsymbol{k}^2 - \eta(\frac{1}{\tau})\boldsymbol{k}^2|\Omega_n|}, \tag{4.42b}$$

where c, d and η are constants that depend on the single-particle relaxation time τ. To lowest order in $1/\tau$,

$$c(1/\tau \to 0) = \frac{\Delta}{6k_{\rm F}^2}, \quad d(1/\tau \to 0) = -\frac{\Delta}{2N_{\rm F}\Gamma_t}, \quad \eta(1/\tau \to 0) = \frac{v_{\rm F}^2}{16\Delta^4\tau}. \tag{4.42c}$$

As $\tau \to \infty$, the damping coefficient η vanishes and Eq. (4.21) is recovered. The structure of the damped Goldstone mode shown in Eq. (4.42b) is different from the one obtained from the Time-Dependent Ginzburg-Landau theory,

$$g^{\pm}(\boldsymbol{k}, i\Omega_n) = \frac{d}{\pm i[\Omega_n + \mathrm{sgn}\,(\Omega_n)\eta\boldsymbol{k}^4] - c\boldsymbol{k}^2}. \tag{4.42d}$$

Using Eq. (4.42b) in Eq. (4.34) and setting $\boldsymbol{k} = 0$, the following relevant dimensionless integral, which is proportional to $\chi_{\rm L}^{(1)}(\boldsymbol{k} = 0, i\Omega_m)$, is obtained at $T = 0$:

$$I_1(\Omega_m) = \frac{1}{V}\sum_{\boldsymbol{p}} \int_{-\infty}^{\infty} d\omega \, \frac{\boldsymbol{p}^4(1+\eta|\omega|)(1+\eta|\omega-\Omega_m|) - \omega(\omega-\Omega_m)}{[\boldsymbol{p}^4(1+\eta|\omega|)^2+\omega^2][\boldsymbol{p}^4(1+\eta|\omega-\Omega_m|)^2+(\omega-\Omega_m)^2]}. \tag{4.43}$$

Performing the integrals, we find

$$I_1(\Omega_m \to 0) = I_1(0) + Z_d\,\eta\,|\Omega_m|^{d/2}, \qquad Z_2 = -\frac{\pi}{6}, Z_3 = -\frac{4\sqrt{2}\,\pi}{35}. \tag{4.44}$$

This result is qualitatively very similar to the results for the "conserved-order-parameter" damped magnons discussed in the previous chapter, Eq. (3.51). Introducing nonmagnetic disorder results in additional fluctuations in the system that couple to the longitudinal magnetization fluctuations and yields nonanalyticities.

Some Finite Temperature Results

Recalling (4.34), the summation over the bosonic Matsubara frequency n_2 is performed and the following result is obtained.

$$\chi_{\rm L}(\boldsymbol{k}, i\Omega_m)|_{\text{one-loop}} = 2\Gamma_t^2 a^2 d^2 \frac{1}{V}\sum_{\boldsymbol{p}}[n_B(c\boldsymbol{p}^2) - n_B(c|\boldsymbol{p}+\boldsymbol{k}|^2)] \times \left(\frac{1}{c|\boldsymbol{p}+\boldsymbol{k}|^2 - c\boldsymbol{k}^2 + i\Omega_m} + \frac{1}{c|\boldsymbol{p}+\boldsymbol{k}|^2 - c\boldsymbol{k}^2 - i\Omega_m}\right) \quad (4.45)$$

where $n_B(x) = 1/(e^{x/T}-1)$, the Bose distribution function. This result is identical to Eq. (3.18) from the previous chapter. The analytic continuation, $i\Omega_m \to \omega + i\delta$ is performed. In the regime $\omega \ll c\boldsymbol{k}^2 \ll T$,

$$\text{Re}[\chi_{\rm L}(\boldsymbol{k},\omega)]\Big|_{\text{one-loop}} \approx \Gamma_t^2 a^2 d^2 \frac{T}{2c^2|\boldsymbol{k}|}, \quad (4.46)$$

which is the classical one-loop result also discussed in the previous chapter, Eq. (3.19). The spectrum of $\chi_{\rm L}$ is given by

$$\chi''_{\rm L}(\boldsymbol{k},\omega) = \Gamma_t^2 a^2 d^2 \frac{T}{4\pi c^2|\boldsymbol{k}|}\log\frac{1-\exp[-\beta(c\boldsymbol{k}^2+\omega)^2/4c\boldsymbol{k}^2]}{1-\exp[-\beta(c\boldsymbol{k}^2-\omega)^2/4c\boldsymbol{k}^2]}, \quad (4.47)$$

which is again identical to the spectrum $\chi''_{\rm L}$ from the previous chapter.

Electrical Conductivity

The Q-matrix field theory with an appropriate source field can also be used to calculate the Goldstone mode contribution to the dynamical electrical conductivity. The following is an identical reproduction of the calculations performed in [20].

In terms of the Grassmannian fields ψ and $\bar{\psi}$, the dynamical electrical conductivity is given by the Kubo formula,

$$\sigma(\Omega) = \frac{i\,n_{\rm e}}{m_{\rm e}\Omega} + \frac{i\,T}{\Omega V m_{\rm e}^2} \sum_{n_1 n_2} \sum_{\sigma\sigma'} \int d\boldsymbol{x}\, d\boldsymbol{x}'\, \langle \bar{\psi}_{n_1,\sigma}(\boldsymbol{x})\, \partial_{x_1} \psi_{n_1+m,\sigma}(\boldsymbol{x})\, \bar{\psi}_{n_2,\sigma'}(\boldsymbol{x}')\, \partial_{x_1'} \psi_{n_2-m,\sigma'}(\boldsymbol{x}') \rangle \Big|_{i\Omega_m \to \Omega + i0}. \tag{4.48}$$

Here, $n_{\rm e}$ is the electron density and $m_{\rm e}$ is the electron effective mass. In order to calculate the one-loop spin-wave contribution to the conductivity, the following source term is added to the action Eq. (4.1), in analogy to Eq. (4.22a).

$$S_j = -\sum_m j_m \int d\boldsymbol{x} \sum_n \sum_\sigma \bar{\psi}_{n,\sigma}(\boldsymbol{x}) \partial_{x_1} \psi_{n-m,\sigma}(\boldsymbol{x}). \tag{4.49}$$

As before, the Grassmannian fields are integrated out, leaving behind an action analogous to Eq. (4.22c) with JL, in this case, defined as

$$(JL)_{12}(\boldsymbol{x}) = \frac{1}{2} \sum_m j_m L_{12,m} \partial_{x_1} = (JL)'_{12} \partial_{x_1} \tag{4.50a}$$

with

$$L_{12,m} = (\tau_- \otimes s_0)\delta_{n_1,n_2+m} - (\tau_+ \otimes s_0)\delta_{n_2,n_1+m}. \tag{4.50b}$$

Once again, the action Eq. (4.22c) is expanded in powers of j and $\delta\tilde{\Lambda}$ to give Eq. (4.24). Then, according to Eq. (4.48),

$$\sigma(\Omega) = -\frac{i n_{\rm e}}{m_{\rm e}\Omega} + \frac{iT}{\Omega V m_{\rm e}^2} \frac{\partial^2}{\partial j_m \partial j_{-m}} \Big|_{\substack{j=0 \\ i\Omega \to \Omega + i0}} \Big[\langle A_{(2,0)} \rangle_{\rm G} + \langle A_{(2,2)} \rangle_{\rm G} + \frac{1}{2} \langle A_{(1,2)}^2 \rangle_{\rm G} \Big]. \tag{4.51}$$

$\langle A_{(2,0)}\rangle_{\rm G}$ yields the Boltzmann conductivity since it does not include the effect of spin waves. The spin-wave contribution comes from $\langle A_{(2,2)}\rangle_{\rm G}$ and $\frac{1}{2}\langle A^2_{(1,2)}\rangle_{\rm G}$. $A_{(2,2)}$ involves one Goldstone propagator whereas $A^2_{(1,2)}$ has two Goldstone propagators and is therefore expected to be the dominant contribution. In the following, we concentrate on calculating

$$\sigma_{(1,2)}(\Omega) = \frac{iT}{2\Omega V m_{\rm e}^2}\frac{\partial^2}{\partial j_m \partial j_{-m}}\bigg|_{\substack{j=0\\ i\Omega\to\Omega+i0}} \langle A^2_{(1,2)}\rangle_{\rm G}. \tag{4.52}$$

Writing out $A_{(1,2)}$ explicitly, we obtain

$$\begin{aligned}
A_{(1,2)} &= -\frac{1}{2}\int d\boldsymbol{x}d\boldsymbol{y}d\boldsymbol{z}\,\mathrm{tr}\Big[G^{n_1n_2}_{\rm sp}(\boldsymbol{x}-\boldsymbol{y})JL^{n_2n_3}(\boldsymbol{y})G^{n_3n_4}_{\rm sp}(\boldsymbol{y}-\boldsymbol{z})\\
&\quad\times\delta\tilde{\Lambda}^{n_4n_5}(\boldsymbol{z})G^{n_5n_6}_{\rm sp}(\boldsymbol{z}-\boldsymbol{x})\delta\tilde{\Lambda}^{n_6n_1}(\boldsymbol{x})\Big]\\
&= -\frac{1}{2}\int d\boldsymbol{x}d\boldsymbol{y}d\boldsymbol{z}\,\mathrm{tr}\Big[G^{n_1n_2}_{\rm sp}(\boldsymbol{x}-\boldsymbol{y})(JL)'_{n_2n_3}\partial_{y_1}G^{n_3n_4}_{\rm sp}(\boldsymbol{y}-\boldsymbol{z})\\
&\quad\times\delta\tilde{\Lambda}^{n_4n_5}(\boldsymbol{z})G^{n_5n_6}_{\rm sp}(\boldsymbol{z}-\boldsymbol{x})\delta\tilde{\Lambda}^{n_6n_1}(\boldsymbol{x})\Big]\\
&\overset{\substack{\boldsymbol{z}\to\boldsymbol{z}+\boldsymbol{x}\\ \boldsymbol{y}\to\boldsymbol{y}+\boldsymbol{x}}}{\longrightarrow} -\frac{1}{2}\int d\boldsymbol{x}d\boldsymbol{y}d\boldsymbol{z}\,\mathrm{tr}\Big[G^{n_1n_2}_{\rm sp}(-\boldsymbol{y})(JL)'_{n_2n_3}\partial_{y_1}G^{n_3n_4}_{\rm sp}(\boldsymbol{y}-\boldsymbol{z})\\
&\quad\times\underbrace{\delta\tilde{\Lambda}^{n_4n_5}(\boldsymbol{z}+\boldsymbol{x})}_{\approx\delta\tilde{\Lambda}(\boldsymbol{x})+\boldsymbol{z}.\vec{\nabla}\delta\tilde{\Lambda}(\boldsymbol{x})}G^{n_5n_6}_{\rm sp}(\boldsymbol{z})\delta\tilde{\Lambda}^{n_6n_1}(\boldsymbol{x})\Big].
\end{aligned}\tag{4.53}$$

It turns out that only $\boldsymbol{z}.\vec{\nabla}\delta\tilde{\Lambda}$ contributes to $A_{(1,2)}$. As before, all non-singular $\boldsymbol{p}$ and m, n_2 dependencies are neglected. Then,

$$A_{(1,2)} \approx \sum_m A_{(1,2)m} j_m, \tag{4.54a}$$

with

$$A_{(1,2)m} = -\frac{1}{4}\sum_{n_1 n_2}\sum_{rs,ij}\frac{1}{V}\sum_{\boldsymbol{p}} ip_x \sum_{\sigma=\pm}\sigma\ {}^{ij}_{rs}N^{-\sigma}_{n_1}\ {}^{i}_{r}(\delta\tilde{\Lambda})_{n_1,n_1+n_2}(\boldsymbol{p})\ {}^{j}_{s}(\delta\tilde{\Lambda})_{n_1+n_2,n_1+\sigma m}(-\boldsymbol{p}), \tag{4.54b}$$

where

$$\begin{aligned}
{}^{ij}_{rs}N^{-\sigma}_{n} &= \sum_{a,b,c=0,3}\mathrm{tr}(\tau_a\tau_{-\sigma}\tau_b\tau_r\tau_c\tau_s)\,\mathrm{tr}(s_a s_b s_i s_c s_j)\underbrace{\int d\boldsymbol{x}d\boldsymbol{y}G^a_n(\boldsymbol{x})\partial_{x_1}G^b_n(\boldsymbol{x}-\boldsymbol{y})y_1 G^c_n(\boldsymbol{y})}_{(M')^{abc}_n}\\
&= \sum_{a,b,c=0,3}\mathrm{tr}(\tau_a\tau_{-\sigma}\tau_b\tau_r\tau_c\tau_s)\,\mathrm{tr}(s_a s_b s_i s_c s_j)(M')^{abc}_n\\
&= [(-1)^r\delta_{rs}+i\sigma(1-\delta_{rs})]\,[-4N^{(2)}_n\delta_{ij}+(\delta_{i2}\delta_{j1}-\delta_{i1}\delta_{j2})\,4i\,\sigma\,N^{(1)}_n],
\end{aligned} \tag{4.54c}$$

and

$$\begin{aligned}
N^{(1)}_n &= (M')^{003}_n-(M')^{030}_n-(M')^{300}_n+(M')^{333}_n\\
N^{(2)}_n &= (M')^{000}_n-(M')^{033}_n-(M')^{303}_n+(M')^{330}_n.
\end{aligned} \tag{4.54d}$$

This yields

$$\begin{aligned}
\sigma_{(1,2)}(\Omega) = & -\frac{iT}{16\Omega V m_{\mathrm{e}}^2}\sum_{n_1,n_2,n_1',n_2'}\sum_{i,j,i',j'}\sum_{r,s,r',s'}\sum_{\sigma,\sigma'}\sigma\sigma'\ {}^{ij}_{rs}N^{-\sigma}_{n_1}\ {}^{i'j'}_{r's'}N^{-\sigma'}_{n_1'}\frac{1}{V^2}\sum_{\boldsymbol{p},\boldsymbol{p}'}p_x\,p_x'\\
&\times\Big[\langle {}^{i}_{r}(\delta\tilde{\Lambda})_{n_1,n_1+n_2}(\boldsymbol{p})\ {}^{i'}_{r'}(\delta\tilde{\Lambda})_{n_1',n_1'+n_2'}(\boldsymbol{p}')\rangle_{\mathrm{G}}\\
&\times\langle {}^{j}_{s}(\delta\tilde{\Lambda})_{n_1+n_2,n_1+\sigma m}(-\boldsymbol{p})\ {}^{j'}_{s'}(\delta\tilde{\Lambda})_{n_1'+n_2',n_1'-\sigma' m}(-\boldsymbol{p}')\rangle_{\mathrm{G}}\\
&+\langle {}^{i}_{r}(\delta\tilde{\Lambda})_{n_1,n_1+n_2}(\boldsymbol{p})\ {}^{j'}_{s'}(\delta\tilde{\Lambda})_{n_1'+n_2',n_1'-\sigma' m}(-\boldsymbol{p}')\rangle_{\mathrm{G}}\\
&\times\langle {}^{j}_{s}(\delta\tilde{\Lambda})_{n_1+n_2,n_1+\sigma m}(-\boldsymbol{p})\ {}^{i'}_{r'}(\delta\tilde{\Lambda})_{n_1',n_1'+n_2'}(\boldsymbol{p}')\rangle_{\mathrm{G}}\Big].
\end{aligned} \tag{4.55}$$

The above expression can be rewritten in terms of the δQ fields via the following substitutions, which is valid for $i, j = 1, 2$ (which correspond to the spin waves):

$$\begin{aligned} {}^{ij}_{rs}N^{\sigma}_{n} &\implies 4\,{}^{ij}_{rs}N^{\sigma}_{n}/B^2_n \\ \delta\tilde{\Lambda} &\implies \delta Q, \end{aligned} \tag{4.56}$$

where

$$B_n = \frac{1}{V}\sum_{\boldsymbol{p}}[\mathcal{G}^2_n(\boldsymbol{p}) - \mathcal{F}^2_n(\boldsymbol{p})]. \tag{4.57}$$

Therefore, the leading ferromagnetic Goldstone mode contribution to $\sigma_{(1,2)}$ is

$$\begin{aligned} \sigma_{(1,2)}(\Omega) = & -\frac{iT}{\Omega V m_{\rm e}^2}\sum_{n_1,n_2,n_1',n_2'}\sum_{i,j,i',j'}\sum_{r,s,r',s'}\sum_{\sigma,\sigma'}\sigma\sigma'\,\frac{{}^{ij}_{rs}N^{-\sigma}_{n_1}}{B^2_n}\,\frac{{}^{i'j'}_{r's'}N^{-\sigma'}_{n_1'}}{B^2_{n_1'}}\frac{1}{V^2}\sum_{\boldsymbol{p},\boldsymbol{p}'}p_x^2 \\ & \times\Big[-\langle {}^{i}_{r}(\delta Q)_{n_1,n_1+n_2}(\boldsymbol{p})\,{}^{i'}_{r'}(\delta Q)_{n_1',n_1'+n_2'}(\boldsymbol{p}')\rangle_{\rm G} \\ & \times\langle {}^{j}_{s}(\delta Q)_{n_1+n_2,n_1+\sigma m}(-\boldsymbol{p})\,{}^{j'}_{s'}(\delta Q)_{n_1'+n_2',n_1'-\sigma' m}(-\boldsymbol{p}')\rangle_{\rm G} \\ & +\langle {}^{i}_{r}(\delta Q)_{n_1,n_1+n_2}(\boldsymbol{p})\,{}^{j'}_{s'}(\delta Q)_{n_1'+n_2',n_1'-\sigma' m}(-\boldsymbol{p}')\rangle_{\rm G} \\ & \times\langle {}^{j}_{s}(\delta Q)_{n_1+n_2,n_1+\sigma m}(-\boldsymbol{p})\,{}^{i'}_{r'}(\delta Q)_{n_1',n_1'+n_2'}(\boldsymbol{p}')\rangle_{\rm G}\Big]. \end{aligned} \tag{4.58}$$

With $\mathcal{C}^{ij}_{rs}$ defined as before Eq. (4.31b) and carrying out the spin and quaternion sums,

$$\begin{aligned} \sigma_{(1,2)}(\Omega) = & \frac{-64T}{\Omega m_{\rm e}^2 V}\sum_{n_1,n_2,n_1',n_2'}\sum_{\sigma,\sigma'}\sum_{\boldsymbol{p}}p_x^2\frac{\sigma\sigma'}{B^2_{n_1}B^2_{n_1'}} \\ \times\Big\{ & [N^{(1)}_{n_1'}N^{(1)}_{n_1}\Big[(\sigma\mathcal{C}^{11}_{00}-\sigma'\mathcal{C}^{11}_{33})(\sigma'\mathcal{C}^{11}_{00}-\sigma\mathcal{C}^{11}_{33})-(\sigma\mathcal{C}^{12}_{03}+\sigma'\mathcal{C}^{12}_{30})(\sigma\mathcal{C}^{12}_{30}+\sigma'\mathcal{C}^{12}_{03})\Big] \\ & -N^{(1)}_{n_1'}N^{(2)}_{n_1}\Big[(\sigma\mathcal{C}^{12}_{30}+\sigma'\mathcal{C}^{12}_{03})(\sigma'\mathcal{C}^{11}_{00}-\sigma C^{11}_{33})-(\sigma\mathcal{C}^{11}_{00}-\sigma'\mathcal{C}^{11}_{33})(\sigma\mathcal{C}^{12}_{03}+\sigma'\mathcal{C}^{12}_{30})\Big]\Big\}. \end{aligned} \tag{4.59}$$

The sums over indices σ and σ' are performed. Keeping only the leading terms, the above expression can be expressed in terms of the Goldstone propagators Eq. (4.21) as

$$\begin{aligned}\sigma_{(1,2)}(\Omega) = \; & -\frac{i\Gamma_t^2\, a^2\, T}{\Omega\, m_{\mathrm{e}}^2\, V}\sum_{\boldsymbol{p}} p_x^2 \sum_{n_2}\Theta(n_2) \\ & \times\Big\{g^+(\boldsymbol{p}, i\Omega_{n_2})\Big[g^+(\boldsymbol{p}, i\Omega_{n_2}-i\Omega_m)+g^+(\boldsymbol{p}, i\Omega_{n_2}+i\Omega_m)\Big] \\ & + \text{complex conjugate}\Big\}\Big|_{i\Omega_m\to\Omega+i0}, \end{aligned} \tag{4.60}$$

with a as defined previously in Eq. (4.33b), albeit with $(M')_n^{abc}$ instead of M_n^{abc}. The above expression is almost exactly the same as Eq. (4.33a), except for an additional factor of p_x^2 which comes from the vertex. Considering the undamped Goldstone propagators Eq. (4.21), the relevant dimensionless integral at $T=0$ is

$$I_1(\Omega_m) = \frac{1}{V}\sum_{\boldsymbol{p}} \boldsymbol{p}^2 \int_{-\infty}^{\infty} d\omega\, \frac{\boldsymbol{p}^4 - \omega(\omega-\Omega_m)}{(\boldsymbol{p}^4+\omega^2)(\boldsymbol{p}^4+(\omega-\Omega_m)^2)}, \tag{4.61}$$

which evaluates to zero. Therefore, the spin waves do not contribute any nonanalytic frequency dependence to the conductivity at zero temperature. This is due to the fact that the current-current correlation function can be expressed purely in terms of the magnon-number fluctuations. This result differs from the original one-loop result for the conductivity given in [20]. According to [20],

$$\begin{aligned}\sigma_{(1,2)}(\Omega) = \; & -\frac{i\Gamma_t^2\, a^2\, T}{\Omega\, m_{\mathrm{e}}^2\, V}\sum_{\boldsymbol{p}} p_x^2 \sum_{n_2}\Theta(n_2) \\ & \times\Big\{g(\boldsymbol{p}, i\Omega_{n_2})\Big[g(\boldsymbol{p}, i\Omega_{n_2}-i\Omega_m)+g(\boldsymbol{p}, i\Omega_{n_2}+i\Omega_m)\Big]\Big\}\Big|_{i\Omega_m\to\Omega+i0}, \end{aligned} \tag{4.62a}$$

where

$$\begin{aligned} g(\boldsymbol{p}, i\Omega_n) &= g^+(\boldsymbol{p}, i\Omega_n) + g^-(\boldsymbol{p}, i\Omega_n) \\ &= \frac{-2dc\boldsymbol{p}^2}{\Omega_n^2 + (c\boldsymbol{p}^2)^2}. \end{aligned} \tag{4.62b}$$

Then, the relevant dimensionless integral at $T = 0$ is

$$\begin{aligned} I_1(\Omega_m) &= \int_0^\infty dp\, p^{d+1} \int_0^\infty d\omega\, \frac{p^4}{\omega^2 + p^4} \\ &\quad \times \left[\frac{1}{p^4 + (\omega - \Omega_m)^2} + \frac{1}{p^4 + (\omega + \Omega_m)^2} \right] \end{aligned} \tag{4.63a}$$

$$I_1(\Omega_m \to 0) = I_1(0) - \frac{\pi^2}{2^{3+d/2} \sin(\pi d/4)} |\Omega_m|^{d/2}. \tag{4.63b}$$

However, Eq. (4.62a) is not correct. This is because in [20], there was an error in performing the sums over σ and σ' in Eq. (4.59), which led to some terms being omitted. The correct result is Eq. (4.60), which shows that undamped spin waves have a vanishing one-loop contribution to the conductivity at $T = 0$.

If the damped Goldstone propagators from Eq. (4.42b) are used, we obtain (with $\Omega \equiv \Omega_m$)

$$I_1(\Omega) = \frac{1}{V} \sum_{\boldsymbol{p}} \boldsymbol{p}^2 \int_{-\infty}^{\infty} d\omega \frac{\boldsymbol{p}^4 (1 + \eta|\omega|)(1 + \eta|\omega - \Omega|) - \omega(\omega - \Omega)}{[\boldsymbol{p}^4 (1 + \eta|\omega|)^2 + \omega^2][\boldsymbol{p}^4 (1 + \eta|\omega - \Omega|)^2 + (\omega - \Omega)^2]} \tag{4.64a}$$

$$I_1(\Omega \to 0) = I_1(0) + \begin{cases} R_2 |\Omega|^2 \log(\dfrac{c p_0^2}{|\Omega|}) & \text{if } d = 2 \\ R_3 |\Omega|^2 + Y_3 |\Omega|^{5/2} & \text{if } d = 3 \end{cases}, \tag{4.64b}$$

where R_2, R_3 and Y_3 are negative finite constants, all proportional to η. p_0 is some momentum cutoff. Then, the one-loop contribution of damped spin waves to the conductivity is given by

$$\begin{aligned} \sigma_{(1,2)}(\Omega) &\propto \left.\frac{-i[I_1(\Omega_m) - I_1(0)]}{\Omega}\right|_{i\Omega_m \to \Omega + i0} \\ \mathrm{Re}[\sigma_{(1,2)}(\Omega)] &= \begin{cases} (1/12\pi)\,\eta\, k_{\mathrm{F}}^2\, |\dfrac{\Omega}{\Delta}| & \text{if } d = 2 \\ (4/63\pi^2)\,\eta\, k_{\mathrm{F}}^3\, |\dfrac{\Omega}{\Delta}|^{3/2} & \text{if } d = 3 \end{cases} . \end{aligned} \tag{4.65}$$

The above contribution is a positive quantity, which means that it is localizing in nature, i.e. the conductivity decreases with decreasing frequency.

Density of States

The single-particle density of states is another quantity that gets contributions from the spin-waves. In terms of Q fields, the frequency or energy dependent single-particle density of states, with energy measured from the chemical potential μ (which is the Fermi energy ϵ_{F} at $T = 0$), is

$$N(\mu + \omega) = \frac{4}{\pi}\,\mathrm{Re}\,\langle\, {}^0_0 Q_{nn}(\boldsymbol{x})\rangle\Big|_{i\omega_n \to \omega + i0} . \tag{4.66}$$

Using

$$\langle\, {}^0_0 Q_{nn}(\boldsymbol{x})\rangle = {}^0_0 Q_{nn}|_{\mathrm{sp}} + \langle\, {}^0_0 (\delta Q)_{nn}(\boldsymbol{x})\rangle, \tag{4.67a}$$

Eq. (4.66) becomes

$$\begin{aligned} N(\mu + \omega) &= N_{\mathrm{F}} + \frac{4}{\pi}\,\mathrm{Re}\,\langle\, {}^0_0 (\delta Q)_{nn}(\boldsymbol{x})\rangle|_{i\omega_n \to \omega + i0} \\ &= N_{\mathrm{F}} + \mathrm{Re}\, Q^{GM}(i\omega_n)\Big|_{i\omega_n \to \omega + i0} . \end{aligned} \tag{4.67b}$$

To calculate this quantity, we start by recalling the action in Eq. (4.6a). This action is written as a sum of the saddle-point contribution, the Gaussian part Eq. (4.14) which is quadratic in Q and $\tilde{\Lambda}$, and non-Gaussian (cubic and higher order) terms.

$$\mathcal{A}[Q,\tilde{\Lambda}] = \mathcal{A}[Q_{\rm sp},\tilde{\Lambda}_{\rm sp}] + \mathcal{A}_{\rm G}[\delta Q,\delta\tilde{\Lambda}] + \sum_{l=3}^{\infty}\mathcal{A}_l[\delta\tilde{\Lambda}] \tag{4.68a}$$

where

$$\mathcal{A}_l[\delta\tilde{\Lambda}] = -\frac{1}{2l}\mathrm{Tr}\,(iG_{\rm sp}\delta\tilde{\Lambda})^l. \tag{4.68b}$$

The fields $\delta\tilde{\Lambda}$ and δQ in $\mathcal{A}_{\rm G}$ can be decoupled by introducing a new field $\delta\bar{\Lambda}$ as defined in Eq. (4.17). Then,

$$\mathcal{A}[Q,\bar{\Lambda}] = \mathcal{A}_{\rm sp} + \mathcal{A}_{\rm G}[\delta Q,\delta\bar{\Lambda}] + \sum_{l=3}^{\infty}\mathcal{A}_l[2A^{-1}(\delta\bar{\Lambda}-\delta Q)]. \tag{4.68c}$$

The diagrammatic loop expansion for the irreducible part of $\langle\delta Q\rangle$, or equivalently for the one-point vertex function, is shown in Fig. 15.

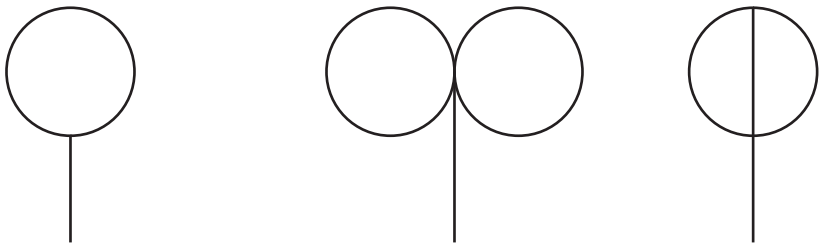

FIGURE 15. One-loop (a) and two-loop (b) contribution to the one-point vertex function $\langle\delta Q\rangle$

The one-loop term, Fig. 15(a), is given analytically by

$$\langle\delta Q_{nn}(\boldsymbol{x})\rangle|_{\text{1-loop}} = \langle\delta Q_{nn}(\boldsymbol{x})\,\mathcal{A}_3[2A^{-1}(\delta\bar{\Lambda}-\delta Q)]\rangle_{\rm G}. \tag{4.69}$$

The leading nonanalyticities are given by contributions where the loop in Fig. 15(a) is a soft mode. That is, the loop must be a Q-propagator, since the $\bar{\Lambda}$-propagator is massive.

Thus,

$$
\begin{aligned}
Q^{GM}(i\omega_n)\Big|_{\text{1-loop}} &= \frac{4}{\pi V}\sum_{\boldsymbol{q}} \langle {}^0_0(\delta Q)_{nn}(\boldsymbol{q}) \times -\frac{1}{6}\operatorname{Tr}\left(-iG_{\text{sp}}\, 2A^{-1}\delta Q\right)^3\rangle_{\text{G}} \\
&= -\frac{16i}{3\pi V^4}\sum_{\boldsymbol{q}}\sum_{\boldsymbol{p}_1,\boldsymbol{p}_2,\boldsymbol{p}_3}\sum_{n_1,n_3,n_5}\sum_{rst,ijk}\sum_{a,b,c=0,3}\operatorname{tr}\left(\tau_a\tau_r\tau_b\tau_s\tau_c\tau_t\right) \\
&\quad\times \operatorname{tr}\left(s_a s_i s_b s_j s_c s_k\right) G^a_{n_1}(\boldsymbol{p}_3)\, G^b_{n_3}(\boldsymbol{p}_3-\boldsymbol{p}_1)\, G^c_{n_5}(\boldsymbol{p}_3-\boldsymbol{p}_2-\boldsymbol{p}_1) \\
&\quad\times A^{-1}_{n_1n_3}(\boldsymbol{p}_1)A^{-1}_{n_3n_5}(\boldsymbol{p}_2)A^{-1}_{n_5n_1}(-\boldsymbol{p}_1-\boldsymbol{p}_2) \\
&\quad\times \underbrace{\langle {}^0_0(\delta Q)_{nn}(\boldsymbol{q})\, {}^i_r(\delta Q)_{n_1n_3}(\boldsymbol{p}_1)\, {}^j_s(\delta Q)_{n_3n_5}(\boldsymbol{p}_2)\, {}^k_t(\delta Q)_{n_5n_1}(-\boldsymbol{p}_1-\boldsymbol{p}_2)\rangle_{\text{G}}}_{\text{Apply Wick's theorem}} \\
&= -\frac{16i}{\pi V^4}\sum_{\boldsymbol{q}}\sum_{\boldsymbol{p}_1,\boldsymbol{p}_2,\boldsymbol{p}_3}\sum_{n_1,n_3,n_5}\sum_{rst,ijk}\sum_{a,b,c=0,3}\operatorname{tr}\left(\tau_a\tau_r\tau_b\tau_s\tau_c\tau_t\right) \\
&\quad\times \operatorname{tr}\left(s_a s_i s_b s_j s_c s_k\right) G^a_{n_1}(\boldsymbol{p}_3)\, G^b_{n_3}(\boldsymbol{p}_3-\boldsymbol{p}_1)\, G^c_{n_5}(\boldsymbol{p}_3-\boldsymbol{p}_2-\boldsymbol{p}_1) \\
&\quad\times A^{-1}_{n_1n_3}(\boldsymbol{p}_1)A^{-1}_{n_3n_5}(\boldsymbol{p}_2)A^{-1}_{n_5n_1}(-\boldsymbol{p}_1-\boldsymbol{p}_2) \\
&\quad\times \underbrace{\langle {}^0_0(\delta Q)_{nn}(\boldsymbol{q})\, {}^k_t(\delta Q)_{n_5n_1}(-\boldsymbol{p}_1-\boldsymbol{p}_2)\rangle_{\text{G}}}_{=\frac{V}{16}\delta_{\boldsymbol{q},\boldsymbol{p}_1+\boldsymbol{p}_2}\,\delta_{0k}\,\delta_{0t}\,\delta_{n,n_5}\,\delta_{n,n_1}A_{nn}(\boldsymbol{q})}\ \langle {}^i_r(\delta Q)_{n_1n_3}(\boldsymbol{p}_1)\, {}^j_s(\delta Q)_{n_3n_5}(\boldsymbol{p}_2)\rangle_{\text{G}} \\
&= -\frac{i}{\pi V^3}\sum_{\boldsymbol{q}}\sum_{\boldsymbol{p}_1,\boldsymbol{p}_3}\sum_{n_3}\sum_{rs,ij}\sum_{a,b,c=0,3}\operatorname{tr}\left(\tau_a\tau_r\tau_b\tau_s\tau_c\right)\operatorname{tr}\left(s_a s_i s_b s_j s_c\right) \\
&\quad\times G^a_n(\boldsymbol{p}_3)\, G^b_{n_3}(\boldsymbol{p}_3-\boldsymbol{p}_1)\, G^c_n(\boldsymbol{p}_3-\boldsymbol{q})\, A^{-1}_{nn_3}(\boldsymbol{p}_1)A^{-1}_{n_3n}(\boldsymbol{q}-\boldsymbol{p}_1) \\
&\quad\times \langle {}^i_r(\delta Q)_{nn_3}(\boldsymbol{p}_1)\, {}^j_s(\delta Q)_{n_3n}(\boldsymbol{q}-\boldsymbol{p}_1)\rangle_{\text{G}}
\end{aligned}
\tag{4.70}
$$

$$Q^{GM}(i\omega_n)\Big|_{\text{1-loop}} = -\frac{i}{\pi V^2}\sum_{\boldsymbol{p}_1}\sum_{n_3}\sum_{rs,ij}(-1)^s \begin{pmatrix} + \\ - \\ - \\ - \end{pmatrix}_j A^{-2}_{nn_3}(\boldsymbol{p}_1)\,\langle {}^i_r(\delta Q)_{nn_3}(\boldsymbol{p}_1)\,{}^j_s(\delta Q)_{nn_3}(-\boldsymbol{p}_1)\rangle_{\text{G}}$$
$$\times\frac{1}{V}\sum_{a,b,c=0,3}\text{tr}\,(\tau_a\tau_r\tau_b\tau_s\tau_c)\,\text{tr}\,(s_a s_i s_b s_j s_c)\,G^a_n(\boldsymbol{p}_3)\,G^b_{n_3}(\boldsymbol{p}_3-\boldsymbol{p}_1)\,G^c_n(\boldsymbol{p}_3).$$

Performing the sum over the indices a, b, c and assuming $\omega_n > 0$,

$$\begin{aligned} Q^{GM}(i\omega_n) &= -\frac{4i}{\pi V^2}\sum_{m<0}\sum_{\boldsymbol{k}}\sum_{r,s=0,3}\sum_{i,j=1,2}\Big[\varphi^{(3)}_{nnm}(\boldsymbol{k})\Big]^{ij}_{rs} \\ &\quad\times D^{-2}_{nm}(\boldsymbol{k})\,(-1)^{s+1}\Big\langle {}^i_r(\delta Q)_{nm}(\boldsymbol{k})\,{}^j_s(\delta Q)_{nm}(-\boldsymbol{k})\Big\rangle\ , \end{aligned} \tag{4.71a}$$

where

$$\begin{aligned} \Big[\varphi^{(3)}_{nnm}(\boldsymbol{k})\Big]^{ij}_{rs} &= (-1)^{r+1}\,\delta_{rs}\delta_{ij}A^{nnm}(\boldsymbol{k}) - (1-\delta_{rs})(\delta_{i1}\delta_{j2}-\delta_{i2}\delta_{j1})B^{nnm}(\boldsymbol{k}) \\ A^{nnm}(\boldsymbol{k}) &= \frac{1}{2V}\sum_{\boldsymbol{p}}[G^+_n(\boldsymbol{p})G^+_n(\boldsymbol{p})G^-_m(\boldsymbol{p}+\boldsymbol{k}) + G^-_n(\boldsymbol{p})G^-_n(\boldsymbol{p})G^+_m(\boldsymbol{p}+\boldsymbol{k})] \\ B^{nnm}(\boldsymbol{k}) &= \frac{1}{2V}\sum_{\boldsymbol{p}}[G^+_n(\boldsymbol{p})G^+_n(\boldsymbol{p})G^-_m(\boldsymbol{p}+\boldsymbol{k}) - G^-_n(\boldsymbol{p})G^-_n(\boldsymbol{p})G^+_m(\boldsymbol{p}+\boldsymbol{k})] \\ D_{nm}(\boldsymbol{k}) &= \frac{1}{2V}\sum_{\boldsymbol{p}}[G^+_n(\boldsymbol{p})G^-_m(\boldsymbol{p}+\boldsymbol{k}) + G^-_n(\boldsymbol{p})G^+_m(\boldsymbol{p}+\boldsymbol{k})] \end{aligned} \tag{4.71b}$$

with

$$G^\pm_n(\boldsymbol{k}) = \frac{1}{(i\omega_n - \xi_{\boldsymbol{k}} \pm \Delta)}. \tag{4.71c}$$

The constants c and d are the ones defined in Eq. (4.21b). In the above equations, r, s and i, j are restricted to $\{0, 3\}$ and $\{1, 2\}$, respectively, so that the δQ propagators exclusively represent the spin-waves. The quantities $A^{nnm}(\boldsymbol{k})$ and $B^{nnm}(\boldsymbol{k})$ are

calculated using the AGD (Abrikosov-Gor'kov-Dzhyaloshinskii) approximation. This yields

$$\begin{aligned} A^{nnm}(\boldsymbol{k}) &\approx N_F\pi i\Big[\frac{1}{(i\Omega_{n-m}+2\Delta)^2-(v_{\rm F}k)^2}+(\Delta\to-\Delta)\Big] \\ B^{nnm}(\boldsymbol{k}) &\approx N_F\pi i\Big[\frac{1}{(i\Omega_{n-m}+2\Delta)^2-(v_{\rm F}k)^2}-(\Delta\to-\Delta)\Big]. \end{aligned} \tag{4.72a}$$

We note that as $m\to n$ and $\boldsymbol{k}\to 0$, $A^{nnm}(\boldsymbol{k})$ and $B^{nnm}(\boldsymbol{k})$ remain finite, due to the nonzero Δ. Therefore, to leading order in $\boldsymbol{k}$ and Ω_{n-m},

$$\begin{aligned} A^{nnm}(\boldsymbol{k}) &= \frac{N_F\pi i}{2\Delta^2} \\ B^{nnm}(\boldsymbol{k}) &= -\frac{N_F\pi i}{2\Delta^2}\left(\frac{i\Omega_{n-m}}{\Delta}\right). \end{aligned} \tag{4.72b}$$

Clearly, $B^{nnm}(\boldsymbol{k})$ has an additional Ω_{n-m}/Δ factor relative to $A^{nnm}(\boldsymbol{k})$. Therefore, the leading contribution to the DOS correction comes from the A term, with the B term contribution a subleading correction.

Thus, taking

$$\langle {}^i_r(\delta Q)_{nm}(\boldsymbol{k})\, {}^i_r(\delta Q)_{nm}(-\boldsymbol{k})\rangle = -\frac{V}{8}\Gamma_t T D^2_{nm}(\boldsymbol{k})\frac{d\,c\,\boldsymbol{k}^2}{c^2\boldsymbol{k}^4+\Omega^2_{n-m}} \tag{4.73}$$

in Eq. (4.71a) and analytically continuing ω_n, the leading spin-wave correction to the DOS turns out to be

$$\delta N^{GM}(\omega) = \mathrm{Re}\, Q^{GM}(i\omega_n)\Big|_{i\omega_n\to\omega+i0} = \frac{1}{8}\,6^{d/2}\,\frac{S_{d-1}}{d(2\pi)^d}\,\frac{k_F^d}{\Delta}\left|\frac{\omega}{\Delta}\right|^{d/2}, \tag{4.74}$$

S_{d-1} is the surface area of a d dimensional hypersphere with unit radius.

Conclusions

In summary, we have calculated the leading spin-wave contribution to the longitudinal susceptibility, electrical conductivity and the density of states in itinerant ferromagnets using the framework of a Q-matrix theory for the electrons and a Stoner saddle-point solution of this field theory. For simplicity, a single parabolic band of electrons has been considered and the effects of the spin waves on the transport and thermodynamic properties have been calculated. Microscopic details like band structure etc. do not affect the universal properties that are due to the soft modes in the system.

As seen in the preceding sections and Chapter III, the one-loop spin-wave contribution to the longitudinal susceptibility vanishes at $T = 0$, when undamped spin waves are considered. If the disorder is neglected in the model, the spin waves are not damped at long wavelengths and low frequencies, even by electron-hole excitations. When nonmagnetic disorder is explicitly included in the model, the spin waves are damped and the leading spin-wave contribution to the longitudinal susceptibility at $T = 0$ is proportional to $(1/\tau)|\Omega|^{d/2}$. This result is in agreement with the very general results presented in the previous chapter. When the single-particle scattering or relaxation time, τ tends to infinity the nonanalytic behavior turns off.

We have also calculated the leading spin-wave contribution to the electrical conductivity. It turns out this contribution is structurally very similar to the one-loop contribution to the longitudinal susceptibility, only differing by a factor of momentum-squared in the relevant integral, which comes from the vertex. This is a result of the current-current correlation function, like the longitudinal susceptibility, being purely related to the magnon-number fluctuations. Naive power counting arguments and previously published results suggested that the undamped spin waves contribute a

$\Omega^{(d-2)/2}$ term to the conductivity at $T = 0$. However, a careful calculation of the same revealed that this nonanalyticity has a zero prefactor, akin to the longitudinal susceptibility. The damped spin-waves lead to a positive $(1/\tau)|\Omega|^{d/2}$ contribution; the positive sign signifies the localizing nature of the spin waves.

The leading spin-wave correction to the electronic density of states has also been calculated. Unlike the other two observables, the undamped spin waves lead to a nonzero correction, consistent with power counting. The correction is positive and behaves like $|\omega/\Delta|^{d/2}$, where 'ω' is the energy measured from the Fermi level. The Stoner gap, Δ, provides a natural energy scale for this nonanalyticity. This behavior can be probed using scanning tunneling experiments and measuring the zero-bias tunneling anomalies.

CHAPTER V

SUMMARY

To summarize, the work presented in this dissertation leads to a better understanding of the fundamental properties of metallic ferromagnets at low temperatures and the various effects caused by the accompanying Goldstone modes. This could have long-term implications on practical applications. As modern electronic devices get smaller, quantum mechanical effects become more relevant and therefore, knowledge of these effects will be helpful in the design and achieving the desired performance of these devices. Hence, understanding the dynamics of ferromagnets and the effects of Goldstone modes is important.

In Chapter II, the ferromagnon contribution to the single-particle and transport relaxation rate was calculated using a model based on simple symmetry arguments that did not depend on the origin of the magnetization. It was noted that the ferromagnon-mediated electron-electron interaction is purely inter-Stoner-band in nature and requires the flipping of the electronic spin. As a result, the relaxation rates display an activation-barrier-like behavior at asymptotically low temperature,s and below a certain temperature the ferromagnon contribution freezes out. Therefore, the ferromagnon contribution is markedly different from the power-law contributions of magnons in antiferromagnets and helimagnets. The previously reported T^2 behavior of the ferromagnon contribution to the transport relaxation rate [19] was found to be valid only in a preasymptotic temperature window. The results of Chapter II are compatible with the low-temperature helimagnet results [26, 27, 28], which was the primary motivation in re-examining the validity of the T^2 result.

Chapter III explored the magnon-induced nonanalyticities in the long-wavelength/low-frequency behavior of correlation functions in quantum magnets. Specifically, the correlation function of the longitudinal order-parameter fluctuations was considered. Naively, the coupling between statics and dynamics in the quantum case is expected to lead to a weaker nonanalyticity compared to the classical case. However, for quantum ferromagnets, it was found that the one-loop undamped-magnon contribution to the longitudinal susceptibility vanished at $T = 0$. This null result is not an artifact of the nonlinear sigma model used for the calculations, or the one-loop approximation; rather, it is a property of correlation functions that can be expressed entirely in terms of magnon-number fluctuations. The longitudinal susceptibility in quantum ferromagnets is one such correlation function. This is in contrast to quantum antiferromagnets: the longitudinal order-parameter susceptibility is not such a correlation function and the expected nonanalyticity exists at $T = 0$. This difference between the quantum ferromagnets and quantum antiferromagnets is highlighted in the longitudinal dynamical structure factor, a quantity relevant in neutron-scattering experiments. Further, damped ferromagnons were considered and a nonvanishing one-loop contribution to the longitudinal susceptibility was obtained. The damping can be due to some disorder in the system. The quenched disorder introduces new fluctuations in the system, which restore the nonanalyticity. A simple renormalization-group scaling analysis showed that the one-loop result is exact, as far as the exponent of the nonanalyticity is concerned.

Chapter IV considered the Stoner model of itinerant ferromagnets and briefly introduced an effective field theory in terms of quaternionic fields. The magnonic soft modes were identified and their contributions to the longitudinal susceptibility and the dynamical electrical susceptibility were calculated using a source formalism

with the appropriate source field. It is found that that the dynamical electrical conductivity, like the susceptibility, is given purely in terms of magnon-number fluctuations. Therefore, the $T = 0$ undamped ferromagnon contribution to the conductivity vanishes, in disagreement with a previous result [20]. As before, introducing quenched nonmagnetic disorder restored the nonanalytic low-frequency dependence of the conductivity. The leading spin-wave correction to the single particle density of states was also calculated and a nonanalyticity, consistent with power-counting arguments, was found.

APPENDIX

CAUSAL FUNCTIONS AND LONG-TIME TAILS

The following are some properties of the class of causal functions that the longitudinal susceptibility belongs to. The proofs can be found in [74].

Non-integer Powers

Consider a causal function χ of complex frequency z that behaves, for $z \to 0$, as

$$\chi(z) = \frac{1}{\cos(\alpha\pi/2)} \left[z^\alpha + (-z)^\alpha\right], \tag{A.1}$$

with α real and not integer. Here and in what follows, only even functions of z are considered, since the magnetic susceptibility has this property. Only the asymptotic small-frequency, or long-time behavior is given here; for $z \to \infty$ χ, or any causal function vanishes.

On the imaginary axis, χ takes the values

$$\chi(i\Omega_n) = |\Omega_n|^\alpha. \tag{A.2}$$

Then, the reactive part χ' and the spectrum χ'', respectively of χ read as

$$\chi''(\omega) = -\sin(\alpha\pi/2)\,|\omega|^\alpha \operatorname{sgn}\omega, \tag{A.3}$$

$$\chi'(\omega) = \cos(\alpha\pi/2)\,|\omega|^\alpha. \tag{A.4}$$

The real-time behavior of χ is given by the Fourier transform of $\chi''(\omega)$,

$$\chi(t) = \int_{-\infty}^{\infty} \frac{d\omega}{\pi}\, e^{-i\omega t}\, \chi''(\omega). \tag{A.5}$$

In the long-time limit, the Hardy-Littlewood tauberian theorem yields a long-time tail:

$$\chi(t \to \infty) = i\, \frac{\Gamma(\alpha+1)}{\pi}\, \sin(\alpha\pi)\, \frac{1}{|t|^{\alpha+1}}. \tag{A.6}$$

The ferromagnet with damped magnons in $d = 3$ is an example of this behavior, with $\alpha = 1/2$ and $\alpha = 3/2$ for a nonconserved and a conserved order parameter, respectively. This behavior is also realized by both ferromagnets and antiferromagnets in generic dimensions.

Even Powers

Considering the following causal function,

$$\chi(z) = \frac{(-)^m}{2}\, z^{2m}\, [\ln z + \ln(-z)], \tag{A.7}$$

with an integer m. On the imaginary axis this yields,

$$\chi(i\Omega_n) = |\Omega_n|^{2m}\, \ln|\Omega_n|. \tag{A.8}$$

The spectrum and the reactive part are

$$\chi''(\omega) = \frac{(-)^{m+1}\pi}{2}\, \omega^{2m}\, \mathrm{sgn}\,\omega, \tag{A.9}$$

$$\chi'(\omega) = (-)^m\, \omega^{2m}\, \ln|\omega|. \tag{A.10}$$

and the long-time behavior is

$$\chi(t \to \infty) = i \, \frac{(2m)!}{|t|^{2m+1}}. \tag{A.11}$$

The above behavior is seen in antiferromagnets in $d = 3$ and ferromagnets in $d = 2$ with a nonconserved order parameter.

Odd Powers

Finally, taking

$$\chi(z) = \frac{(-)^{m+1}}{2} \, z^{2m+1} \, [\ln z - \ln(-z)] \tag{A.12}$$

with m integer, which leads to

$$\chi(i\Omega_n) = |\Omega_n|^{2m+1}, \tag{A.13}$$

and

$$\chi''(\omega) = (-)^{2m+1} \, \omega^{2m+1}. \tag{A.14}$$

A distinction needs to be made between $m \geq 0$ and $m < 0$. For $m \geq 0$, the spectrum is analytic and the reactive part vanishes,

$$\chi'(\omega) = 0, \tag{A.15}$$

and there is no long-time tail in the real-time domain. However, there is a long-time tail in the limit of large imaginary time $\tau \to \infty$. $\chi(\tau)$ is given by

$$\chi(\tau) = T \sum_{i\Omega_n} e^{-i\Omega_n \tau} \, \chi(i\Omega_n). \tag{A.16}$$

At $T = 0$, the sum turns into an integral and one finds,

$$\chi(\tau \to \infty) = \frac{1}{\pi} (-)^{2m+1} (2m+1)! \frac{1}{\tau^{2(m+1)}}. \tag{A.17}$$

An example for this behavior is the ferromagnet with damped magnons in $d = 2$ with a conserved order parameter.

For $m < 0$, the spectrum is singular at $\omega = 0$ and there is a long-time tail even in real-time domain. For $m = -1$,

$$\chi'(\omega) = \delta(\omega), \tag{A.18}$$

and the long-real-time behavior is a constant,

$$\chi(t) = -i. \tag{A.19}$$

An example is the antiferromagnet in $d = 2$.

REFERENCES CITED

[1] P. A. M. Dirac. *The Principles of Quantum Mechanics*. Oxford University Press, New York, 1935. second edition, Chapter X.

[2] J. H. Van Vleck. *Rev. Mod. Phys.*, 17:27, 1945.

[3] C. Kittel. *Introduction to Solid State Physics*. Wiley, New York, 2005.

[4] E. C. Stoner. *Proc. Roy. Soc. London A*, 165:372, 1938.

[5] L. Néel. Magnetic properties of ferrites: Ferrimagnetism and antiferromagnetism. *Ann. Phys.-Paris*, 3:137–198, 1948.

[6] I. E. Dzyaloshinski. *J. Phys. Chem. Solids*, 4:241, 1958.

[7] T. Moriya. *Phys. Rev.*, 120:91, 1960.

[8] P. Bak and M. H. Jensen. *J. Phys. C*, 13:L881, 1980.

[9] O. Nakanishi, A. Yanase, A. Hasegawa, and M. Kataoka. *Solid State Commun.*, 19:525, 1976.

[10] D. Sherrington and S. Kirkpatrick. *Phys. Rev. Lett.*, 35:1792, 1975.

[11] S. F. Edwards and P. W. Anderson. *Journal of Physics F: Metal Physics*, 5:965, 1975.

[12] P. W. Anderson. *Mater. Res. Bull.*, 8:153, 1973.

[13] E. Fawcett. *Rev. Mod. Phys.*, 60:209, 1988.

[14] S.-K. Ma. *Modern Theory of Critical Phenomena*. Benjamin, Reading, MA, 1976.

[15] L. D. Landau. *Zh. Eksp. Teor. Fiz.*, 7:19, 1937. translated and reprinted in *Collected Papers of L. D. Landau*, edited by D. Ter Haar, Pergamon, Oxford 1965.

[16] P. M. Chaikin and T. C. Lubensky. *Principles of Condensed Matter Physics*. Cambridge University Press, 2000.

[17] P. W. Higgs. *Phys. Rev. Lett.*, 13:508, 1964.

[18] V. L. Ginzburg and L. D. Landau. *Zh. Eksp. Teor. Fiz.*, 20:1064, 1950. translated and reprinted in *Collected Papers of L. D. Landau*, edited by D. Ter Haar, Pergamon, Oxford 1965.

[19] K. Ueda and T. Moriya. *J. Phys. Soc. Jpn*, 39:605, 1975.

[20] T. R. Kirkpatrick and D. Belitz. *Phys. Rev. B*, 62:952, 2000.

[21] J. M. Ziman. *Electrons and Phonons*. Clarendon Press, Oxford, 1960.

[22] T. Kasuya. *Progr. Theor. Phys.*, 16:58, 1956.

[23] D. A. Goodings. *Phys. Rev.*, 132:542, 1963.

[24] Tôru Moriya. *Spin fluctuations in Itinerant Electron Magnetism*. Springer, Berlin, 1985.

[25] I. Dzyaloshinksy. *J. Phys. Chem. Solids*, 4:241, 1958.

[26] D. Belitz, T. R. Kirkpatrick, and A. Rosch. *Phys. Rev. B*, 74:024409, 2006.

[27] T. R. Kirkpatrick, D. Belitz, and R. Saha. *Phys. Rev. B*, 78:094407, 2008.

[28] T. R. Kirkpatrick, D. Belitz, and R. Saha. *Phys. Rev. B*, 78:094408, 2008.

[29] K. Ueda. *J. Phys. Soc. Jpn*, 43:1497, 1977.

[30] N. D. Wagner and H. Wagner. *Phys. Rev. Lett.*, 17:1133, 1966.

[31] K. Y. Ho, T. R. Kirkpatrick, Y. Sang, and D. Belitz. *Phys. Rev. B*, 82:134427, 2010.

[32] F. J. Himpsel, J. E. Ortega, G. J. Mankey, and R. F. Willis. *Adv. Phys.*, 47:511, 1998.

[33] G. D. Mahan. *Many-Particle Physics*. Plenum, New York, 1981.

[34] L. P. Kadanoff and G. Baym. *Quantum Statistical Mechanics*. W. A. Benjamin, New York, 1962.

[35] A. A. Abrikosov, L. P. Gorkov, and I. E. Dzyaloshinksi. *Methods of Quantum Field Theory in Statistical Physics*. McGraw-Hill, New York, 1963.

[36] D. Belitz and T. R. Kirkpatrick. *Physica E*, 42:497, 2010.

[37] D. Forster. *Hydrodynamic Fluctuations, Broken Symmetry, and Correlation Functions*. Benjamin, Reading, MA, 1975.

[38] F. J. Himpsel. *Phys. Rev. Lett.*, 67:2363, 1991.

[39] P. Böni, B. Roessli, and K. Hradil. *J. Phys. Cond. Matt.*, 23:254209, 2011.

[40] N. R. Bernhoeft, I. Cole, G. G. Lonzarich, and G. L. Squires. *J. Appl. Phys.*, 53:8204, 1982.

[41] C. Pfleiderer. *J. Low Temp. Phys.*, 147:231, 2007.

[42] I. A. Campbell and A. Fert. *Ferromagnetic Materials*, volume 3, pg. 747. North-Holland, Amsterdam, 1982. edited by E. P. Wohlfarth.

[43] V. G. Vaks, A. I. Larkin, and S. A. Pikin. *Zh. Eksp. Teor. Fiz.*, 53:1089, 1967. [Sov. Phys. JETP **26**, 647 (1968)].

[44] E. Brézin and D. J. Wallace. *Phys. Rev. B*, 7:1967, 1973.

[45] D. Belitz and T. R. Kirkpatrick. *Phys. Rev. B*, 56:6513, 1997.

[46] D. Belitz, T. R. Kirkpatrick, and Thomas Vojta. *Rev. Mod. Phys.*, 77:579, 2004.

[47] B. L. Altshuler and A. G. Aranov. *Electron-Electron Interactions in Disordered Systems*. North-Holland, Amsterdam, 1984. edited by M. Pollak and A. L. Efros.

[48] P. A. Lee and T. V. Ramakrishnan. *Rev. Mod. Phys.*, 57:287, 1985.

[49] J. Zinn-Justin. *Quantum Field Theory and Critical Phenomena*. Oxford University Press, Oxford, 1996.

[50] S. Bharadwaj, D. Belitz, and T. R. Kirkpatrick. *Phys. Rev. B*, 94:144404, 2016.

[51] Eduardo Fradkin. *Field Theories of Condensed Matter Systems*. Addison Wesley, New York, 1991.

[52] Subir Sachdev. *Quantum Phase Transitions*. Cambridge University Press, Cambridge, 1999.

[53] J. R. Klauder. *Phys. Rev. D*, 19:2349, 1979.

[54] B. Schlittgen and U. J. Wiese. *Phys. Rev. D*, 63:085007, 2001.

[55] H. Watanabe and H. Murayama. *Phys. Rev. Lett.*, 108:251602, 2012.

[56] L. D. Landau and E. M. Lifshitz , Phys. Z. Sowjet. 8, 153 (1935), reprinted in. *Collected Papers of L. D. Landau*. Pergamon, Oxford, 1965. edited by D. Ter Haar.

[57] P. C. Hohenberg and B. I. Halperin. *Rev. Mod. Phys.*, 49:435, 1977.

[58] H. Kohno, G. Tatara, and J. Shibata. *J. Phys. Soc. Jpn. 75, 113706*, 75:113706, 2006.

[59] N. Umetsu, D. Miura, and A. Sakuma. *J. Phys. Soc. Jpn.*, 81:114716, 2012.

[60] M Isoda. *J. Phys. Condes. Matter*, 2:3579, 1990.

[61] V. Korenman and R. E. Prange. *Phys. Rev. B*, 6:2769, 1972.

[62] Y. Tserkovnyak, E. M. Hankiewicz, and G. Vignale. *Phys. Rev. B*, 79:094415, 2009.

[63] J. Kötzler, D. Görlitz, R. Dombrowski, and M. Pieper. *Z. Phys. B*, 94:9, 1994.

[64] J. Eisert, M. Cramer, and M. B. Plenio. *Rev. Mod. Phys.*, 82:277, 2010.

[65] V. Popkov and M. Salerno. *Phys. Rev. A*, 71:012301, 2005.

[66] W. Ding, N. E. Bonesteel, and K. Yang. *Phys. Rev. A*, 77:052109, 2008.

[67] H. F. Song, N. Laflorencie, S. Rachel, and K. Le Hur. *Phys. Rev. B*, 83:224410, 2011.

[68] M. Metlitski and T. Grover. *arXiv:1112.5166*, 2011.

[69] G. Misguich, V. Pasquier, and M. Oshikawa. *arXiv:1607.02465*, 2016.

[70] J. M. O. de Zarate and J. V. Sengers. *Hydrodynamic fluctuations in fluids and fluid mixtures*. Elsevier, Amsterdam, 2007. ch. 7.5.

[71] T. R. Kirkpatrick, E. G. D. Cohen, and J. R. Dorfman. *Phys. Rev. A*, 26:995, 1982.

[72] T. R. Kirkpatrick and D. Belitz. *Phys. Rev. B*, 93:125130, 2016.

[73] D. Belitz, F. Evers, and T. R. Kirkpatrick. *Phys. Rev. B*, 58:9710, 1998.

[74] M. J. Lighthill. *Introduction to Fourier analysis and generalised functions*. Cambridge University Press, Cambridge, 1958.